# Potential of Pulsed Corona Discharges Generated in Water for the Degradation of Recalcitrant Pharmaceutical Residues and for Water Disinfection

I n a u g u r a l d i s s e r t a t i o n

zur

Erlangung des akademischen Grades eines

Doktors der Naturwissenschaften
(Dr. rer. nat.)

der

Mathematisch-Naturwissenschaftlichen Fakultät

der

Ernst-Moritz-Arndt-Universität Greifswald

vorgelegt von

Robert Banaschik

geboren am 08.06.1983

in Rostock

Greifswald, den 17.07.2017

Dekan:                     Prof. Dr. Werner Weitschies

1. Gutachter:              Prof. Dr. Patrick J. Bednarski

2. Gutachter:              Prof. Dr. Bruce R. Locke

Tag der Promotion:         21.11.2017

# Index

# Chapter 1

# Introduction (P1)

Earth is often called the "Blue Planet" due to the abundance of water on its surface; in fact, water covers about 71 percent of the Earth's ground level. However, to break the number down, 96.5 percent of all the water on earth is contained within the oceans as salt water. Another percent (0.94%) exists beneath the Earth's surface as saline groundwater. About 2.6 percent of global water is available as freshwater but 69 percent of this is trapped in ice caps, glaciers and as permanent snow [1]. From a global perspective, only about 0.8 percent of the Earth's water therefore meet the requirements for usable freshwater, namely not-saline ground water (0.76%), surface water in lakes (0.007%), swamps (0.0008%) and rivers (0.0002%).

According to Cosgrove and Rijsberman, perhaps half of all available freshwater is being used by humans, which is twice what it was only 35 years ago. Water consumption has multiplied six times in the last 100 years, while the world population tripled [2]. The situation is even more serious when the local perspective and water quality are considered [3]. In this context, the limited and precious nature of freshwater becomes clear. The protection and conservation of natural resources is therefore one of the main priorities of modern societies. Because freshwater is a limited resource, it needs to be recycled and harmful pollutants have to be removed. This idea constitutes the basis of all modern water and waste water purification techniques. However, during recent years, several new threats to fresh and potable water have been identified. Anthropogenic pollutants, and in particular pharmaceutical residues, have been found in increasing concentrations and different environmental effects could already be linked to the presence of these chemicals.

## 1.1    Pharmaceutical Residues and their Environment Fate

The needs of a steady ageing society, have been going along with the development and growing use of pharmaceuticals. QuintilesIMS, formerly known as IMS Health, reported a steady increase in dispensed prescription drugs of 5.4% between 2008 (3870 million) and 2012 (4078 million). In 2015, total amount dispensed for the US reached 4.4 billion prescriptions [4, 5]. Due to the continuing progress in pharmaceutical sciences and expected population growth, a further increase can be assumed.

Pharmaceuticals can follow two primary pathways into the environment: by deliberate disposal, or by excretion of drugs and metabolites from the patient's body [6]. In fact, most pharmaceuticals prescribed for treatment are excreted from the body by either the renal or the biliary system [7]. Since pharmaceuticals should be able to reach their target location without destruction by enzymes and the metabolism in general, many pharmaceuticals are essentially not biodegradable and withstand destruction by conventional sewage treatment plants [8, 9].

More than 80 pharmaceuticals and drug metabolites, such as antiepileptic drugs (diazepam, carbamazepine) and analgesics (ibuprofen, diclofenac), have been detected in the aquatic environment [10] and can be found in increasing concentrations [9]. About 32 common drugs, were found in effluents of German sewage treatment plants [11]. In the Netherlands, hormones from oral contraceptives (17α-ethinylestradiol) were found in concentrations of 62 ng/l and 47 ng/l in sewage effluents and surface water, respectively [12, 13]. These compounds, but also others, escape most efforts of filtration and destruction and are a burden on the environment.

Although detected concentrations are lower than used for therapeutic dosages, continuously administered pharmaceuticals can be harmful to aquatic life forms. Benzodiazepines were reported to alter the behavior and feeding rate of perches in drug concentrations as low as 1.8 µg/l [14]. A decrease in the reproduction rates of snails (*P. antipodarum*) may be caused by the antidepressant drug fluoxetine in concentrations of 0.81 µg/l [15]. Estrogens in doses as low as 0.296 ng/l were linked to the disruption of amphibian mating behavior and can affect the gender distribution of fish populations [16, 17].

Long-term effects on human health, however, are difficult to predict and are of growing public concern. To investigate the potential risks for human health, the European Commission (EC) started monitoring of pollutants including diclofenac (analgesic), 17α-ethinylestradiol and 17β-estradiol (both hormones) in 2015 [18]. The next step would be the implementation of novel water purification techniques to address this problem. Advanced Oxidation Processes (AOP) and especially physical plasmas with their ability to generate highly reactive species directly in water, offer potentially promising solutions. The field of plasmas for water purification is introduced in this study, with special focus on pulsed corona discharges.

## 1.2   Plasma: "The fourth state of matter"

The term "plasma" was first introduced by Irwing Langmuir and describes a gas that is at least partially ionized [19]. Sometimes plasma is also referred to as the "fourth state of matter" due to similarities with other phase transitions [20].

Matter, such as for example water, can generally exist in different distinct physical states, namely solid, liquid or gaseous. The state or phase can be changed from one to another depending on ambient parameters and by supplying or depleting internal energy. A well-known example is the melting of water-ice (Fig. 1). This takes place at a constant temperature for a given pressure, and requires an amount of energy known as latent heat. When energy is continuously provided, water becomes gaseous with molecules that can be compressed and move about freely. Further application of energy in form of heat, electrical energy or radiation can promote the transition from a gas to a plasma.
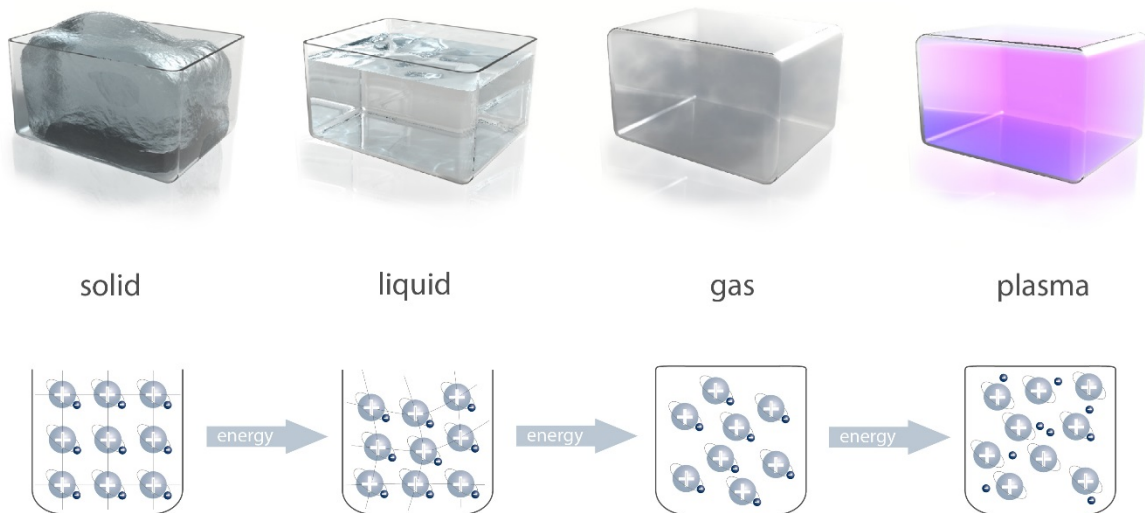
**Fig. 1 "The four states of matter"**. Matter can exist in different physical states (solid, liquid, gaseous). Further application of energy (heat, electrical energy or radiation) favors the transition from the gaseous-state to the plasma-state. Plasmas are characterized by mixtures of neutral particles, positive ions and free, negatively charged electrons. **©Graphic: C. Desjardins, INP**

Plasmas are essentially mixtures of neutral particles, positive ions and free, negatively charged electrons. Operating and ambient conditions determine the degree of ionization of a plasma, i.e. partial or full ionization. The individual respective energies of electrons, ions and neutrals, determine whether plasma is in equilibrium (thermal plasma) or non-equilibrium state (non-thermal plasma).

In equilibrium plasmas, all particles (neutrals, ions and electrons) do have the same thermal energy. Electron temperature and gas temperature are therefore the same. Prominent examples for equilibrium plasmas in nature are solar winds or the inside of the sun. However, in non-equilibrium plasmas, electrons, ions and neutrals do have different temperatures. Such plasmas are consisting of fast-moving, energetic electrons and relatively slow-moving ions and neutrals, corresponding to lower kinetic energies. Northern lights (*aurora borealis*) are a typical example for this kind of plasma.

Plasmas can provide and combine physical effects, such as elevated temperatures, energetic electrons and ions, strong electric fields and the formation of reactive species. Thus, plasmas are used in notable industrial applications, such as plasma modification of materials, plasma spraying, plasma welding, plasma cutting and semiconductor electronics [20]. Recently, novel fields of applications, such as plasmas in medicine, and plasmas for pollutant removal have raised interest [21, 22].

## 1.3    Scope of this Work

The aim of this work is a better understanding of fundamental plasma-chemistry and how plasmas can potentially be applied for water purification. As outlined in the previous section, different kinds of plasmas have different unique properties. Thus, in a first step, plasmas suitable for water purification had to be identified. Plasmas considered suitable, as well as the plasma setup developed in this work, are presented in Chapter 2. This chapter also discusses how plasmas can be generated in water and what challenges and difficulties need to be addressed.

Chapter 3 discusses the question whether plasma can be effectively used for the degradation of recalcitrant compounds. Representative substances from important drug groups, such as analgesics, hormones, hypnotics, antibiotics and X-ray contrast agents were selected and treated accordingly. To evaluate water quality after plasma treatment, important water parameters, such as pH-value and concentration of nitrate and nitrite were monitored.

In Chapter 4, first insights into plasma chemistry and the degradation of recalcitrant organic pollutants are provided. Special focus was given to the degradation of phenol, which was used as a chemical probe for the detection of reactive species. The chapter also deals with the corrosion of ground electrodes, which appeared to substantially affect plasma chemistry.

The knowledge about plasma chemical processes was further expanded in Chapter 5. Since for most pharmaceuticals detailed reaction pathways and associated possible risks (e.g. from toxic degradation products) are not known, this was studied by using diclofenac as an example. Consequently, an initial first risk assessment of hazardous byproducts that potentially form when pharmaceuticals are exposed to plasma generated in water was performed.

After it has been demonstrated that plasmas generated directly in water do have a variety of physical and chemical effects that are effective for pollutant degradation, a closer examination was given to antimicrobial properties that can be used for water disinfection and the killing of bacteria in Chapter 6. Plasma and pulsed electric fields were assessed for their capacity to kill pathogenic microorganisms persisting in water tanks, cooling systems and water pipes. As a result, it was shown that the killing of *L. pneumophila* was possible with both methods. However, pulsed corona plasma appeared to be more efficient.

A Summary and an outlook for further research is given in Chapter 7.

# Chapter 2

# Plasma Generation (P1, P2 & P3)

Water purification by plasma can be distinguished into methods where the plasma is either generated in gaseous atmosphere above or close to liquid surface or methods where the plasma is generated directly in the liquid. Representative operating systems for plasmas generated in gaseous atmosphere are Dielectric Barrier Discharges (DBD) [23-27] and Pulsed Corona Discharges (PCD) [28-32]. Plasmas generated in gaseous atmosphere can be considered as an indirect treatment since species that are formed in the gas phase must diffuse into the liquid first. A modification of this approach is the treatment of water droplets or water sprays [30]. The issue of a necessary diffusion can be avoided by plasma generation directly in water.

## 2.1    Plasmas for Water Purification

The generation of spark discharges, generally in point-to-point or point-to-plane (needle-plate) geometries is an obvious possibility for the generation of a plasma directly in water. However, the technique is mostly described for small volumes and associated research on degradation of organic compounds has primarily focused on discoloration of dyes and the decomposition of phenolic derivatives [33-36]. A second method is the application of Pulsed Corona Discharges (PCD) generated directly in water. Required energies are generally about three orders of magnitude lower than needed for spark discharges [37]. When compared with spark discharges, corona discharges also offer the advantage of generating them in extended geometries [38, 39]. A summary of different discharge concepts, including investigated organic pollutants and model substances, is given in Table 1.

      Considering the potential of plasmas for water purification, pulsed corona discharges, do have inherent advantages. They are able to generate active species directly in the liquid, which then attack aqueous pollutants. Depending on the electrode configuration, they can also treat larger volumes of liquid than spark discharges in point-to-plane or needle-tip geometries [40]. Moreover, corona discharges should not lead to nitrification or big changes in pH-value as reported for surface discharges [41, 42]. Pulsed corona discharges generated in water are therefore an appealing research subject for water purification. However, pollutant degradation, degradation mechanisms, as well as associated risks, have not yet been fully investigated and are hence the topic of this work.

**Table 1**

Comparison of treatment efficacies and treatment parameters for the degradation of organic compounds. **Reprinted from Publication P2**

| Study, reference | Substances investigated | Concentration | Treated volume | Plasma system | Degradation | Treatment time | Energy cost |
|---|---|---|---|---|---|---|---|
| (Magureanu et al. 2010) | Pentoxifylline | 100 mg/l | 200 ml | coaxial DBD[a] | 92.5% | 60 min | 16 g/kWh |
| (Magureanu et al. 2011) | Amoxicillin, Oxacillin, Ampicillin | 100 mg/l | 200 ml | coaxial DBD[a] | > 90% | 30, 10, 20 min | 27, 105, 29 g/kWh |
| (Magureanu et al. 2013) | Enalapril | 50 mg/l | 300 ml | coaxial DBD[a] | > 90% | 20 min | 20.66 g/kWh |
| (Hijosa-Valsero et al. 2013) | Atrazine, Chlorfenvinfos, 2,4-Dipbromphenol Lindane | 15 mg/l | 175 ml | coaxial DBD[a] | 87–89% | 5 min | 47–447 mg/kWh |
| (Krause et al. 2009) | Clofibric acid, Carbamazepin, Iopromide | 0.1 mM (22–79 mg/l) | 200 ml | two barrier electrodes | > 98% | 30 min | 500 W |
| (Gerrity et al. 2010) | Meprobamate, Phenytoin, Primidone, Carbamazepine, Atenolol, Trimethoprim, (Atrazine) | 36–378 ng/l | 150 l | needle-plate | > 90% | 19 min | 2.2–6.4 kWh/m$^3$ (Eec°) |
| (Panorel et al. 2012, 2013) | Paracetamol, 17β-estradiol, Salicylic acid, Indometacin, Ibuprofen | 3–100 mg/l | 40-50 l | PCD[b] | 70–99% | 30 min | 1.5-150 g/kWh |
| (Minamitani et al. 2008) | Indigo carmine | 20 mg/l | 1 l | PCD[b] | > 99% | 1-60 min | 9–360 J/mg |
| (Dobrin et al. 2013) | Diclofenac | 50 mg/l | 55 ml | PCD[b] | >99% | 15 min | 0.76 g/kWh (90% conversion) |
| (Sugiarto and Sato 2001) | Phenol | 50 mg/l | 1 l | needle-plate | >99% | 30-60 min | 20 kV, 50 Hz |
| (Sato 2009) | Rhodamine B | 10 mg/l | n.s. | needle-plate | 80% | n.s. | 70–360 J/ml |
| (Malik et al. 2002) | Methylene blue | 13.25 mg/l | 20 ml | needle-plate | 95% | 90 min | 41 mg/kWh |
| (Lukes and Locke 2005) | Phenol derivatives | 500 µmol/l (47–70 mg/l) | 400 ml | needle-plate | 47–80% | 60 min | 281–457 kWh/m3 (EEO°) |

[a] Dielectric Barrier Discharge.

[b] Pulsed Corona Discharges in gaseous atmosphere.

[c] The EEO-value is defined as the amount of electrical energy (kWh), required to reduce the concentration of a pollutant by one order of magnitude (90%).

## 2.2    Experimental Setup

Corona discharges are plasmas in which many plasma filaments (streamers) are initially formed at the high voltage electrode, which then have a crown-like appearance. Pulsed corona discharges in water can be generated by applying short high voltage pulses in the sub-microsecond range to electrodes with high curvatures [43]. The short duration of the high voltage pulses ensures that no transition to sparks takes places for a given electrode gap, whereas the high electrode curvature provides locally the necessary electrical-field strength to start a plasma-filament.

In gases, the most popular geometry for laboratory studies is the point-to-plane geometry. A needle is placed above a grounded plane and the high voltage pulses are applied to the needle electrode. For industrial applications, however, this geometry is not sufficient, as the plasma can only develop in rather small volumes. Popular geometries for industrial applications are therefore the wire-cylinder or wire-to-plate geometries [44]. For scalability, a coaxial geometry was investigated for this work.

First setups were based on a thin tungsten wire of 50 µm in diameter that was used as high voltage electrode along the center of a glass tube. A metal mesh, fixed to the inner wall of the tube, served as ground electrode and permitted optical access to the discharge chamber (Fig. 2).
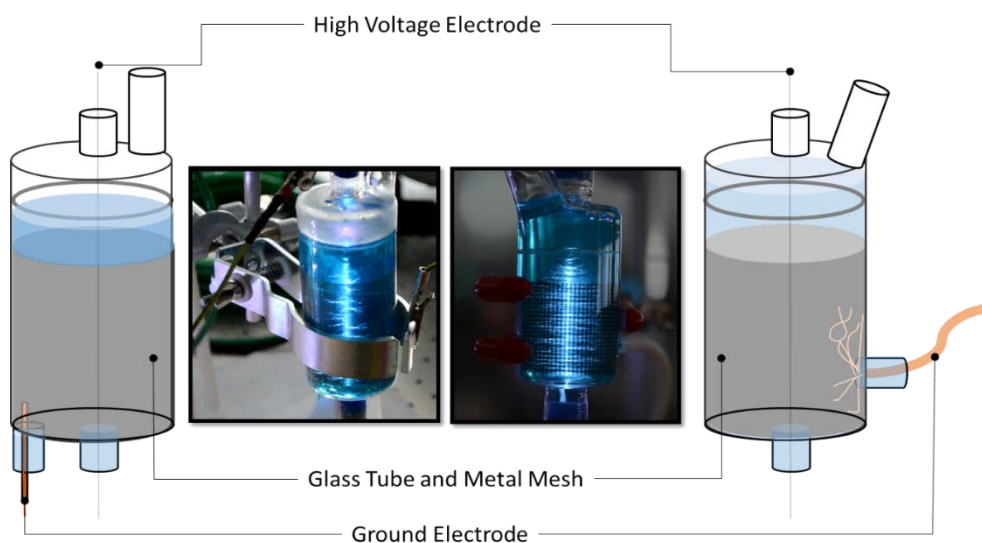


**Fig. 2** First discharge concepts that based on a thin tungsten wire of 50 µm used as high voltage electrode. The ground-electrode was a steel mesh fixed to the inner glass wall of the reactor. Plasma filaments (streamer) were generated along the wire by applying positive high voltage pulses

A disadvantage of the design is the air volume on top of the water. Since the breakdown voltage in air is considerable lower than for water, this often led to sparks and breakdowns along the air-water interface in the reaction chamber. Although insights into plasma generation in water could be obtained, reactors of this generation were difficult to build and suffered from a lack of robustness. Electrodes had to be enclosed directly onto the glass and the entire reactor had to be built from several parts that had to be melted together.

A more sophisticated design concept is shown in Fig. 3. The reactor was constructed modularly and two acrylic plates and commercially available glass tubes were bolted together. Sealing was realized by O-rings in the upper and bottom plate. Under standard experimental conditions, the glass tubes had a diameter of 47 mm and a length between the acrylic plates of 138 mm, hence retaining a volume of 240 ml. The ground electrode connection was attached directly to the metal mesh inside the reactor through a small hole in the glass. In case of glass breakage, only the standard glass tube had to be replaced, which considerably increased the robustness of the system.
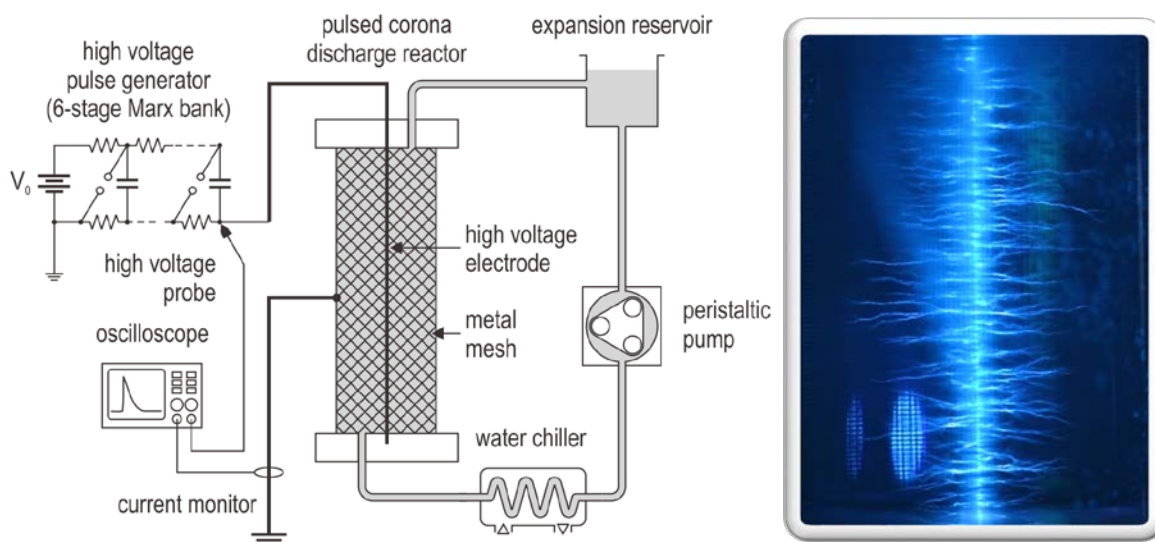


**Fig. 3** Pulsed corona discharges were generated in a coaxial reactor with an inner diameter of 47 mm and length of 138 mm along a tungsten wire with a diameter of 50 mm. Positive high voltage pulses were applied from a 6-stage Marx-Generator with 20 Hz. A volume of 300 ml of water was treated in a continuous flow system with a flow rate of 120 ml/min. **Reprinted from Publication P2**

With an interchangeable metal mesh, different electrode materials could be investigated. Including tubes and excess container, the entire system had a capacity of 300 ml. The liquid was driven through the system by a peristaltic pump. Electrical parameters, such as pulsed currents through the reactor, were measured with a Pearson current monitor (Model 5046, Pearson Electronics, Palo Alto, CA) and recorded on a fragmented memory storage oscilloscope (Wave Surfer 64MXs-B, LeCroy, Chestnut Ridge, NY).

## 2.3    Experimental Parameters

Earlier results for the decomposition of model substances, such as methylene blue, showed that decomposition efficacies correlated with the length of streamers [45]. Both number and length ($\ell$) of the plasma filaments depend on the conductivity ($\sigma$) of the liquid and the amplitude of the applied high voltage pulses ($V_p$). Peak voltages were fixed at 82 kV, whereas the conductivity of the water was adjusted from 25 µS/cm to 500 µS/cm with sodium chloride (Table 2).

**Table 2** Peak voltage, $V_p$, mean streamer length, $\ell$, with respect to water conductivity, $\sigma$. Initial peak voltage was adjusted to 82 kV for a conductivity of 25 µS/cm. **Reprinted from Publication P1**

| σ (µS/cm) | 25 | 60 | 80 | 100 | 250 | 500 |
|---|---|---|---|---|---|---|
| $V_p$ (kV) | 82 | 79 | 80 | 79 | 76 | 70 |
| $\ell$ (mm) | 16 | 6.5 | 6 | 6 | 5.5 | 4.5 |

As the conductivity gradually increased, streamer length decreased, with a gradually lower rate of change for higher conductivities. It was found during experiments that the water conductivity had to be adjusted to at least 25 µS/cm since lower values encouraged the formation of sparks. In addition, high voltage pulses above 82 kV considerably increased the risk of breaking the reactor chamber due to the formation of sparks that crossed the gap between the electrodes. Consequently, liquid conductivities between 30 µS/cm and 40 µS/cm were chosen for the experiments with peak voltages not higher than 80 kV.

Streamers, as shown in Fig. 3, were generated along the entire length of the wire when positive high voltage pulses were applied from a 6-stage Marx-Generator. Repetition rate for most experiments was set to 20 Hz. Pulses had an exponentially decaying pulse shape with a duration of about 200-300 ns (FWHM) and a rise time of 30 ns (Fig. 4).
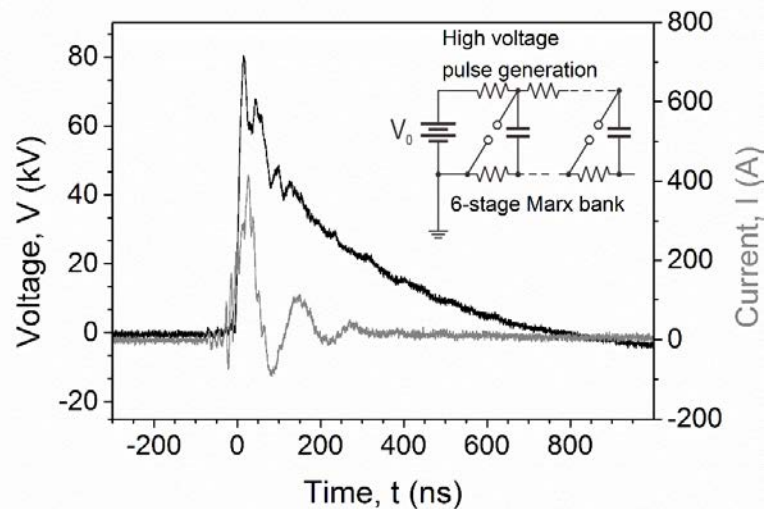


**Fig. 4** Current and voltage characteristics for a single positive high voltage pulse that was applied to the reactor containing a ground electrode made of titanium or stainless-steel. Positive voltage pulses were generated by a 6-stage Marx-Generator with a repetition rate of 20 Hz and applied to the high voltage electrode. Pulses are characterized by short rise times of about 20-30 ns, a peak voltage of 80 kV and an exponential decay resulting in pulse lengths (FWHM) of about 200-300 ns. **Reprinted from Publication P3**
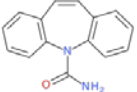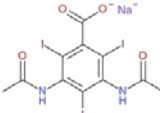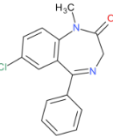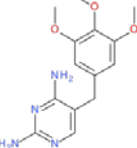
> Pulsed corona discharges generated directly in water are suitable for the treatment of recalcitrant pharmaceuticals. The plasma reactor was constructed modularly and by applying high voltage pulses of positive polarity, several luminous plasma filaments (streamer) were formed along a thin tungsten wire and propagated to a grounded metal mesh.

# Chapter 3

# Efficacy of Pulsed Corona Discharges (P2)

Efficacy and potential of pulsed corona discharges for water purification were evaluated with seven recalcitrant pharmaceuticals that were chosen as model substances. All compounds represent problematic substances for water purification technologies and a summary of their characteristics is given in Table 3. Pharmaceuticals were dissolved in a concentration of 0.5 mg/l to allow quantification via standard analytical methods.

**Table 3** Overview of investigated pharmaceuticals with their key characteristics and occurance in the environment.

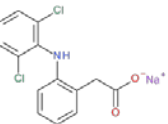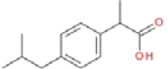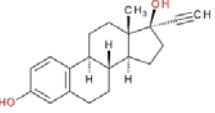| Pharmaceutical | Indication | Environmental concentrations | Remarks |
|---|---|---|---|
| Carbamazepine  | epilepsy, neuropathic pain | 0.258 µg/l – 6.3 µg/l [9, 11] | screening parameter [46, 47], hardly biologically degradable [48] |
| Diatrizoate  | X-ray contrast agent | 0.23 µg/l – 5.7 µg/l [49, 50] | resistant against $O_3$, $H_2O_2$, UV [50] |
| Diazepam  | anxiety, insomnia | 0.04 µg/l in STP-effluent [11] | hardly biologically degradable [51] |
| Diclofenac  | pain, inflammation, fever | 2.1 µg/l – 4.7 µg/l [11, 52] | hardly biologically degradable [53] |
| Ibuprofen  | pain, inflammation, fever | 3.4 µg/l in STP-effluent [11] | extensively used, screening parameter [47] |
| 17α-Ethinylestradiol  | contraceptive | 7.5 ng – 62 ng/l [12, 13] | environmental effects in very low concentrations [16] |
| Trimethoprim  | antibiotic | 0.2 µg/l – 0.66 µg/l in [54] | commonly used in aquacultures [55] |

## 3.1    Degradation of Recalcitrant Pharmaceuticals

Analytic separations were conducted by HPLC (Agilent 1200 Infinity Series, Agilent Technologies Santa Clara, CA) and concentrations before and after the treatment were quantified with a single quadrupole mass analyzer (Agilent series 6130).

The retrieval rate, R, is defined as the amount of unchanged analyte that could be recovered after the treatment. As summarized in Fig. 5, all pharmaceuticals showed a decrease in the retrieval rate when the applied discharges were doubled. Diclofenac and 17α-ethinylestradiol decomposed most readily (more than 97%) after the application of 80,000 discharges. Both pharmaceuticals are on the watch list of the European Union for harmful substances or substance groups that are monitored since March 2015. Ibuprofen, carbamazepine and trimethoprim decomposed at a three to four times slower rate. The concentration of diatrizoate was reduced by 45% and concentration of diazepam by 53%, thus both compounds were the most stable of the investigated substances. Notable is the degradation of the X-ray contrast agent diatrizoate, whose concentration was almost halved. In contrast, Ternes et al. reported only a 14% degradation for a suspension of diatrizoate when the pharmaceutical was subjected to an ozone treatment of 10 mg/l [50].
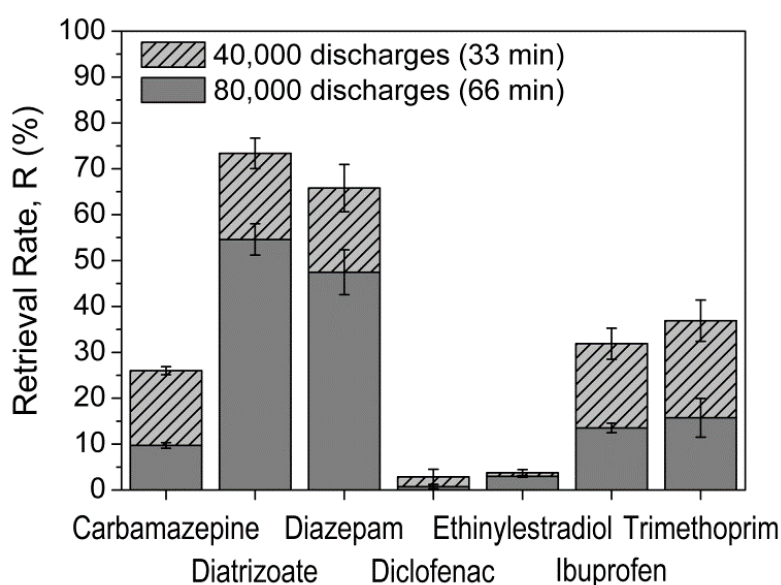


**Fig. 5** Different pharmaceuticals were dissolved at a concentration of 500 µg/l in water and treated with 40,000 or 80,000 discharges, corresponding to total treatment times of 33 min and 66 min, respectively. All experiments have been conducted at least in triplicates. **Reprinted from Publication P2**

The amount of electrical energy (kWh) required to reduce the concentration of a pollutant by one order of magnitude (90%) was in the range of 27-430 kWh/m³. Although the laboratory scale of the plasma reactor only serves as a proof-of-concept, and since the experimental setup was not optimized with respect to energy efficiency, energy consumption and degradation efficiencies are comparable to other water plasmas as depicted in Table 1 for methylene blue and phenol derivatives [35, 36].

For a more detailed study of operation costs and energy efficiencies, pilot installations will need to gather data on energy consumption and general long-term efficiencies, which is beyond the scope of this work. Nevertheless, from a fundamental point of view, it has been shown for the first time that pulsed corona discharges generated directly in water can effectively decompose even recalcitrant pharmaceuticals such as diatrizoate.

## 3.2    Water Quality after Plasma Treatment

Similar trends and characteristics were observed for all investigated pharmaceuticals with no adverse effects regarding water quality (Table 4). Whereas pH-value and liquid conductivity stayed almost constant, the most difference was observed for the amount of dissolved oxygen, which nearly doubled during the treatments.

**Table 4** Important water quality parameters before (Start) and after the application of 80,000 consecutive pulsed corona discharges (End). All experiments were repeated at least three times with results and errors determined as mean values and standard deviations, accordingly.

|  | pH-Value | | Conductivity (µS/cm) | | Dissolved oxygen (mg/l) | |
|---|---|---|---|---|---|---|
|  | Start | End | Start | End | Start | End |
| Carbamazepine | 6.4 ±0.1 | 6.4 ±0.1 | 30.4 ±0.5 | 42.3 ±2.2 | 4.9 ±0.1 | 10.1 ±0.3 |
| Diatrizoate | 7.1 ±0.3 | 6.6 ±0.2 | 29.0 ±0.0 | 44.3 ±1.0 | 5.9 ±0.4 | 11.0 ±0.8 |
| Diazepam | 6.7 ±0.2 | 6.3 ±0.0 | 30.7 ±0.8 | 43.3 ±1.1 | 4.5 ±0.0 | 9.4 ±0.6 |
| Diclofenac | 6.5 ±0.5 | 6.4 ±0.3 | 28.7 ±0.8 | 40.1 ±3.2 | 3.6 ±0.4 | 6.9 ±0.5 |
| Ethinylestradiol | 7.0 ±0.2 | 6.7 ±0.2 | 30.3 ±0.4 | 42.6 ±1.2 | 5.3 ±0.1 | 11.2 ±0.2 |
| Ibuprofen | 6.4 ±0.2 | 6.3 ±0.0 | 30.0 ±0.0 | 40.0 ±1.6 | 4.3 ±0.1 | 8.7 ±0.7 |
| Trimethoprim | 6.7 ±0.3 | 6.2 ±0.0 | 31.3 ±0.4 | 44.6 ±0.4 | 6.3 ±0.2 | 13.6 ±0.6 |

Moreover, corona discharges did not lead to a notable nitrification of the liquid as reported for plasmas above water [41, 42]. After 10,000 discharges, the concentrations of nitrate and nitrite increased to 0.51 mg/l and 0.35 mg/l, respectively. Consecutive treatments with up to 80,000 discharges only resulted in a small further increase of these values with final concentrations of 1.29 mg/l for nitrate and 0.39 mg/l for nitrite. Thus, with respect to the measured parameters and according to the German Drinking Water Ordinance, water quality following corona discharges is sufficient for drinking water.

> Pulsed corona discharges have been shown to effectively decompose recalcitrant pharmaceuticals. Some pharmaceuticals, such as diclofenac and 17α-ethinylestradiol decomposed readily when subjected to pulsed corona plasma while others, such as diatrizoate, have shown to be more recalcitrant. In case of selected water quality parameters, no adverse effects were observed.

# Chapter 4

# Plasma Chemistry and Catalytic Effects (P2 & P3)

Plasmas generated directly in water are known to have a variety of physical and chemical effects that can potentially be used for pollutant degradation and the killing of bacteria [21, 33, 56-58]. As depicted in Fig. 6, strong electric fields, ultraviolet radiations, shockwaves and, most importantly, chemical reactive species are generated by the plasma streamers [59].
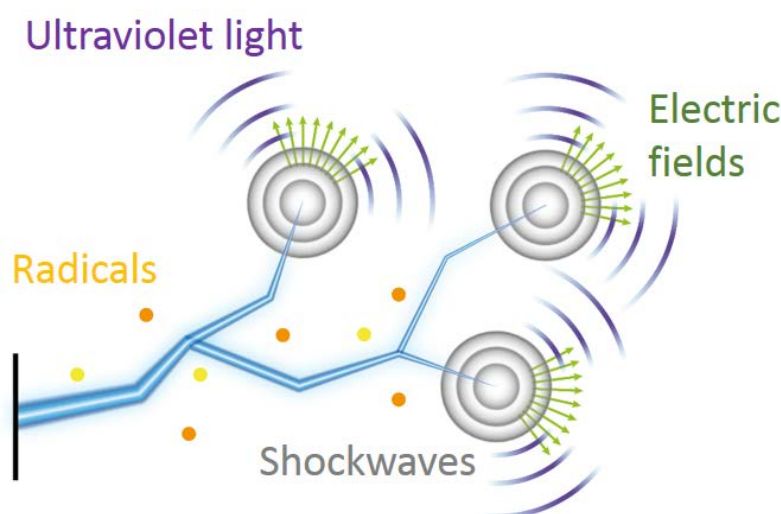


**Fig. 6** A single branching streamer propagating through the liquid is capable of producing strong electric fields, ultraviolet radiations, shockwaves and, chemical reactive species. ©**Graphic: C. Desjardins, modified by R. Banaschik**

Decomposition of organic compounds is primarily mediated by the formation of reactive species. In particular, plasmas in water can either interact with gas molecules dissolved in the liquid (nitrogen, oxygen) or the water molecules itself. Consequently, transient species, such as $^\bullet OH$, $HO_2^\bullet$, $^\bullet O_2^-$, $^\bullet NO_2$, $^\bullet NO$ and long-lived chemical products $O_3$, $H_2O_2$, $NO_3^-$ $NO_2^-$ can be formed. To investigate mechanisms of action that lead to the decomposition of pharmaceutical residues in pulsed corona discharges, it first must be known which radicals are primarily responsible for pollutant degradation.

## 4.1    Hydroxyl Radicals and the Formation of Hydrogen Peroxide

A first insight in plasma chemistry was gained by the measurement of hydrogen peroxide during the application of 80,000 discharges to pure water. The concentration of hydrogen peroxide ($H_2O_2$) was measured by a colorimetric assay containing a saturated solution of titanyl sulfate and 15% sulfuric acid [60]. After 80,000 consecutive discharges in pure water, $H_2O_2$ concentration reached values of about 100-120 mg/l.

As a more long-lived species, hydrogen peroxide is often considered a useful indicator for hydroxyl radicals in plasma systems, since OH-radical recombination is expected to be a major pathway for $H_2O_2$ generation in non-oxygenated solutions (Eq. (1)), followed by the pH-value dependent recombination of hydroperoxyl radicals in the presence of high levels of molecular oxygen ((Eq. (2) and (3)) [61].

$$\bullet OH + \bullet OH \rightarrow H_2O_2 \tag{1}$$

$$\bullet H + O_2 \rightarrow 2HO_2^\bullet \tag{2}$$

$$HO_2^\bullet + HO_2^\bullet \rightarrow H_2O_2 + O_2 \tag{3}$$
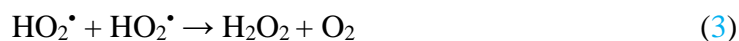
Hydroperoxyl radicals can be considered a conjugated acid (Eq. (4)) with a $po_{ke}$-value of 4.8 [62].

$$HO_2^\bullet + OH^- \rightleftharpoons \bullet O_2^- + H_2O \tag{4}$$

Roughly estimating the degree of dissociation with the Henderson–Hasselbalch equation reveals that during the degradation experiments with pH-values between 6.2 to 6.7, less than 5% of the superoxide existed in the protonated form $HO_2^\bullet$. Consequently, this makes an $H_2O_2$ formation due to $HO_2^\bullet$ recombination doubtful. Accordingly, it was assumed that hydroxyl radicals, with their strong oxidation potential and almost diffusion controlled reaction rates, might be the dominant species responsible for the degradation of the pharmaceuticals. However, since many different reactive species could also have formed during the treatment, further possibilities had to be explored.

## 4.2    Phenol as a Chemical Probe

The specific detection of reactive species in aqueous solutions proves to be rather challenging and time consuming, especially when a variety of reactive species can be present in the solution. Thus, a more reliable and consistent approach was the detection of reactive species, which evidently were not involved in reactions with the target compounds. For this purpose, phenol was used as a chemical probe.

Phenol has specific analytic advantages with a reaction chemistry that is understood in detail. Decomposition products can be easily detected by HPLC-MS and provide conclusions about the reactive species responsible for its degradation. Transient species, such as hydroxyl radicals, but also long-lived species, such as ozone, may lead to hydroxylated products, whereas reactive nitrogen species or chlorine form nitrated or chlorinated phenols [42].

Studies were conducted with aqueous solutions prepared from deionized water containing 500 mmol/l phenol. The solution conductivity was adjusted to at least 30 mS/cm with sodium chloride in a total treated volume of 300 ml. Altogether 80,000 discharges (treatment time 66 min) were applied to the reactor chamber containing a tungsten high voltage electrode and

a grounded metal mesh made of stainless steel. All analytics were carried out with the addition of 250 µl methanol to stop ongoing degradation reactions, which were observed even after the plasma was switched off.

The results of this study indicate that mainly hydroxylated decomposition products, such as benzoquinone (BQ), hydroxybenzoquinone (HBQ), catechol (CC), and hydroquinone (HQ), were formed during the plasma treatment Fig. 7.
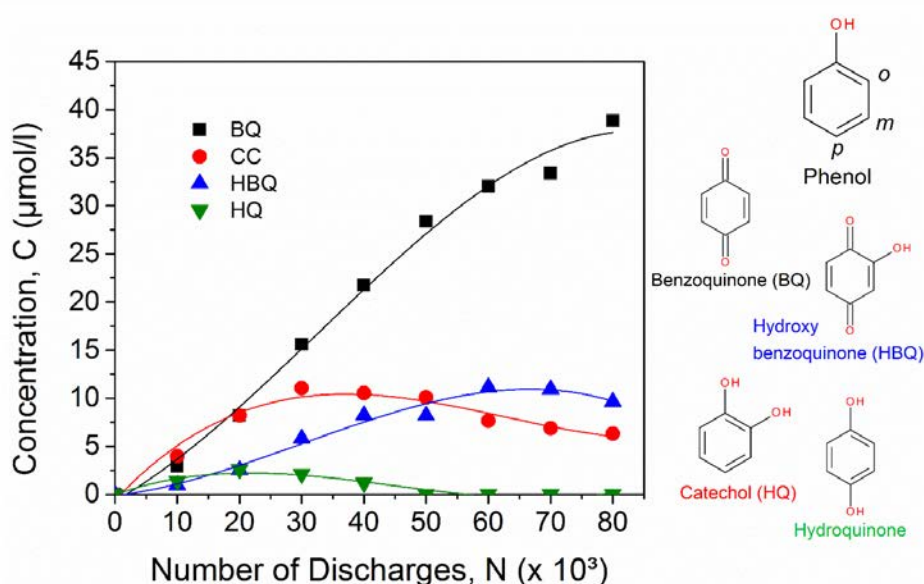


**Fig. 7** Formation of hydroxylated products of phenol during the application of 80,000 discharges. Reaction products identified by HPLC-MS are: benzoquinone (BQ), hydroxybenzoquinone (HBQ), catechol (CC), hydroquinone (HQ). **Reprinted from Publication P2**

Since no nitrated phenols or muconic acid was found, there was no evidence for chemical reactions involving reactive nitrogen species or ozone. For reactions with ozone, muconic acid is typically formed after the benzene ring cleavage [42]. Thus, hydroxyl radicals seem to be primarily responsible for phenol decomposition. In particular, hydroxyl radicals are regarded strong electrophiles, thus abstraction of hydrogen und further hydroxylation of the *ortho* and *para* position of phenol can be expected, since these C-atoms have relatively high electron densities and are stabilized due to resonance effects [63, 64].

## 4.3    How Ground Electrodes can affect Phenol Decomposition.

Due to an ongoing degradation chemistry, which was observed even after the plasma was switched off, samples had to be quickly mixed with methanol. Methanol acted as a scavenger for radicals that formed independently from the plasma and were presumably responsible for the ongoing degradation processes.

It is known that high voltage electrodes can suffer from erosive and corrosive processes when enveloped by a plasma [65]. Consequently it was first presumed that released metal ions from the tungsten high voltage electrode catalytically decomposed hydrogen peroxide to hydroxyl radicals via Fenton-chemistry [66]. However, compared to the size and surface of the high voltage electrode, the ground electrode often exceeds these dimensions. Corrosive processes at the ground electrode interface, therefore, might had conceivably affected overall bulk reaction chemistries and needed to be evaluated.

Subsequent phenol degradation experiments were conducted with different ground electrode materials made of either titanium (Ti008710/11, Goodfellow, Huntingdon, England) or stainless steel (AISI 316Ti). For the sake of simplicity, the stainless-steel electrode is hereinafter referred to as "iron electrode" or "iron mesh".

Samples of the continuously treated solution were taken in intervals every 10,000 discharges Fig. 8. Corrosion of the metal meshes was assessed by quantifying the amount of titanium and iron released into the solution with atomic absorption spectroscopy (AAS). In a volume of 300 ml, an amount of 0.31±0.01 mg titanium was found after plasma treatment, which corresponds to a titanium concentration of 1.02 mg/l. When the ground electrode was changed to the iron mesh, 0.41±0.09 mg of the metal was determined (1.35 mg/l) after treatment in subsequent experiments.
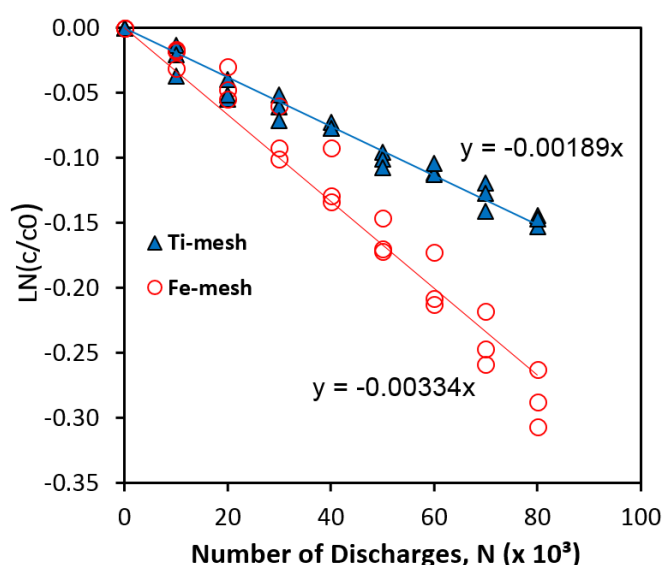


**Fig. 8**. Degradation of phenol for the continuous application of 80,000 discharges at 20 Hz. Different symbols reflect three independent experiments. Experiments were conducted with titanium (closed symbols) and stainless steel (open symbols) as ground electrode material. Linear fits of the half-logarithmic plot represent degradation rate constants of -0.00189 and -0.00334 (1/1000 pulses) for either the titanium or the iron mesh. Starting concentration of phenol was 500 µM, treated volume: 300 ml. **Reprinted from Publication P3**

Decomposition of phenol was again accompanied by the formation of several hydroxylated products. Nevertheless, absolute concentrations for titanium electrodes were lower when compared to iron electrodes (Fig. 9).

For titanium ground electrodes, phenol concentration decreased by 13.8% (69 µmol/l), whereas 24.8% (124 µmol/l) of the phenol was decomposed using iron electrodes. Notable is a slight exponential increase in the formation of 1,4-benzoquinone for the iron mesh. The differences became distinct after the application of 20,000 discharges. Presumably had the continuous release of electrode material an increasing effect on phenol decomposition.
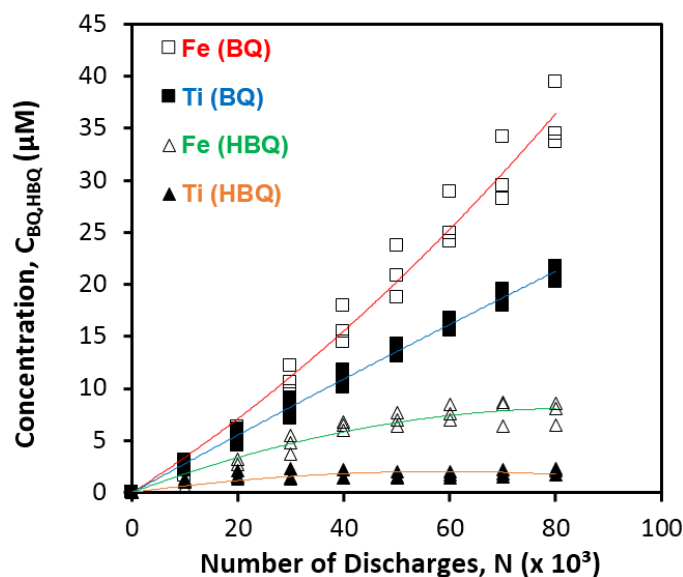


**Fig. 9** Effect of ground electrode material (titanium, iron) on 1,4-benzoquinone (BQ) and hydroxy-1,4-benzoquinone (HBQ) formation after treatment with pulsed corona discharges. Starting concentration of phenol was 500 µM, treated volume: 300 ml. Different symbols reflect three independent experiments. Experiments were conducted with titanium (closed symbols) and iron (open symbols) as ground electrode material. **Reprinted from Publication P3**

Taking energy consumption into account, degradation efficiencies were calculated to be 68.4 mg/kWh for titanium electrodes and 119.6 mg/kWh for iron electrodes, which is an efficiency increase by three quarters (74.9%), presumably mediated by metal ions released in the bulk liquid.

## 4.4    Catalytic chemistry promoted by ground electrode materials

While hydroxyl radicals are rather short-lived, their recombination product hydrogen peroxide is more stable and can be seen as an intermittent storage for OH-radicals that are not consumed in other chemical reactions (Eq. (1)). Hydrogen peroxide can diffuse into the bulk liquid. During phenol degradation experiments concentrations of about 2.5 mmol/l were reached with yields of 1.08 g/kWh for titanium and 1.04 g/kWh for iron ground electrodes (Fig. 10).
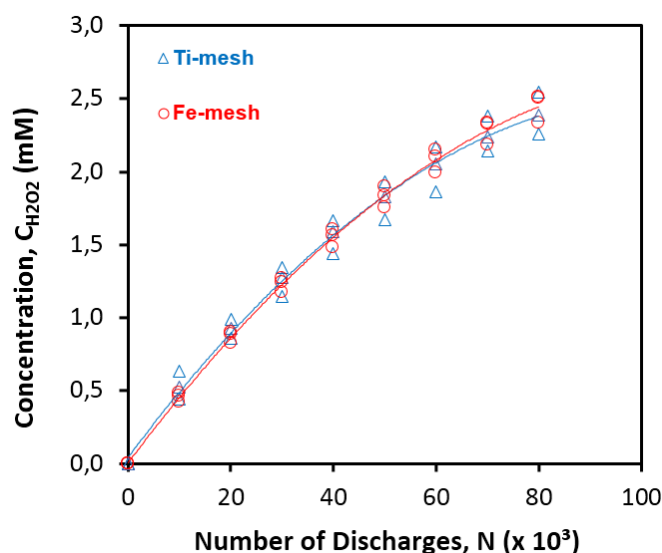
**Fig. 10** Formation of hydrogen peroxide after application of 80,000 discharges as a function of different electrode materials. Different symbols reflect three independent sets of measurements. The measurements were conducted with titanium (triangles) and iron (circles) as ground electrode materials. Concentrations reached a maximum of about 2.4±0.1 mmol/l (titanium) and 2.45±0.1 mmol/l (iron). **Reprinted from Publication P3**

Concentrations and achieved yields of $H_2O_2$ during experiments are so similar that it is doubtful that observed differences in phenol decomposition can be explained by either energy input or hydrogen peroxide production alone. Metal ions, however, can induce a decomposition of $H_2O_2$ into OH-radicals via Fenton chemistry as exemplary shown for $Fe^{2+}$ ions in Eq. (5).

$$Fe^{2+} + H_2O_2 \rightarrow Fe^{3+} + {}^\bullet OH + OH^- \tag{5}$$
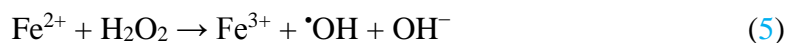
With increasing concentrations of $H_2O_2$ due to a prolonged treatment, hydrogen peroxide also acts as a hydroxyl radical scavenger forming superoxide anion radicals, which then can start a catalytic cycle (Eq. 6 and 7).

$$ {}^\bullet OH + H_2O_2 \rightarrow H_2O + {}^\bullet O_2{}^- + H^+ \tag{6}$$

$$Fe^{3+} + {}^\bullet O_2{}^- \rightarrow Fe^{2+} + O_2 \tag{7}$$
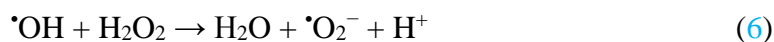
Although the cycle can be started by $Ti^{3+}$ ions as well as by $Fe^{2+}$ ions, the reverse reaction i.e. the reduction of the oxidized metal ion is primarily mediated by $Fe^{3+}$ ions. Titanium ions ($Ti^{4+}$) are rather small, have a high charge density and will easily react with water molecules. The formed titanium oxo precipitations are only dissolvable in water under high acidic conditions [67]. It has been shown that these precipitations neither release reduced titanium ions ($Ti^{3+}$) nor can decompose hydrogen peroxide to form free OH-radicals [68]. As a consequence, the catalytic cycle is disrupted.

Furthermore, phenol byproducts may also induce additional reactions with iron ions, since $Fe^{3+}$ ions can be reduced by dihydroxybenzenes [69]. In the case of *para*-hydroxybenzene, the hydroquinone – benzoquinone equilibrium is shifted to the benzoquinone form (Fig. 11) with an inherent regeneration of $Fe^{2+}$-ions, which then further facilitate the generation of hydroxyl radicals by subsequent Fenton-cycles.
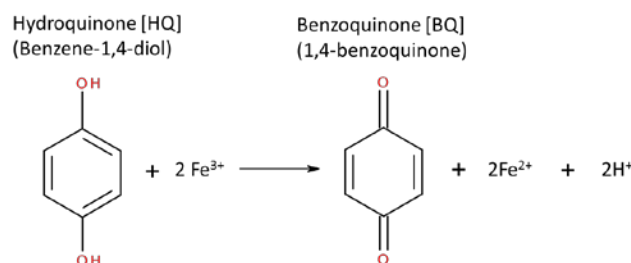


**Fig. 11**. The reaction of hydroquinone with iron ions released from the iron mesh is shifting the reaction equilibrium to the benzoquinone form. **Reprinted from Publication P3**

An increased releases of hydroxyl radicals in the bulk liquid does also explain why the formation of benzoquinone (BQ) increases exponentially when iron ground electrodes were used (Fig. 9). Considering Fenton-chemistry as a source of increased phenol decomposition leads to the conclusion that about 69 µmol/l phenol was decomposed when using a titanium ground electrode and 124 µmol/l when using an iron electrode. Thus, when normalized to the titanium mesh, about 80% (55 µmol/l) of the increased phenol degradation was not caused by direct plasma - phenol interactions (streamer channels), but by secondary reactions in the bulk liquid when OH-radicals were formed from $H_2O_2$ decomposition.

## 4.5     Mechanisms of ground electrode corrosion

Plasmas in liquids are generally associated with high voltage electrode corrosion because of the generation of reactive species, intensive heat and direct electro-physical and electro-chemical processes at the electrode [70-72]. However, ground electrodes in pulsed corona discharges are not directly subjected to the plasma and there are no obvious reasons why they should suffer from such corrosive processes as observed during experiments (Fig. 12).

As a reasonable initial assumption, hydrogen peroxide was suspected to be responsible for ground electrode corrosion, but the hypothesis was discarded after sham experiments with aqueous solutions of 3 mmol/l hydrogen peroxide did not lead to any observable corrosion of the mesh electrodes at all. Further experiments with iron ground electrodes revealed that thermal damage by the plasma was also negligible since propagating streamers were not long enough to reach the grounded electrodes. Nevertheless, the effect of streamer length was evaluated in successive experiments by suppressing streamer propagation with increased solution conductivities and increased high voltage electrode diameter. Although streamer did stop far short of the metal mesh, comparable amounts of iron were found with otherwise the same operating parameters as used during phenol degradation experiments.
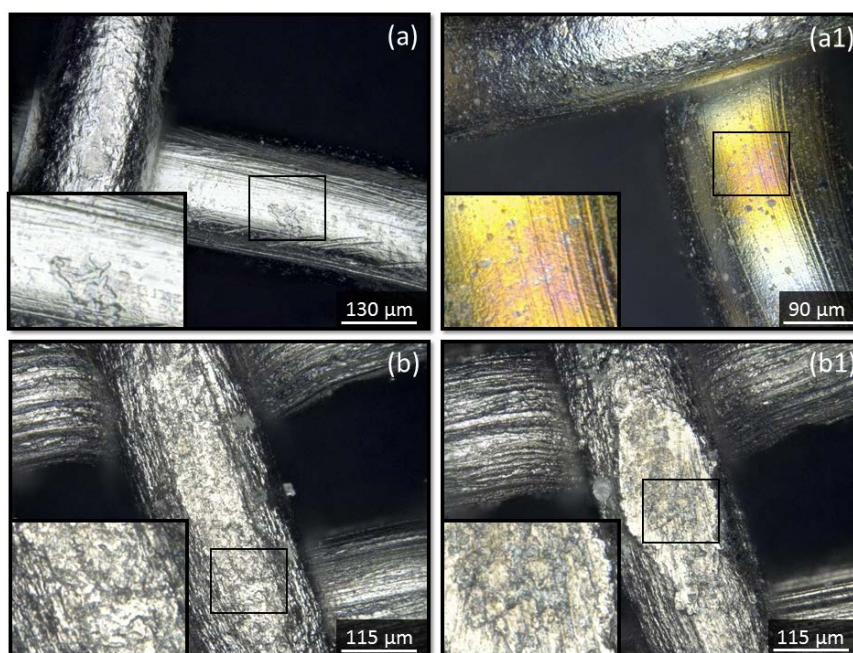
**Fig. 12** Images of the iron (a) and titanium (b) ground electrode before the application of 80,000 discharges. After treatment, small, randomized spots of discoloration and changes in surface structure were visible for iron (a1) and titanium (b1) ground electrodes. **Reprinted from Publication P3**

Plasma formation was then suppressed completely with a 0.2 mm diameter wire as high voltage electrode and a liquid conductivity of 400 µS/cm by adding sodium chloride. In this case, a monopolar current pulse of about 100 ns (FWHM) with a peak current of about 500 A was applied (Fig. 13). Corrosion of the ground electrode was observed after an application of 80,000 pulses. The net charge transferred for pulsed electric field (PEF) treatment ($2.83 \times 10^{-5}$ C) was even a little higher than those observed for plasma generation ($2.55 \times 10^{-5}$ C). Thus, it was unexpectedly found that the current between the electrodes i.e. charge transferred, was responsible for the corrosive processes, regardless of the extent of plasma that was generated.
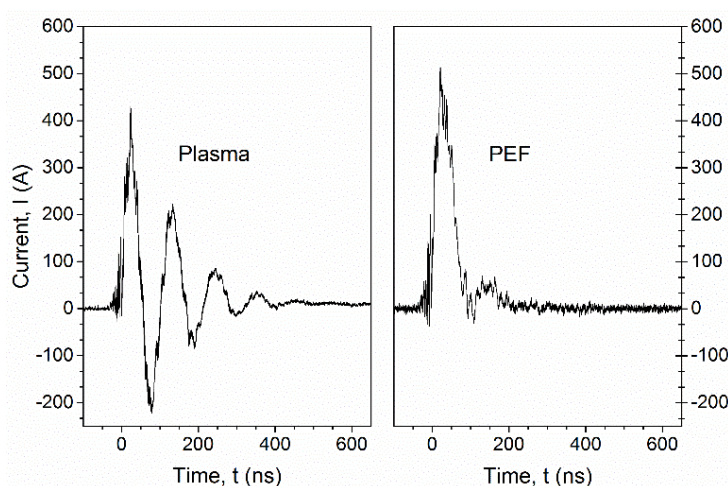


**Fig. 13** Current pulses after plasma and pulsed electric field (PEF) treatment. Diameter of the high voltage electrode was 0.2 mm. In case of PEF-treatment, solution conductivity had to be increased to 400 µS/cm to suppress plasma generation. **Reprinted from Publication P3**

From an electrochemical point of view, when pulses of positive polarity are applied to the high voltage tungsten wire electrode (anode), the ground electrode serves as a cathode and should therefore not suffer from electrochemical corrosion [73].

However, differences in electrolytic processes during the application of short high voltage pulses (300 ns) have been described recently. Electrolysis in such a system takes place with a mechanism dominated by electron transfer and electrons are emitted from the cathode metal directly into the electrolyte [74, 75]. It seems plausible that positively charged metal ions can go in solution when the ground electrode suffers from a fast and substantial emission of electrons into the liquid. According to this proposed assumption, the amount of charge, $Q$, transferred in a typical applied high voltage pulse was multiplied with the number of pulses applied, $x_{Pulse}$ (80,000). In the case of iron ground electrodes, about 31.1 µC were transferred during the treatment. When divided by the elementary electrical charge, $e$, the total number of electrons possibly emitted from the cathode is obtained. Iron ions are mostly present as ferrous ($Fe^{2+}$) or ferric ($Fe^{3+}$) ions, thus two or three electrons can be withdrawn from elemental iron. With the Avogadro constant, $N_A$, and the molar mass of the metal, $M_{metal}$, the amount of possible corrosion can be calculated and compared with the AAS measurements (Eq. (8)).

$$C_{metal} = \frac{Q \times M_{metal}}{e \times z_{ion} \times N_A} \times x_{Pulse} \tag{8}$$

Despite a lack of detail, for example not taking the electrode composition into account, the calculated values for metal that can be theoretically released from the ground electrode, agreed well with the measurements shown in Table 5.

**Table 5** Comparison of electrode corrosion after the application of 80,000 high voltage pulses. Experimental data was obtained from atomic absorption spectroscopy (AAS). According to Eq. (8), theoretical electrode corrosion (release of metal) was calculated for different ion charges ($z_{ion}$). **Reprinted from Publication P3**

| **THEORETICAL ERROSION DUE TO CHARGE TRANSFER** | | | | | **EXPERIMENT** |
|---|---|---|---|---|---|
| **ERROSION** | Charge transferred | $M^{2+}$ ($z_{ion}$) | $M^{3+}$ ($z_{ion}$) | $M^{4+}$ ($z_{ion}$) | AAS (mean) |
| | **in µC** | **in mg** | **in mg** | **in mg** | **in mg** |
| **TITANIUM** | 32.5 | 0.64 | 0.43 | 0.32 | 0.31 ±0.01 |
| **IRON** | 31.1 | 0.72 | 0.48 | - | 0.41 ±0.09 |

Phenol was applied as a chemical probe to provide first insights into plasma chemistry and hydroxyl radicals seem to be primarily responsible for the degradation of recalcitrant compounds the formation of hydrogen peroxide. It was further found that corrosion of the grounded metal meshes can substantially affected decomposition efficiency of target pollutants. It appeared that electrode corrosion is not mediated by the plasma itself, but mediated by the net charge transfer that corresponds to the applied pulsed electric fields.

# Chapter 5

# Degradation Chemistry of Recalcitrant Compounds (P3 & P4)

Pulsed corona discharges generated directly in water have been demonstrated to effectively decompose organic compounds and recalcitrant pharmaceuticals. The underlying principle is the generation of reactive species, which then degrade dissolved pollutants. The generation of hydroxyl radicals ($^\bullet$OH) is of special interest due to their high oxidizing potential. Hydroxyl radicals are presumably formed in the plasma channels or close to the plasma-liquid boundary [76, 77] and can either react with the target pollutants or recombine to hydrogen peroxide. Hydrogen peroxide herby acts as a storage for hydroxyl radicals not consumed in reactions with target pollutants and can be spilt to hydroxyl radicals again. Depending, especially on ground electrode materials, indirect degradation through the assumed splitting of hydrogen peroxide (Fenton chemistry) can overlap and exceed degradation induced by plasma formation directly. Since hydroxyl radicals seems to be primarily responsible for pollutant degradation, they should be clearly detectable in the bulk liquid. Degradation pathways of recalcitrant pharmaceuticals should reflect this. However, for pharmaceutical residues, degradation pathways and mechanisms of action, as well as associated risks, have not yet been investigated.

## 5.1    Detection of Hydroxyl Radicals for Sub-Microsecond Pulsed Corona Discharges

In a first attempt, the light emitted by the excited species formed in the plasma was collected with an optical fiber immersed into the water during plasma generation. For pulsed electrical discharges that are generated in liquids with microsecond high voltage pulses, prominent emissions of the OH radical are in the range of $\lambda = 306.4 - 314$ nm [78, 79].

The emission from atomic hydrogen Balmer series ($H_\alpha$), as well as emission lines that are associated with metals ions were observed independently of the ground electrode material. However, emissions of excited hydroxyl radicals were not observed. As stated in the scientific literature, detection of excited $^\bullet$OH depends on configurations and plasma generation schemes, as well as on diagnostic setups. Whereas OH-lines are often found for corona discharges that are generated with longer (microsecond) high voltage pulses [59, 79-81], they are often absent for plasmas generated with pulses in the range of nanoseconds [82, 83]. For a better understanding of the underlying processes, more detailed studies are necessary. However, it can be concluded so far that plasma generation with sub-microsecond high voltage pulses provide an environment that is not conducive for the detection of OH-radicals via optical emission spectroscopy.

A more promising approach for the detection of free radicals in plasma treated solution was conducted by spin trap enhanced electron paramagnetic resonance spectroscopy (EPR). The spin trap 5-*ter*t-butoxycarbonyl-5-methyl-1-pyrroline-*N*-oxide (BMPO) also had the inherent advantage to distinguish between formed hydroxyl radicals and superoxide anion radicals [84]. Both radicals were detected with concentrations in the µmol/l-range from their respective BMPO-adducts. The $^\bullet$OH adduct was almost immediately observed, whereas the $^\bullet$O$_2^-$ adduct was detected about 38 minutes after the start of the treatment (Fig. 14).
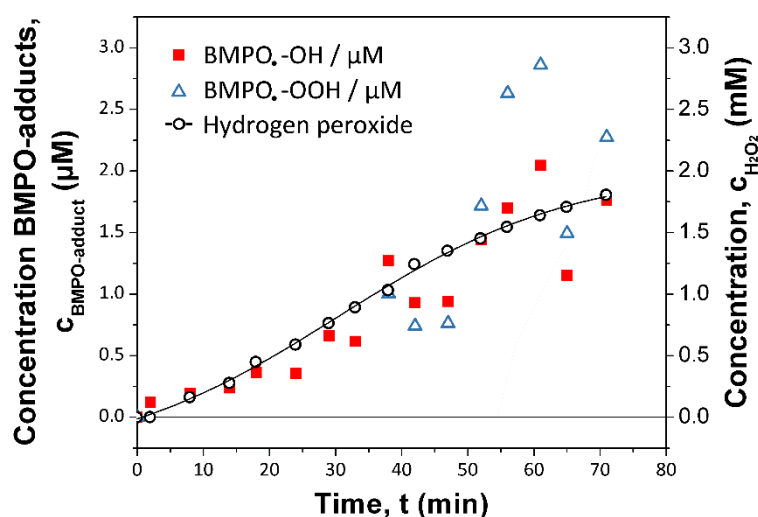


**Fig. 14** Formation of $^\bullet$OH and $^\bullet$O$_2^-$ spin trap adducts and hydrogen peroxide (-) during plasma treatment. Initial concentration of BMPO was 10 mmol/l. **Reprinted from Publication P4**

The spin trap efficacy for $^\bullet$O$_2^-$ trapping is about 90% [85] and for $^\bullet$OH about 0.6% [86]. Responsible for the small trapping efficacy for $^\bullet$OH is the high reactivity of the radical with almost every molecule in its vicinity before it is caught by the spin trap. In multi species systems, such as plasmas, effective trapping efficacies for OH-radicals might be even lower. In fact can the concentration measured with the BMPO-adduct considered an estimation for OH-radicals that are available in the bulk, whereas a considerable part of the OH-radicals almost instantaneously recombine to hydrogen peroxide and is not available for pollutant degradation anymore.

Concentration of radicals available for pollutant degradation were estimated to be in the range of at least 300 µmol/l for $^\bullet$OH and 2.5 µmol/l for $^\bullet$O$_2^-$ after 70 min of plasma treatment. In accordance to the conducted experiments with different ground electrode materials, the time delayed detection of $^\bullet$O$_2^-$ suggest the formation of $^\bullet$O$_2^-$ due to secondary reactions in the bulk liquid (Fig. 15). About 1.8 mmol/l hydrogen peroxide was formed during the experiment, which equals 3.6 mmol/l $^\bullet$OH. By comparing the mass balances, this implies that hydroxyl radicals were at least generated in a 10-fold higher concentration than described by the spin-trap measurements. In this concentrations, hydrogen peroxide can also act as a radical scavenger, forming the observed superoxide anion radical (Eq. (9)).

$$^\bullet OH + H_2O_2 \rightarrow H_2O + {}^\bullet O_2^- + H^+ \tag{9}$$

The start of subsequent Fenton-cycles and the generation of hydroxyl radicals diffusely in the bulk hereby acts in a supportive way for the degradation of the target pollutants.



**Fig. 15** Formation and evolution of hydroxyl radicals ($^\bullet$OH) during application of pulsed corona plasma. Plasma generated hydroxyl radicals can react with organic pollutants or recombine to form hydrogen peroxide. Metal ions ($Me^{red}$/$Me^{ox}$), released by electrode corrosion, can catalytically decompose hydrogen peroxide providing hydroxyl radicals again. Hydrogen peroxide can further act as $^\bullet$OH scavenger and form the superoxide anion radical ($^\bullet O_2^-$). **Reprinted from Publication P4**

## 5.2   Degradation Pathways of the Pharmaceutical Diclofenac

It has been shown that pulsed corona discharges generated in water are an efficient means to generate hydroxyl radicals. Plasma chemistry mediated by pulsed corona discharges thereby share some similarities with traditional Fenton-chemistry. However, only absolute degradation was measured, but degradation pathways and mechanisms of actions were not discussed. For a detailed understanding of reaction mechanism responsible for pollutant degradation, diclofenac was chosen as model substance, since it is on the watch list of the European Commission (Water Framework Directive). Oxidation by OH-radicals seems to be the most interesting process; thus, plasma degradation was compared with an alternative production of $^\bullet$OH-radicals by Fenton-chemistry.

    With both methods diclofenac was readily decomposed. In the case where hydroxyl radicals were formed by Fenton-chemistry, the decomposition of diclofenac (initial concentration of 0.5 mmol/l) followed an exponential decay and was associated with the ongoing consumption of hydrogen peroxide (Fig. 16).
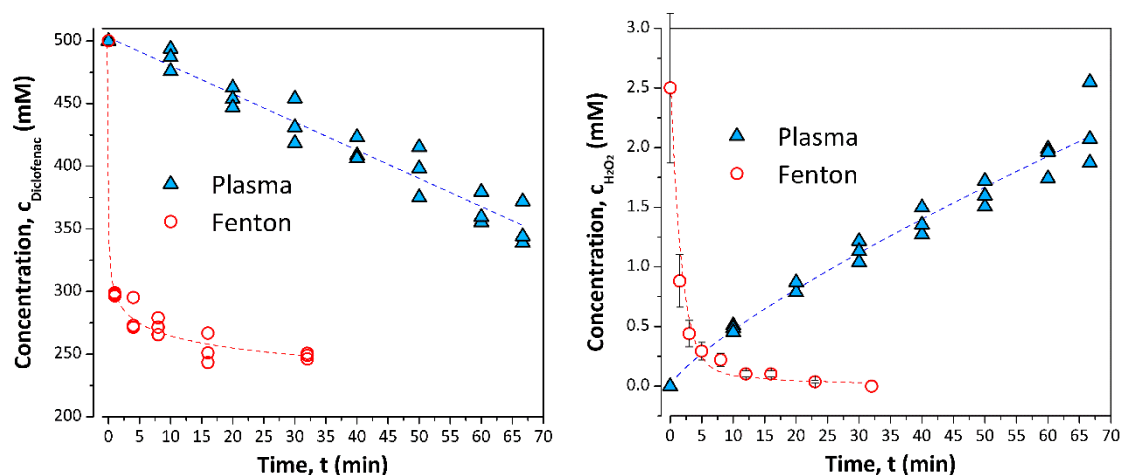
**Fig. 16** On the left: Decomposition of diclofenac by pulsed corona plasma (solid triangles) or by the generation of OH-radicals initiated with 2.5 mmol/l $H_2O_2$ and 0.75 mmol/l iron(II) chloride (open circles). On the right: Hydrogen peroxide concentrations for plasma treatment (solid triangles), or for $^\bullet$OH-chemistry with an initial admixture of 2.5 mmol/l together with 0.75 mmol/l iron(II) chloride (open circles). **Reprinted from Publication P4**

After about 32 minutes, hydrogen peroxide was consumed completely with 50% of the diclofenac being decomposed. For the plasma treatment, however, hydroxyl radicals were continuously generated and hydrogen peroxide concentrations increased to about 1.13 mmol/l after 30 min and 2.2 mmol/l after 67 min. Assuming an ongoing linear decomposition kinetic, degradation of 50% diclofenac would have been achieved after about 113 min (135.600 plasma discharges).

After either treatment, samples were pretreated by solid phase extraction (SPE) and analyzed by gas chromatographic (GC) methods. With this method, about 60 different chemical compounds were identified, whereas 21 chemical compounds could be related directly with the diclofenac degradation. Similar to previous studies in which phenol was used as a chemical probe, no evidence was found for chemistry involving reactive chlorine, ozone or peroxynitrites. Moreover, observed intermediates for the degradation of diclofenac by plasma treatment (P) or by Fenton-processes (F) were almost similar when compared among the experiments and with the literature data (Fig. 17).

Degradation of diclofenac is predominantly characterized by four reaction steps (**I-IV**), whereas an attack of the benzene rings is probably one of the key starting reactions [87-89]. In the diclofenac molecule, the most reactive C-atoms are expected at the 4 and 4' position of the two phenyl rings, since radicals would best be stabilized due to resonance effects. Hydroxyl radials can first abstract a hydrogen atom from carbon and a second $^\bullet$OH can combine with the carbon based radical. Cleavage of the C-N bond (**II**) results in several characteristic byproducts (**D5**-**D10**). Further hydroxylation (**III**) and dechlorination (**D11**-**D16**), leads to cleavage of the benzene ring structure (**IV**) and the formation of small organic acids (**D17**-**D21**).
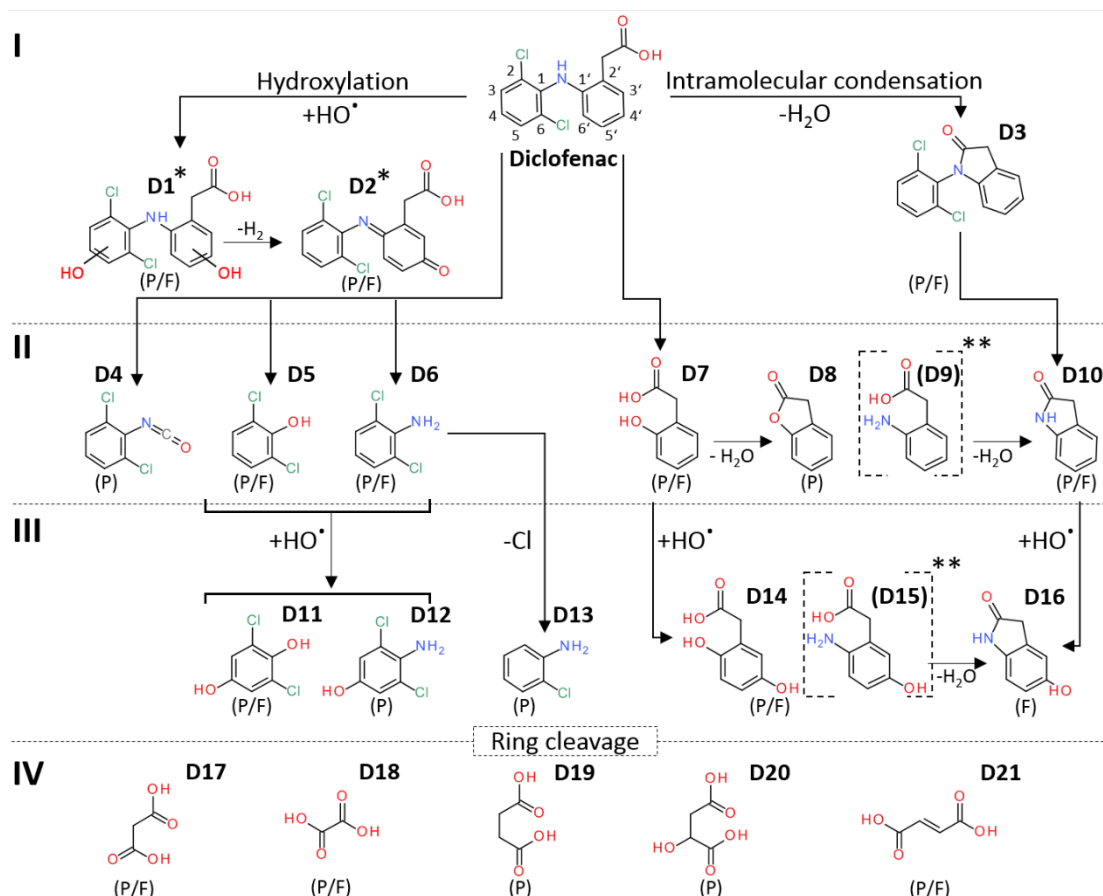
* Products were identified due to their molecular mass, physicochemical properties and description in literature
** Intermediate was not detected

**Fig. 17** Proposed degradation pathway and intermediates for the degradation of diclofenac by hydroxyl radicals formed during plasma treatment (P) or due to hydroxyl radicals generated by Fenton-processes (F). Apart from intermediates D9 and D15, all other byproducts were experimentally identified and verified. **Reprinted from Publication P4**

## 5.3 Degradation Chemistry of Recalcitrant Pharmaceuticals

Hydroxyl radicals can predominantly react with target pollutants by abstraction of hydrogen atoms (Eq. (10)) or electrophilic addition to unsaturated bonds (Eq. (11)). Because of steric hindrance, or if reactions described above are disfavored by multiple halogen substitutes, also electron transfers (Eq. (12)) can occur [44].

$$^{\bullet}OH + RH \rightarrow {}^{\bullet}R + H_2O \qquad (10)$$

$$^{\bullet}OH + R_2C{=}CR_2 \rightarrow {}^{\bullet}R_2C\text{-}CR_2(OH) \qquad (11)$$

$$^{\bullet}OH + RX \rightarrow {}^{\bullet}RX^+ + OH^- \qquad (12)$$

It has been shown during experiments that pharmaceuticals can be classified in distinctly different reactivity groups. Some pharmaceuticals decomposed readily when subjected to pulsed corona plasma while others, such as diatrizoate, have shown to be more recalcitrant. (Fig. 18).
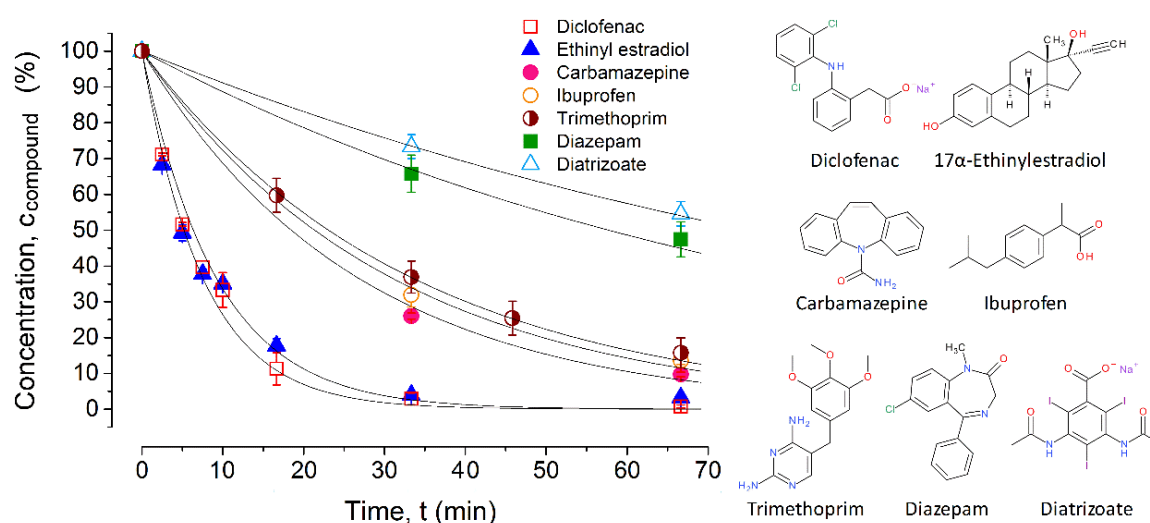


Fig. 18 Degradation of pharmaceuticals that were treated in individual experiments for an initial concentration in water of 0.5 mg/l with pulsed corona plasma. The plasma was instigated with a frequency of 20 Hz and a treatment with 80,000 consecutive discharges, hence, corresponding to a treatment time of 67 min. **Reprinted from Publication P4**

In diatrizoate, all reactive C-atoms are blocked by functional groups and abstraction of hydrogen atoms is hindered. Moreover, some functional groups withdraw electrons from the aromatic ring system. When compared to diclofenac or 17α-ethinylestradiol, electron density in the aromatic ring system is considerably lower due to inductive effects (-*I* effect, iodine) and resonance effects (-*M*, carbonyl group). As shown in Table 6, this is also reflected by the reaction rate constants of OH-radicals with the pharmaceuticals.

**Table 6** Reaction rate constants of OH radicals with investigated pharmaceutical residues. Starting with diclofenac, pharmaceuticals are sorted by their response to the plasma treatment as shown in Fig. 18. **Reprinted from Publication P4**

| Pharmaceutical | reaction rate constants ($k_{OH}$ in $10^9\,M^{-1}\,s^{-1}$) | Reference |
|---|---|---|
| Diclofenac | $9.29 \pm 0.11$ | [90] |
| 17α-Ethinylestradiol | $9.8 \pm 1.2$ | [91] |
| Carbamazepine | $8.8 \pm 1.2$ | [91] |
| Ibuprofen | $7.4 \pm 1.2$ | [91] |
| Trimethoprim | $8.66$ | [92] |
| Diazepam | $7.2 \pm 1$ | [91] |
| Diatrizoate | $0.96 \pm 0.02$ | [93] |

Carbamazepine, ibuprofen, trimethoprim and diazepam have approximately the same reaction rate constants. Consequently, their response to plasma treatment was found to be between diclofenac/17α-ethinylestradiol and diatrizoate. In summary, molecular reactivity towards the

plasma treatment is increased by aromatic ring systems, unsaturated bonds and electron donating functional groups ($+I/+M$).

## 5.4    Possible Hazardous Byproducts formed during Plasma Treatment

Plasma degradation of compounds, such as pharmaceuticals residues, can be subjected to risks associated with the formed byproducts. As shown for the diclofenac degradation experiments, the formation of phenol derivatives can be expected when chemical compounds contain aromatic rings, which are common in many pharmaceuticals. Phenols and their derivatives are well-known for their bio-recalcitrance and acute toxicity [94].

The Globally Harmonized System of Classification and Labelling of Chemicals (GHS), classifies diclofenac as "harmful to aquatic life with long lasting effects" (H412, category 3). This category is exceeded by the decomposition products 2,6-dichlorophenol (**D5**) and 2,6-dichloroaniline **(D6),** which are classified as category 2 (H411) and category 1 (H400/H410), respectively [95]. Chemical compounds in category 2 are considered "toxic to aquatic life with long-lasting effects", whereas category 1 is considered "very toxic to aquatic life with long lasting effects".

Thus, for sewage water with high loads of pharmaceuticals there is the inherent risk of generating chemical compounds that are even more toxic than the targeted substances. However, it has to be noted that the risk is not limited to plasma but is common to all AOPs that rely on the generation of OH-radicals and can be addressed with a sufficiently long or intense treatment as it was shown for step **IV** during diclofenac decomposition.

It should be mentioned that the release of metal ions, especially iron ions, might have undesirable effects in terms of water quality. However, dissolved iron occurs naturally in water and does not present a danger to human health or the environment in general. Iron can be present in groundwater or can occur due to the corrosion of iron pipes. Higher concentrations of iron result in a rust color of water and a metallic taste and thus, the water might be unpleasant for consumption. In raw fresh water, the iron concentration is usually on the order of less than 50 mg/l. Several methods for iron removal, such as oxidation and filtration or electro-coagulation are possible and already used in water treatment facilities [96]

> In contrast to initial assumptions, degradation processes cannot be described as a straight forward process. Secondary reactions due to the decomposition of hydrogen peroxide can considerably contribute to degradation processes. Degradation efficiency is increased by aromatic rings, unsaturated bonds and electron donating functional groups. However, if sewage water with high loads of pharmaceutical residues is treated with purification techniques that rely on the generation of OH-radicals, there is the inherent risk of generating toxic byproducts. Accordingly, treatment times must be increased.

# Chapter 6

# Potential for Water Disinfection (P5)

Apart from their capability to degrade recalcitrant organic pollutants, plasma generated in water can also be applied for the killing of microorganisms persisting in pipes, water tanks, or cooling systems. Of special interest is the eradication of *Legionella sp.,* which are Gram-negative bacteria and associated with severe infections [97]. The prevalence of this microorganism is of growing concern and efficient disinfection systems are needed to reduce *Legionella* species in water containing environments [98]. Physical and chemical disinfection methods, such as thermal treatment, copper/silver ionization, UV-light or hyperchlorination have been described, but are known to be not free from disadvantages [99].

Motivated by this circumstance, alternative disinfection methods have to be developed. As demonstrated by recent studies, pulsed electric fields (PEF) and pulsed corona plasma have already proved to be effective, bio-compatible and environmental friendly [58]. While PEF are generally effective, the combination with plasma might have an added advantage. Of particular scientific interest is the role of the pulsed electric field in comparison to the effects mediated by the plasma itself.

## 6.1 Differences in the Antimicrobial Mode of Action between Plasma and Pulsed Electric Fields

The experimental setup described in this study is capable of generating either a pulsed corona plasma by applying a high voltage pulse of positive polarity, or of providing a pulsed electrical field by using negative polarity. In a coaxial discharge system, a strong electric field is found in both cases close to the high voltage electrode (wire). With high voltage pulses of positive polarity, the strong electric field at the wire will promote the initiation of a plasma-channel with electrons moving along this channel in an avalanche process towards the anode. Since electrons are moving much faster than ions, a positive space charge is left behind at the streamer head. The space charge enhances the strength of the electrical field in front of the streamer head and further electrons are attracted towards the high-voltage electrode [100]. Plasma filaments formed this way are longer and more fractured in appearance when compared to streamers that are obtained for negative high voltages pulses [101].

For negative polarity pulses and higher solution conductivity, at least for the experimental setup described in this work, plasma formation is almost completely suppressed, while pulses with positive polarity would still form a plasma. In the following experiments, parameters, such as peak voltage, energy input and strength of the electric field were kept constant, but polarity of the power source was changed. This allowed a comparative study on the effectiveness and differences in killing mechanisms of both methods.

Suspensions of *Legionella pneumophila* were individually exposed to both treatment methods for 25 min and bacterial survival was determined. As depicted in (Fig. 19), the treatment with pulsed corona plasma for 12.5 min resulted in a complete inactivation of *Legionella* and no viable bacteria were detected after 25 min.
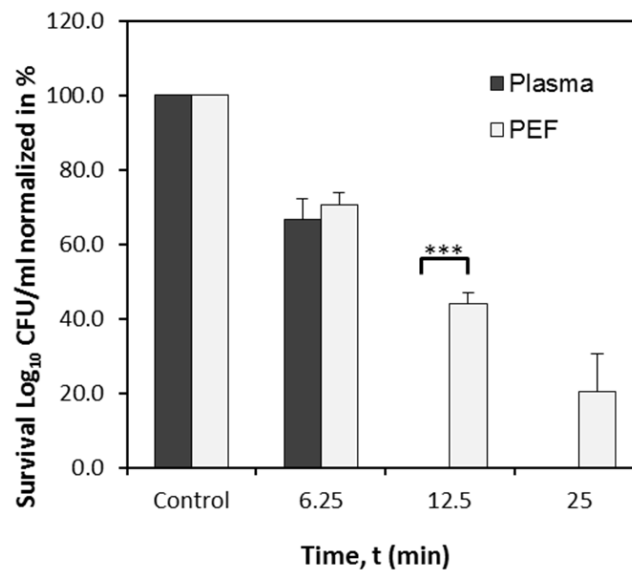


**Fig. 19** Treatment of Legionella suspensions with pulsed corona plasma and PEF. Each bar represents the mean of three independent experiments with standard deviation (n=3). Detection limit: 10 CFU/ml.

Applying the same pulse energy with negative polarity, thus pulsed electric fields only, resulted in a decrease of approximately log 2 after 12.5 min. Almost log 1 of *Legionella* survived this experiment after a treatment time of 25 min.

Scanning electron microscopy (Fig. 20) revealed severe damage to the *Legionella* for both treatment methods when compared to untreated bacteria. However, for increasing treatment times, ruptured cells observed post-exposure to PEF were substantially lower when compared with cells after plasma treatment. In addition, longer plasma treatment times encouraged the formation of plaque-like structures.
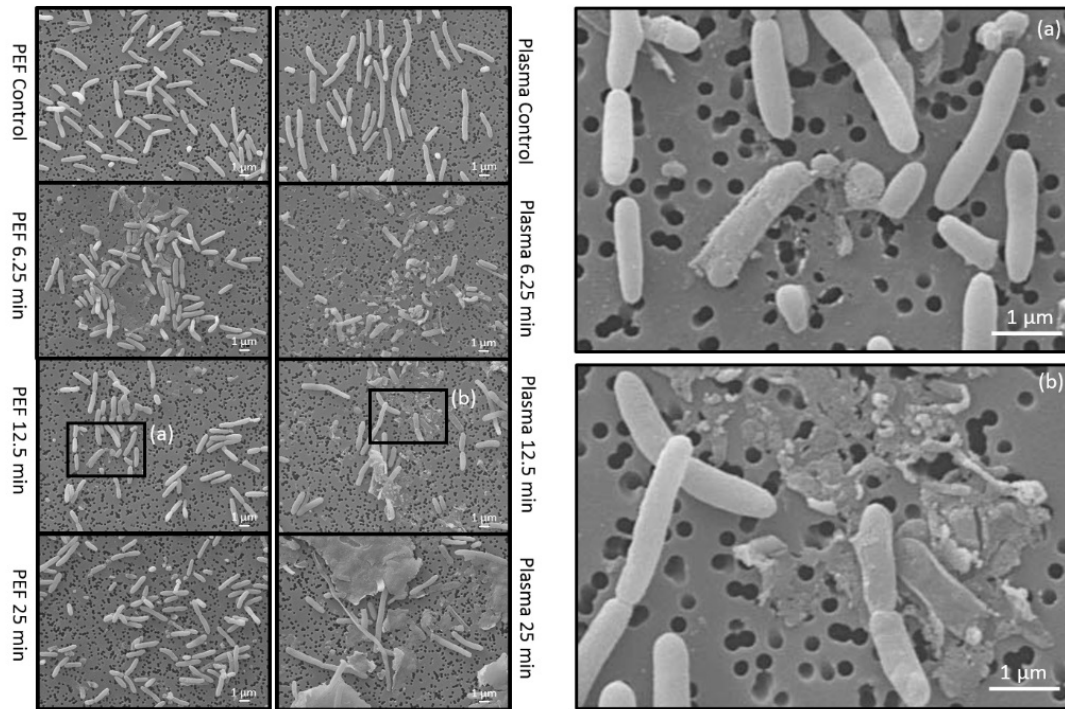
**Fig. 20** Scanning electron microscopy pictures of *L. pneumophila* after plasma and PEF treatment, respectively. **Reprinted from Publication P5**

## 6.2     Synergistic Effects of Plasma and Pulsed Electric Fields

The strength of the electric field was equal for both treatment methods and was calculated to be in the range of 2745 kV/cm close to the high voltage electrode. The field strength was decreasing exponentially to 8.1 kV/cm close to the outer electrode. Killing effects of the electric field were mediated in a cylindrical zone around the high voltage electrode that had a volume of 4.1 to 4.3 cm³. If the killing of *L. pneumophila* would have been mediated primarily by the strength of the electric field, no differences between the two treatment methods should have been observed.

The superior effectiveness of pulsed corona discharges was presumably caused by the synergistic combination of strong electric fields, shockwaves and the formation of reactive species. During plasma treatment, hydrogen peroxide in a concentration of 1 mmol/l after 12.5 min was detected. Nevertheless, differences in bacterial killing could not be fully linked to hydrogen peroxide concentrations alone. When a suspension of *Legionella* was spiked with hydrogen peroxide to a concentration of 1 mmol/l and left to act, CFU/ml decreased by only 23% (log 1.47) after 12.5 min. More likely the established electric field favored the uptake of reactive species into *Legionella* due to electroporation. Once inside the cell, radicals formed during plasma treatment developed their cytotoxic effects resulting in an enhanced killing of *L. pneumophila*. In addition, shockwaves instigated by propagating streamers could also induce shear forces, which disrupted cell membrane integrity.

**Table 7** Energy efficiency for plasma treatment and PEF treatment for killing of *Legionella pneumophila*. Each column represents the mean of three independent experiments (n=3) **Reprinted from Publication P5**

|  | Killing after 12.5 min | Killing after 25 min | Energy per Pulse applied | Efficiency per log reduction | Efficiency for eradication |
|---|---|---|---|---|---|
|  | in CFU/ml | in CFU/ml | in J | in kJ/l | in kJ/l |
| PLASMA (MEAN) | log 5.4 | log 5.4 | 1.16 | 23.03 | 124.44 |
| SD | ±0.15 | ±0.15 | ±0.02 | ±0.85 | ±5.15 |
| PEF (MEAN) | log 3.42 | log 4.82 | 1.03 | 46.97 | > 221.15 |
| SD | ±0.46 | ±0.57 | ±0.08 | ±5.90 | ±35.60 |

Altogether, the combination of plasma induced mechanism resulted in a much more efficient inactivation of *L. pneumophila*. For the investigated setup and for the applied pulsed corona discharges, about 124 kJ were necessary for a complete inactivation of *L. pneumophila* in one liter of waters (Table 7). Thus, the required energy was much lower than for thermal treatment, which is currently being used for the killing of *Legionella*. For the thermal treatment, water temperature has to be increased to 70 °C [102]. Assuming a starting temperature of around 25 °C and taking the heat capacity of water ($C_W$ =4.182 kJ·kg$^{-1}$·K$^{-1}$) into account, this change in temperature ($\Delta T = 45$ K) would require approximately 188 kJ/l.

Plasma and pulsed electric fields were assessed for their capacity to kill pathogenic microorganisms persisting in water tanks, cooling systems and water pipes. As a result, it was shown that the killing of *L. pneumophila* was possible with both methods. However, pulsed corona plasma appeared to be more efficient due to the accumulation of synergistic effects. Hydrogen peroxide is of particular importance, since it can enter *L. pneumophila*, presumably supported by electroporation, and develop its cytotoxic effects directly in the cell.

# Chapter 7

# Summary and Outlook

The potential of pulsed corona discharges for water purification and water disinfection was investigated. Degradation of organic pollutants and the inactivation of bacteria are based on the generation of short-lived species, such as in particular hydroxyl radicals, but also long-lived species, such as hydrogen peroxide. It has been found that the absence of nitrified, chlorinated or ozonated reaction products is an advantage for the maintenance of good water quality.

However, degradation processes cannot be described as a straight forward process and secondary reactions in the bulk liquid can contribute more significantly than direct plasma interactions. Especially hydrogen peroxide, as an intermediate storage for hydroxyl radicals, is important for reactions in the bulk. Metal ions released into the bulk liquid due to ground electrode corrosion can induce Fenton-chemistry that can substantially contribute to the degradation of recalcitrant compounds. The source of ground electrode corrosion is probably mediated by electrochemical processes when positive pulses in the sub-microsecond range are applied.

When pharmaceuticals are subjected to plasma, it has been found that degradation efficiency is increased by aromatic rings, unsaturated bonds and electron donating functional groups (+*I*/+*M*). These findings also explain why some pharmaceuticals, such as diatrizoate, are more recalcitrant than others. The degradation by hydroxyl radical chemistry in principle has the associated risk of forming harmful compounds. This was investigated in detail for the degradation of diclofenac. Consequently, with respect to energy efficiency, AOPs that rely on hydroxyl radical generation should aim for a complete mineralization of organic pollutants.

For the inactivation of *Legionella pneumophila* in water, electroporation of the cell membrane due to the established electric field was assumed to favor the uptake of reactive species into the microorganisms; thus, enhancing their cytotoxic effects. Energy consumption for the killing of microorganisms was found to be competitive with other disinfection methods, energy efficiency for water purification is still a critical issue and needs to be improved.

Since most of the radicals recombine to hydrogen peroxide, pulsed corona discharges generated in water should ideally be combined with methods that can split hydrogen peroxide into hydroxyl radicals again. Traditional Fenton-processes, photo-Fenton or electro-Fenton might be promising approaches.

Further studies are also needed for a better understanding of plasma processes that are responsible for the generation of radicals and how processes depend on operating parameters, i.e. duration of applied high voltage pulses. Although hydroxyl radicals are unambiguously generated, OH-emission lines are notably absent in emission spectra. The hypothesized fast electron injection from the ground electrode when subjected to short high voltage pulses warrants also further investigations.

Altogether, however, have pulsed corona plasma generated directly in water in this study already demonstrated their potential for the decomposition of recalcitrant organic compounds and the inactivation of microorganisms. Therefore, corona discharges may provide a solution to a problem that has so far hampered conventional water treatment methods.

# References

[1] M. Drinkwater, Y. Kerr, J. Font, M. Berger, Exploring the Water Cycle of the Blue Planet - The Soil Moisture and Ocean Salinity (SMOS) mission, (2009).

[2] W.J. Cosgrove, F.R. Rijsberman, World water vision: making water everybody's business, Routledge2014.

[3] T. Lévová, M.Z. Hauschild, Assessing the impacts of industrial water use in life cycle assessment, CIRP Annals-Manufacturing Technology, 60 (2011) 29-32.

[4] I. Health, National Prescription Audit, 2012.

[5] I. Health, IMS Health Study: U.S. Drug Spending Growth Reaches 8.5 Percent in 2015, 2016.

[6] V.L. Cunningham, S.P. Binks, M.J. Olson, Human health risk assessment from the presence of human pharmaceuticals in the aquatic environment, Regulatory Toxicology and Pharmacology, 53 (2009) 39-45.

[7] P.K. Jjemba, Excretion and ecotoxicity of pharmaceutical and personal care products in the environment, Ecotoxicology and Environmental Safety, 63 (2006) 113-130.

[8] T.A. Ternes, M. Meisenheimer, D. McDowell, F. Sacher, H.-J. Brauch, B. Haist-Gulde, G. Preuss, U. Wilme, N. Zulei-Seibert, Removal of Pharmaceuticals during Drinking Water Treatment, Environmental Science & Technology, 36 (2002) 3855-3863.

[9] P.E. Stackelberg, E.T. Furlong, M.T. Meyer, S.D. Zaugg, A.K. Henderson, D.B. Reissman, Persistence of pharmaceutical compounds and other organic wastewater contaminants in a conventional drinking-water-treatment plant, Science of the Total Environment, 329 (2004) 99-113.

[10] T. Heberer, Occurrence, fate, and removal of pharmaceutical residues in the aquatic environment: a review of recent research data, Toxicology letters, 131 (2002) 5-17.

[11] T.A. Ternes, Occurrence of drugs in German sewage treatment plants and rivers1, Water research, 32 (1998) 3245-3260.

[12] M. Stumpf, T.A. Ternes, K. Haberer, W. Baumann, Nachweis von natürlichen und synthetischen Östrogenen in Kläranlagen und Fließgewässern, Vom Wasser, 87 (1996) 251-261.

[13] A. Belfroid, A. Van der Horst, A. Vethaak, A. Schäfer, G. Rijs, J. Wegener, W. Cofino, Analysis and occurrence of estrogenic hormones and their glucuronides in surface water and waste water in The Netherlands, Science of the Total Environment, 225 (1999) 101-108.

[14] T. Brodin, J. Fick, M. Jonsson, J. Klaminder, Dilute Concentrations of a Psychiatric Drug Alter Behavior of Fish from Natural Populations, Science, 339 (2013) 814-815.

[15] G. Nentwig, Effects of pharmaceuticals on aquatic invertebrates. Part II: The antidepressant drug fluoxetine, Archives of environmental contamination and toxicology, 52 (2007) 163-170.

[16] F. Hoffmann, W. Kloas, Estrogens can disrupt amphibian mating behavior, PloS one, 7 (2012) e32097.

[17] C.E. Purdom, P.A. Hardiman, V.V.J. Bye, N.C. Eno, C.R. Tyler, J.P. Sumpter, Estrogenic Effects of Effluents from Sewage Treatment Works, Chemistry and Ecology, 8 (1994) 275-285.

[18] E. Commission, Environment and Water: proposal to reduce water pollution risks, European Commission, European Commission - Press release.

[19] I. Langmuir, Oscillations in ionized gases, Proceedings of the National Academy of Sciences, 14 (1928) 627-637.

[20] S. Eliezer, Y. Eliezer, The fourth state of matter: an introduction to plasma science, CRC Press2001.

[21] B. Jiang, J. Zheng, S. Qiu, M. Wu, Q. Zhang, Z. Yan, Q. Xue, Review on electrical discharge plasma technology for wastewater remediation, Chemical Engineering Journal, 236 (2014) 348-368.

[22] T. Von Woedtke, S. Reuter, K. Masur, K.-D. Weltmann, Plasmas for medicine, Physics Reports, 530 (2013) 291-320.

[23] M. Magureanu, D. Piroi, N.B. Mandache, V. David, A. Medvedovici, V.I. Parvulescu, Degradation of pharmaceutical compound pentoxifylline in water by non-thermal plasma treatment, Water Research, 44 (2010) 3445-3453.

[24] M. Magureanu, D. Piroi, N.B. Mandache, V. David, A. Medvedovici, C. Bradu, V.I. Parvulescu, Degradation of antibiotics in water by non-thermal plasma treatment, Water Research, 45 (2011) 3407-3416.

[25] M. Magureanu, D. Dobrin, N. Bogdan Mandache, C. Bradu, A. Medvedovici, V.I. Parvulescu, The Mechanism of Plasma Destruction of Enalapril and Related Metabolites in Water, Plasma processes and polymers, 10 (2013) 459-468.

[26] M. Hijosa-Valsero, R. Molina, H. Schikora, M. Müller, J.M. Bayona, Removal of priority pollutants from water by means of dielectric barrier discharge atmospheric plasma, Journal of Hazardous Materials, 262 (2013) 664-673.

[27] H. Krause, B. Schweiger, J. Schuhmacher, S. Scholl, U. Steinfeld, Degradation of the endocrine disrupting chemicals (EDCs) carbamazepine, clofibric acid, and iopromide by corona discharge over water, Chemosphere, 75 (2009) 163-168.

[28] D. Gerrity, B.D. Stanford, R.A. Trenholm, S.A. Snyder, An evaluation of a pilot-scale nonthermal plasma advanced oxidation process for trace organic compound degradation, Water Research, 44 (2010) 493-504.

[29] I. Panorel, S. Preis, I. Kornev, H. Hatakka, M. Louhi-Kultanen, Oxidation of aqueous pharmaceuticals by pulsed corona discharge, Environmental Technology, 34 (2012) 923-930.

[30] Y. Minamitani, S. Shoji, Y. Ohba, Y. Higashiyama, Decomposition of dye in water solution by pulsed power discharge in a water droplet spray, Plasma Science, IEEE Transactions on, 36 (2008) 2586-2591.

[31] D. Dobrin, C. Bradu, M. Magureanu, N. Mandache, V. Parvulescu, Degradation of diclofenac in water using a pulsed corona discharge, Chemical Engineering Journal, 234 (2013) 389-396.

[32] I. Panorel, S. Preis, I. Kornev, H. Hatakka, M. Louhi-Kultanen, Oxidation of Aqueous Paracetamol by Pulsed Corona Discharge, Ozone: Science & Engineering, 35 (2013) 116-124.

[33] A.T. Sugiarto, M. Sato, Pulsed plasma processing of organic compounds in aqueous solution, Thin Solid Films, 386 (2001) 295-299.

[34] M. Sato, Degradation of organic contaminants in water by plasma, International Journal of Plasma Environmental Science and Technology, 3 (2009).

[35] P. Lukes, B.R. Locke, Degradation of substituted phenols in a hybrid gas-liquid electrical discharge reactor, Industrial & engineering chemistry research, 44 (2005) 2921-2930.

[36] M.A. Malik, Ubaid-ur-Rehman, A. Ghaffar, K. Ahmed, Synergistic effect of pulsed corona discharges and ozonation on decolourization of methylene blue in water, Plasma Sources Science and Technology, 11 (2002) 236.

[37] B.R. Locke, S.M. Thagard, Analysis and review of chemical reactions and transport processes in pulsed electrical discharge plasma formed directly in liquid water, Plasma Chemistry and Plasma Processing, 32 (2012) 875-917.

[38] M.A. Malik, Y. Minamitani, S. Xiao, J.F. Kolb, K.H. Schoenbach, Streamers in water filled wire-cylinder and packed-bed reactors, Ieee Transactions on Plasma Science, 33 (2005) 490-491.

[39] M.A. Malik, J.F. Kolb, K.H. Schoenbach, Streamers in Water and Along the Insulator Surface in a Wire - Cylinder Gap, IEEE Transactions on Plasma Science, 39 (2011) 2626-2627.

[40] M.A. Malik, A. Ghaffar, S.A. Malik, Water purification by electrical discharges, Plasma Sources Science and Technology, 10 (2001) 82.

[41] K. Oehmigen, M. Hähnel, R. Brandenburg, C. Wilke, K.D. Weltmann, T. von Woedtke, The role of acidification for antimicrobial activity of atmospheric pressure plasma in liquids, Plasma Processes and Polymers, 7 (2010) 250-257.

[42] P. Lukes, E. Dolezalova, I. Sisrova, M. Clupek, Aqueous-phase chemistry and bactericidal effects from an air discharge plasma in contact with water: evidence for the formation of peroxynitrite through a pseudo-second-order post-discharge reaction of H2O2 and HNO2, Plasma Sources Science and Technology, 23 (2014) 015019.

[43] J.-S. Chang, P. Lawless, T. Yamamoto, Corona discharge processes, Plasma Science, IEEE Transactions on, 19 (1991) 1152-1166.

[44] V.I. Parvulescu, M. Magureanu, P. Lukes, Plasma chemistry and catalysis in gases and liquids, John Wiley & Sons2012.

[45] J.S. Clements, M. Sato, R.H. Davis, Preliminary investigation of prebreakdown phenomena and chemical reactions using a pulsed high-voltage discharge in water, IEEE Transactions on industry applications, (1987) 224-235.

[46] C. Schramm, O. Gans, M. Uhl, J. Grath, S. Scharf, I. Zieritz, M. Kralik, A. Scheidleder, F. Humer, Carbamazepin und Koffein–Potenzielle Screeningparameter für Verunreinigungen des Grundwassers durch Kommunales Abwasser, (2006).

[47] M. Jekel, W. Dott, A. Bergmann, U. Dünnbier, R. Gnirß, B. Haist-Gulde, G. Hamscher, M. Letzel, T. Licha, S. Lyko, U. Miehe, F. Sacher, M. Scheurer, C.K. Schmidt, T. Reemtsma, A.S. Ruhl, Selection of organic process and source indicator substances for the anthropogenically influenced water cycle, Chemosphere, 125 (2015) 155-167.

[48] T. Kosjek, H.R. Andersen, B. Kompare, A. Ledin, E. Heath, Fate of Carbamazepine during Water Treatment, Environmental Science & Technology, 43 (2009) 6256-6261.

[49] T.A. Ternes, R. Hirsch, Occurrence and Behavior of X-ray Contrast Media in Sewage Facilities and the Aquatic Environment, Environmental Science & Technology, 34 (2000) 2741-2748.

[50] T.A. Ternes, J. Stüber, N. Herrmann, D. McDowell, A. Ried, M. Kampmann, B. Teiser, Ozonation: a tool for removal of pharmaceuticals, contrast media and musk fragrances from wastewater?, Water Research, 37 (2003) 1976-1982.

[51] T.A. Larsen, J. Lienert, A. Joss, H. Siegrist, How to avoid pharmaceuticals in the aquatic environment, Journal of Biotechnology, 113 (2004) 295-304.

[52] T. Heberer, Tracking persistent pharmaceutical residues from municipal sewage to drinking water, Journal of Hydrology, 266 (2002) 175-189.

[53] C. Zwiener, F.H. Frimmel, Short-term tests with a pilot sewage plant and biofilm reactors for the biological degradation of the pharmaceutical compounds clofibric acid, ibuprofen, and diclofenac, Science of The Total Environment, 309 (2003) 201-211.

[54] R. Hirsch, T. Ternes, K. Haberer, K.-L. Kratz, Occurrence of antibiotics in the aquatic environment, Science of the Total Environment, 225 (1999) 109-118.

[55] K. Kümmerer, Antibiotics in the aquatic environment – A review – Part I, Chemosphere, 75 (2009) 417-434.

[56] P. Lukes, M. Clupek, V. Babicky, P. Sunka, Ultraviolet radiation from the pulsed corona discharge in water, Plasma Sources Science and Technology, 17 (2008) 024012.

[57] M. Dors, E. Metel, J. Mizeraczyk, E. Marotta, Coli bacteria inactivation by pulsed corona discharge in water, Int. J. Plasma Environ. Sci. Technol, 2 (2008) 34-37.

[58] Q. Zhang, J. Zhuang, T. von Woedtke, J.F. Kolb, J. Zhang, J. Fang, K.-D. Weltmann, Synergistic antibacterial effects of treatments with low temperature plasma jet and pulsed electric fields, Applied Physics Letters, 105 (2014) 104103.

[59] P. Sunka, V. Babický, M. Clupek, P. Lukes, M. Simek, J. Schmidt, M. Cernák, Generation of chemically active species by electrical discharges in water, Plasma Sources Science and Technology, 8 (1999) 258.

[60] G. Eisenberg, Colorimetric determination of hydrogen peroxide, Industrial & Engineering Chemistry Analytical Edition, 15 (1943) 327-328.

[61] B.R. Locke, K.-Y. Shih, Review of the methods to form hydrogen peroxide in electrical discharge plasma with liquid water, Plasma Sources Science and Technology, 20 (2011) 034006.

[62] B.H. Bielski, D.E. Cabelli, R.L. Arudi, A.B. Ross, Reactivity of HO2/O− 2 radicals in aqueous solution, Journal of Physical and Chemical Reference Data, 14 (1985) 1041-1100.

[63] N. Raghavan, S. Steenken, Electrophilic reaction of the OH radical with phenol: determination of the distribution of isomeric dihydroxycyclohexadienyl radicals, J. Am. Chem. Soc.;(United States), 102 (1980).

[64] G. Albarran, R.H. Schuler, Hydroxyl radical as a probe of the charge distribution in aromatics: phenol, The Journal of Physical Chemistry A, 111 (2007) 2507-2510.

[65] J.F. Bonnen, S. Golovashchenko, S. Dawson, A. Mamutov, Electrode Erosion Observed in Electrohydraulic Discharges Used in Pulsed Sheet Metal Forming, Journal of Materials Engineering and Performance, 22 (2013) 3946-3958.

[66] P. Lukes, M. Clupek, V. Babicky, I. Sisrova, V. Janda, The catalytic role of tungsten electrode material in the plasmachemical activity of a pulsed corona discharge in water, Plasma Sources Science and Technology, 20 (2011) 034011.

[67] S. Sakka, Handbook of sol-gel science and technology. 1. Sol-gel processing, Springer Science & Business Media2005.

[68] P. Tengvall, I. Lundström, L. Sjöqvist, H. Elwing, L.M. Bjursten, Titanium-hydrogen peroxide interaction: model studies of the influence of the inflammatory response on titanium implants, Biomaterials, 10 (1989) 166-175.

[69] R. Chen, J.J. Pignatello, Role of quinone intermediates as electron shuttles in Fenton and photoassisted Fenton oxidations of aromatic compounds, Environmental Science & Technology, 31 (1997) 2399-2406.

[70] Š. Potocký, N. Saito, O. Takai, Needle electrode erosion in water plasma discharge, Thin Solid Films, 518 (2009) 918-923.

[71] P. Lukeš, M. Člupek, V. Babický, P. Šunka, J.D. Skalný, M. Štefečka, J. Novák, Z. Málková, Erosion of needle electrodes in pulsed corona discharge in water, Czechoslovak Journal of Physics, 56 (2006) B916-B924.

[72] F. Holzer, B.R. Locke, Influence of high voltage needle electrode material on hydrogen peroxide formation and electrode erosion in a hybrid gas–liquid series electrical discharge reactor, Plasma Chemistry and Plasma Processing, 28 (2008) 1-13.

[73] B. Roodenburg, J. Morren, H.I. Berg, S.W. de Haan, Metal release in a stainless steel Pulsed Electric Field (PEF) system: Part I. Effect of different pulse shapes; theory and experimental method, Innovative Food Science & Emerging Technologies, 6 (2005) 327-336.

[74] N. Shimizu, S. Hotta, T. Sekiya, O. Oda, A novel method of hydrogen generation by water electrolysis using an ultra-short-pulse power supply, Journal of Applied Electrochemistry, 36 (2006) 419-423.

[75] M. Vanags, G. Bajars, J. Kleperis, Water electrolysis with inductive voltage pulses, INTECH Open Access Publisher2012.

[76] M. Sahni, B.R. Locke, Quantification of Hydroxyl Radicals Produced in Aqueous Phase Pulsed Electrical Discharge Reactors, Industrial & Engineering Chemistry Research, 45 (2006) 5819-5825.

[77] R.P. Joshi, S.M. Thagard, Streamer-like electrical discharges in water: part II. Environmental applications, Plasma Chemistry and Plasma Processing, 33 (2013) 17-49.

[78] B. Sun, M. Sato, J.S. Clements, Optical study of active species produced by a pulsed streamer corona discharge in water, Journal of Electrostatics, 39 (1997) 189-202.

[79] K.-Y. Shih, B.R. Locke, Optical and electrical diagnostics of the effects of conductivity on liquid phase electrical discharge, Plasma Science, IEEE Transactions on, 39 (2011) 883-892.

[80] B. Sun, M. Sato, A. Harano, J.S. Clements, Non-uniform pulse discharge-induced radical production in distilled water, Journal of Electrostatics, 43 (1998) 115-126.

[81] M. Sato, B. Sun, T. Ohshima, Y. Sagi, Characteristics of active species and removal of organic compound by a pulsed corona discharge in water, Journal of Advanced Oxidation Technologies, 4 (1999) 339-342.

[82] D. Dobrynin, Y. Seepersad, M. Pekker, M. Shneider, G. Friedman, A. Fridman, Non-equilibrium nanosecond-pulsed plasma generation in the liquid phase (water, PDMS) without bubbles: fast imaging, spectroscopy and leader-type model, Journal of Physics D: Applied Physics, 46 (2013) 105201.

[83] P. Lukes, M. Clupek, V. Babicky, B. Pongrac, M. Simek, J. Kolb, On the mechanism of OH radical formation by nanosecond pulsed corona discharge in water, Plasma Science (ICOPS), 2016 IEEE International Conference on, IEEE, 2016, pp. 1-1.

[84] H. Tresp, M.U. Hammer, J. Winter, K. Weltmann, S. Reuter, Quantitative detection of plasma-generated radicals in liquids by electron paramagnetic resonance spectroscopy, Journal of Physics D: Applied Physics, 46 (2013) 435401.

[85] N. Bézière, M. Hardy, F. Poulhès, H. Karoui, P. Tordo, O. Ouari, Y.-M. Frapart, A. Rockenbauer, J.-L. Boucher, D. Mansuy, Metabolic stability of superoxide adducts derived from newly developed cyclic nitrone spin traps, Free Radical Biology and Medicine, 67 (2014) 150-158.

[86] H. Tong, A.M. Arangio, P.S. Lakey, T. Berkemeier, F. Liu, C.J. Kampf, W.H. Brune, U. Pöschl, M. Shiraiwa, Hydroxyl radicals from secondary organic aerosol decomposition in water, Atmospheric Chemistry and Physics, 16 (2016) 1761-1771.

[87] J. Hartmann, P. Bartels, U. Mau, M. Witter, W. Tümpling, J. Hofmann, E. Nietzschmann, Degradation of the drug diclofenac in water by sonolysis in presence of catalysts, Chemosphere, 70 (2008) 453-461.

[88] L.A. Pérez-Estrada, S. Malato, W. Gernjak, A. Agüera, E.M. Thurman, I. Ferrer, A.R. Fernández-Alba, Photo-Fenton degradation of diclofenac: identification of main intermediates and degradation pathway, Environmental science & technology, 39 (2005) 8300-8306.

[89] D. Vogna, R. Marotta, A. Napolitano, R. Andreozzi, M. d'Ischia, Advanced oxidation of the pharmaceutical drug diclofenac with UV/H 2 O 2 and ozone, Water Research, 38 (2004) 414-422.

[90] W.J. Cooper, W. Song, Advanced Oxidation Degradation of Diclofenac, Radiation Treatment of Wastewater for Reuse with Particular Focus on Wastewaters Containing Organic Pollutants, (2012) 168.

[91] M.M. Huber, S. Canonica, G.-Y. Park, U. von Gunten, Oxidation of pharmaceuticals during ozonation and advanced oxidation processes, Environmental Science & Technology, 37 (2003) 1016-1024.

[92] X. Luo, Z. Zheng, J. Greaves, W.J. Cooper, W. Song, Trimethoprim: Kinetic and mechanistic considerations in photochemical environmental fate and AOP treatment, water research, 46 (2012) 1327-1336.

[93] F.J. Real, F.J. Benitez, J.L. Acero, J.J. Sagasti, F. Casas, Kinetics of the chemical oxidation of the pharmaceuticals primidone, ketoprofen, and diatrizoate in ultrapure and natural waters, Industrial & Engineering Chemistry Research, 48 (2009) 3380-3388.

[94] S. Ahmed, M. Rasul, W.N. Martens, R. Brown, M. Hashib, Heterogeneous photocatalytic degradation of phenols in wastewater: a review on current status and developments, Desalination, 261 (2010) 3-18.

[95] PubChem, 2,6-DICHLOROANILINE, National Center for Biotechnology Information, 2017.

[96] S. Chaturvedi, P.N. Dave, Removal of iron for safe drinking water, Desalination, 303 (2012) 1-11.

[97] D. García, N. Gómez, P. Mañas, S. Condón, J. Raso, R. Pagán, Occurrence of sublethal injury after pulsed electric fields depending on the micro-organism, the treatment medium ph and the intensity of the treatment investigated, Journal of Applied Microbiology, 99 (2005) 94-104.

[98] K. Neil, R. Berkelman, Increasing incidence of legionellosis in the United States, 1990–2005: changing epidemiologic trends, Clinical Infectious Diseases, 47 (2008) 591-599.

[99] Y.S. Lin, J.E. Stout, V.L. Yu, R.D. Vidic, Disinfection of water distribution systems for Legionella, Semin Respir Infect, 13 (1998) 147-159.

[100] R.P. Joshi, S.M. Thagard, Streamer-like electrical discharges in water: Part I. Fundamental mechanisms, Plasma Chemistry and Plasma Processing, 33 (2013) 1-15.

[101] J. Kolb, R. Joshi, S. Xiao, K. Schoenbach, Streamers in water and other dielectric liquids, Journal of Physics D: Applied Physics, 41 (2008) 234007.

[102] B. Kim, J. Anderson, S. Mueller, W. Gaines, A. Kendall, Literature review—efficacy of various disinfectants against Legionella in water systems, Water Research, 36 (2002) 4433-4444.

# Original Publications

The work presented in this thesis is based on the following peer-reviewed publications. The authors' contributions are briefly summarized in the following section:

## Publication P1

Decomposition of Pharmaceuticals by Pulsed Corona Discharges in Water Depending on Streamer Length
R. Banaschik, F. Koch, J.F. Kolb, K.D. Weltmann, *IEEE Transactions on Plasma Science*, 42 (2014) 2736-2737

Own contribution: RB designed and performed the experiments and data analysis was conducted by RB. The manuscript was written by RB and edited by al co-authors.

## Publication P2

Potential of Pulsed Corona Discharges Generated in Water for the Degradation of Persistent Pharmaceutical Residues
R. Banaschik, P. Lukes, H. Jablonowski, M.U. Hammer, K.-D. Weltmann, J.F. Kolb, *Water research*, 84 (2015) 127-135

Own contribution: RB designed and performed the experiments and data analysis was conducted by RB with the help of PL for phenol decomposition experiments. The manuscript was written by RB and edited by al co-authors.

## Publication P3

Fenton chemistry promoted by sub-microsecond pulsed corona plasmas for organic pollutant degradation in water
R. Banaschik, P. Lukes, C. Miron, R. Banaschik, A. Pipa, K. Fricke, P.J. Bednarski and J. F. Kolb, *Electrochimica Acta*, 245 (2017) 539-548.

Own contribution: RB designed and performed the experiments and data analysis was conducted by RB with the help of PL for phenol decomposition experiments. Data analysis for optical emission spectroscopy (OES) was performed by CM and AP. The manuscript was written by RB and edited by al co-authors.

## Publication P4

Degradation and Metabolites of Diclofenac as Instructive Example for Decomposition of Recalcitrant Pharmaceuticals by Hydroxyl Radicals Generated with Pulsed Corona Plasma in Water
R. Banaschik, H. Jablonowski, P.J. Bednarski and J.F. Kolb, *Journal of hazardous materials,* 342 (2018): 651-660.

Own contribution: RB designed and performed the experiments and data analysis was conducted by RB with the help of HJ for experiments involving spin trap enhanced electron paramagnetic resonance spectroscopy (EPR). The manuscript was written by RB and edited by al co-authors.

## Publication P5

Comparison of Pulsed Corona Plasma and Pulsed Electric Fields for the Decontamination of Water Containing Legionella Pneumophila as Model Organism
R. Banaschik, G. Burchhardt, K. Zocher, S. Hammerschmidt, J.F. Kolb, K.-D. Weltmann, *Bioelectrochemistry*, 112 (2016) 83-90.

Own contribution: RB designed and performed the experiments and data analysis was conducted by RB with the help of GB for the cultivation of *Legionella Pneumophila*. The manuscript was written by RB and edited by al co-authors.

## Confirmed

| | |
|---|---|
| Date | Robert Banaschik |

| | |
|---|---|
| Date | P.J. Bednarski |

## Publication P1

## Decomposition of Pharmaceuticals by Pulsed Corona Discharges in Water Depending on Streamer Length

R. Banaschik, F. Koch, J.F. Kolb, K.D. Weltmann, *IEEE Transactions on Plasma Science*, 42 (2014) 2736-2737

# Decomposition of Pharmaceuticals by Pulsed Corona Discharges in Water Depending on Streamer Length

Robert Banaschik, Friedrich Koch, Juergen F. Kolb, and Klaus-Dieter Weltmann

*Abstract*—Pulsed corona discharges generated in water provide a possibility for the abatement of even stable organic compounds. Decomposition efficacy correlates with the length of streamers, which in turn depends on water conductivity and applied voltage. We investigated the relation between conductivities from 25 to 500 $\mu$S/cm, pulse duration, and visible streamer length for applied peak voltages of 70 and 82 kV. Streamer development for an initially applied peak voltage of 70 kV was related to the decomposition rates of the pharmaceutical carbamazepine that was dissolved in solutions with conductivities in the same range.

*Index Terms*—Atmospheric-pressure plasmas, plasma applications, plasma chemistry.

## I. Introduction

**P**ULSED corona discharges are an appealing method for water treatment primarily for the generation of significant concentrations of hydroxyl radicals [1]. Conceivably, the amount of hydroxyl radicals is correlated to the length of the streamers and the permeation of the treated volume by the plasma, i.e., the number of streamers that are generated. Both number and length of streamers depend on the conductivity of the liquid, which will therefore determine the efficacy of water purification [2].

Corona plasmas were studied in a coaxial discharge geometry. A thin-tungsten wire of 50 $\mu$m in diameter along the center of a glass tube is the high-voltage electrode. The ground electrode is a steel mesh that is fixed to the inner glass wall of the reactor. Streamers were generated along the wire by applying positive high-voltage pulses from a 6-stage Marx bank generator with pulse repetition rates of 20 Hz. Accordingly, the applied high-voltage pulses are fast rising to peak values that were adjusted for a conductivity of 25 $\mu$S/cm to 70 or 82 kV and are subsequently exponentially decreasing. Rise time and pulse duration full-width at half-maximum (FWHM) depend on the resistance of the water filled reactor, i.e., on the conductivity of the liquid. Conversely, the conductivity is gradually increasing with number of applied discharges, while streamer

TABLE I

PEAK VOLTAGE, $V_p$, MEAN STREAMER LENGTH, $l$, AND PULSE DURATION (FWHM), $\tau$, WITH RESPECT TO WATER CONDUCTIVITY, $\sigma$. INITIAL PEAK VOLTAGE WAS ADJUSTED TO 82 kV FOR A CONDUCTIVITY OF 25 $\mu$S/cm

| σ (µS/cm) | 25 | 60 | 80 | 100 | 250 | 500 |
|---|---|---|---|---|---|---|
| $V_p$ (kV) | 82 | 79 | 80 | 79 | 76 | 70 |
| ℓ (mm) | 16 | 6.5 | 6 | 6 | 5.5 | 4.5 |
| τ (ns) | 321 | 234 | 186 | 169 | 116 | 104 |

TABLE II

EFFICACY AND EFFICIENCY FOR THE DECOMPOSITION OF CARBAMAZEPINE. EFFICACY WAS DETERMINED FROM THE REDUCTION OF THE INITIAL CONCENTRATION OF 1 mg/L. EFFICIENCY WAS DETERMINED FROM THE ENERGY REQUIRED FOR THE AMOUNT OF DECOMPOSED CARBAMAZEPINE

| Number of Discharges | Initial Conductivity (µS/cm) | | |
|---|---|---|---|
| | 25 | 100 | 500 |
| **20,000** | -15.52% | -10.94% | -1.9% |
| **mg/kWh** | 6.3 | 4.8 | 0.7 |
| **50,000** | -31.39% | -25.58% | -5.2% |
| **mg/kWh** | 5.1 | 4.5 | 0.8 |

length is decreasing. For each voltage we treated solutions with an initial conductivity of 25, 60, 80, 100, 250, and 500 $\mu$S/cm. Conductivities were controlled by dissolving sodium chloride in Milli-Q (Millipore Corporation, Massachusetts, USA) pure water. We found it necessary to adjust the conductivity to at least 25 $\mu$S/cm since we only observed spark discharges for lower values. A volume of 300 mL was treated in a continuous flow system with a flow rate of 240 mL/min. The reactor itself contained a volume of 240 mL. Table I describes the gradual change of pulseduration and streamer length with water conductivity. For a fixed Marx-bank, applied peak voltages were adjusted with respect to the water conductivity to deliver the same energy per pulse. Accordingly, peak currents were increasing, while peak voltages were decreasing when conductivities were increasing. For a conductivity of 25 $\mu$S/cm, peak voltages were adjusted to initial values of 82 or 70 kV, corresponding to energies per pulse of 2.8 and 1.3 J, respectively.
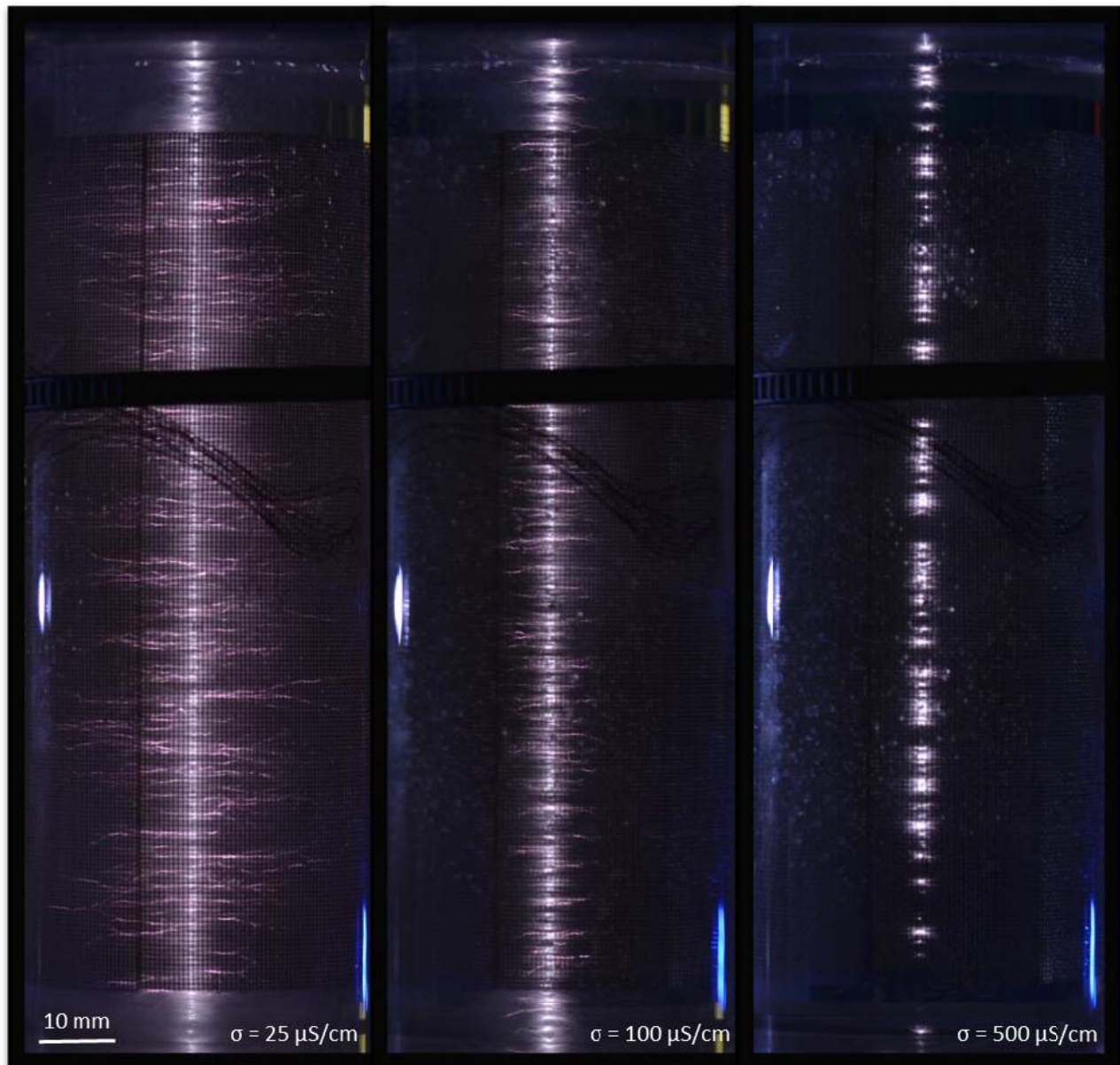
This article has been accepted for inclusion in a future issue of this journal. Content is final as presented, with the exception of pagination.

2                                                                                                          IEEE TRANSACTIONS ON PLASMA SCIENCE



Fig. 1.    Streamer discharges in water have been generated along a 50-$\mu$m tungsten wire in a coaxial reactor with inner diameter of 47 mm and length of 138 mm by applying short positive high-voltage pulses from a Marx bank. Number of streamers and streamer length is changing with water conductivity. For high-voltage pulses with a peak voltage of 82 kV, streamers fill almost the entire reactor volume for a conductivity of $\sigma = 25$ $\mu$S/cm. Without adjusting the Marx bank and when increasing conductivity to 500 $\mu$S/cm, peak voltage drops to 70 kV and streamer length is noticeably reduced. Simultaneously peak current is increasing with increasing conductivity. Without adjusting the applied voltage, the energy delivered per pulse is for all conductivities about the same (2.8 J).

Streamer length is decreasing with increasing conductivities with a gradually lower rate of change for higher conductivities. Examples are shown in Fig. 1. A similar characteristic is also observed for the decrease in pulse duration. For an initial conductivity of 25 $\mu$S/cm dense streamers permeate the entire volume, whereas for a conductivity of 500 $\mu$S/cm both streamer length and streamer density decrease significantly.

In a complementary experiment, we studied the decomposition efficacy for a peak voltage of 70 kV. Three solutions of the antiepileptic carbamazepine with a concentration of 1 mg/L were prepared and adjusted to conductivities of 25, 100, or 500 $\mu$S/cm. Concentrations of carbamazepine were determined by high-pressure liquid chromatography after 20 000 or 50 000

discharges were applied. Decomposition efficacies, as shown in Table II, correlate well with the mean streamer length that was determined for different conductivities (Table I). In conclusion, the decomposition of the pharmaceutical is more effective for longer streamers, i.e., for lower conductivities.

REFERENCES

[1] M. A. Malik, A. Ghaffar, and S. A. Malik, "Water purification by electrical discharges," *Plasma Sources Sci. Technol.*, vol. 10, no. 1, pp. 82–91, 2001.
[2] J. S. Clements, M. Sato, and R. H. Davis, "Preliminary investigation of prebreakdown phenomena and chemical reactions using a pulsed high-voltage discharge in water," *IEEE Trans. Ind. Appl.*, vol. IA-23, no. 2, pp. 224–235, Mar. 1987.

## Publication P2

## Potential of Pulsed Corona Discharges Generated in Water for the Degradation of Persistent Pharmaceutical Residues

# Potential of pulsed corona discharges generated in water for the degradation of persistent pharmaceutical residues

CrossMark
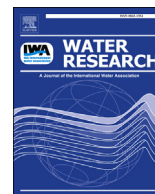
Robert Banaschik [a], Petr Lukes [b], Helena Jablonowski [a], Malte U. Hammer [a], Klaus-Dieter Weltmann [a], Juergen F. Kolb [a, *]

[a] Leibniz Institute for Plasma Science and Technology e.V. (INP Greifswald), Felix-Hausdorff-Strasse 2, 17489 Greifswald, Germany
[b] Department of Pulse Plasma Systems, Institute of Plasma Physics AS CR, Za Slovankou 3, 182 00 Prague 8, Czech Republic

## A R T I C L E   I N F O

## A B S T R A C T

Anthropogenic pollutants and in particular pharmaceutical residues are a potential risk for potable water where they are found in increasing concentrations. Different environmental effects could already be linked to the presence of pharmaceuticals in surface waters even for low concentrations. Many pharmaceuticals withstand conventional water treatment technologies. Consequently, there is a need for new water purification techniques. Advanced oxidation processes (AOP), and especially plasmas with their ability to create reactive species directly in water, may offer a promising solution. We developed a plasma reactor with a coaxial geometry to generate large volume corona discharges directly in water and investigated the degradation of seven recalcitrant pharmaceuticals (carbamazepine, diatrizoate, diazepam, diclofenac, ibuprofen, 17α-ethinylestradiol, trimethoprim). For most substances we observed decomposition rates from 45% to 99% for treatment times of 15—66 min. Especially ethinylestradiol and diclofenac were readily decomposed. As an inherent advantage of the method, we found no acidification and only an insignificant increase in nitrate/nitrite concentrations below legal limits for the treatment. Studies on the basic plasma chemical processes for the model system of phenol showed that the degradation is primarily caused by hydroxyl radicals.

© 2015 Elsevier Ltd. All rights reserved.

## 1. Introduction

Medical advances have always been going along with the development and increasing use of pharmaceuticals. Accordingly, IMS Health, a company that provides information for the US healthcare industry, reported a steady increase in dispensed prescriptions of 5.4% from 2008 to 2012 (Health, 2012). A further increase is expected due to continuing progress in pharmaceutical sciences together with an aging population, especially in industrialized countries. Most of the active compounds prescribed for treatment are in fact excreted from the body by the renal and biliary system (Jjemba, 2006). At the same time, a lot of these substances are essentially not biodegradable and withstand destruction in sewage treatment plants (STP) (Ternes et al., 2002; Stackelberg et al., 2004). As a result, increasing concentrations of pharmaceuticals are now a burden on the environment and a potential risk to

drinking water supplies. A prominent example is the triiodinated X-ray contrast agent, diatrizoate, which resists oxidation by ozone even in combination with UV-irradiation (Ternes et al., 2003). However, in particular the concentrations of antiepileptic drugs (diazepam, carbamazepine), analgesics (ibuprofen, diclofenac) and hormones (ethinylestradiol) are of growing concern (Heberer, 2002). Ternes et al. reported among 32 common drugs, found in effluents of German sewage treatment plants, carbamazepine in concentrations of 6.3 μg/l and ibuprofen and diclofenac in concentrations of 3.4 μg/l and 2.1 μg/l, respectively (Ternes, 1998). Hormones (17α-ethinylestradiol) were detected in effluents from German sewage treatment plants in concentrations of 62 ng/l and in surface water of the Netherlands in concentrations as high as 47 ng/l (Stumpf et al., 1996; Belfroid et al., 1999).

The detected residual concentrations seem to be low in comparison to therapeutic dosages but have already been found to have verifiable environmental effects. Psychiatric drugs (benzodiazepines) were linked to changes in the behavior and feeding rate of perches in concentrations as low as 1.8 μg/l (Brodin et al., 2013). Fluoxetine, an antidepressant drug, may cause a decrease in

* Corresponding author.
  E-mail address: juergen.kolb@inp-greifswald.de (J.F. Kolb).

reproduction rates of snails (*P. antipodarum*) at concentrations of 0.81 μg/l (Nentwig, 2007). Estrogens were reported to disrupt amphibian mating behavior in doses as low as 0.296 ng/l and further affect the gender distribution of fish populations (Hoffmann and Kloas, 2012; Purdom et al., 1994). High concentrations of analgesics were identified as the cause of vulture population decline in Pakistan (Oaks et al., 2004). Increasing concentrations of antibiotics in the environment could further be a factor in the proliferation of antibiotic resistant bacteria (Kümmerer, 2009a, 2009b).

Growing public concern is therefore understandable, particularly since the long term effect of many of these compounds that are continuously administered in low doses are difficult to predict. In response to the potential risk to our surface waters the European Commission (EC) has decided to add the pharmaceuticals diclofenac (analgesic drug), 17α-ethinylestradiol and 17β-estradiol (both hormones) to a watch list of emerging pollutants [Water Framework Directive, Directive 2008/105/EC, Decision (EU) 2015/495 of 20 March 2015] (Commission).

Established water treatment methods, such as filtration and biological degradation are apparently not sufficient to address the problem even when improved and combined with membrane bioreactors, nanofiltration, reverse osmosis filters or activated carbon filters (Foster et al., 2012, 2013; Poyatos et al., 2010). Therefore other approaches are now focusing on advanced oxidation processes (AOPs), i.e. the generation of highly reactive species. Of particular interest is the hydroxyl radical that has a much higher oxidation potential than ozone or chlorine. Interactions with target molecules are primarily diffusion controlled and eventually result in fragmentation of organic compounds and mineralization to $CO_2$ (Giri et al., 2010; Magureanu et al., 2015). The commonly exploited generation mechanisms for hydroxyl radicals are photochemical degradation of ozone and hydrogen peroxide by exposure to ultraviolet light ($O_3$ + UV, $H_2O_2$ + UV). The process can be improved by photo catalysts, e.g. titanium-dioxide ($TiO_2$), or iron ($Fe^{2+}$). Catalytic process by themselves ($TiO_2$ + UV) and other chemical oxidation mechanisms ($O_3/H_2O_2$, $H_2O_2/Fe^{2+}$) are also investigated (Poyatos et al., 2010). Although effective to some degree, all of these methods are associated with some problems on a larger scale. For example is ozone or hydrogen peroxide consumed and has to be supplied accordingly. Assuming the use of UV/$H_2O_2$ for the waste water treatment facility of Hamburg/Dradenau (410,958 m$^3$ waste water/d) hydrogen peroxide in concentrations between 0.2 mM and 5 mM would be required (Katsoyiannis et al., 2011; Vogna et al., 2004). This would correspond to a need for $H_2O_2$ of 2.8—70 tons per day. Hydrogen peroxide production is further associated with hazards due to its corrosive nature and the risk of explosions during storage and transport of large volumes. Furthermore photo catalysts that are suspended in water have to be removed again, since they have been found to be potentially toxic (Mantzavinos and Psillakis, 2004; Pintar et al., 2004). Another efficient method for the generation of hydroxyl radicals and other reactive species is offered by plasmas. Dielectric barrier discharges (DBD) that are generated outside the water but close to water are often employed for this purpose. However, species that are generated in the plasma have to diffuse into the liquid first and as a consequence this approach is most effective only for shallow water layers. Magureanu et al. investigated the decomposition of different pharmaceutical compounds that were dissolved in water in a coaxial DBD configuration with the plasma generated in air (Magureanu et al., 2010, 2011, 2013). Hijosa-Valsero et al. also investigated a coaxial DBD configuration for the removal of organic micro pollutants (Hijosa-Valsero et al., 2013) Krause et al. studied barrier electrodes (Krause et al., 2009) and Gerrity et al. investigated a pilot-scale unit of an "electrode-to-plate" configuration (Gerrity et al., 2010). Pulsed corona discharges are another method for the

creation of plasma in air (Locke and Thagard, 2012). Panorel et al. used a pulsed corona discharge (PCD), created along horizontal wires for the degradation of pharmaceuticals with solutions that were dispersed and showered in jets, droplets and films into the electrode array (Panorel et al., 2012, 2013). Dobrin et al. used pulsed corona discharges in oxygen in an array of 15 copper wires for the degradation of diclofenac (Dobrin et al., 2013). Results on the degradation that were achieved with these respective systems for different pharmaceuticals are summarized in Table 1.

Methods using corona discharges generated in a gaseous atmosphere outside the liquid are likewise facing the problem of a necessary diffusion of reactive species into and throughout the liquid for the method to be effective. This problem is avoided by creating plasma directly in water. One possibility is the generation of spark discharges, generally in point-to-point or point-to-plane (needle-plate) geometries in small volumes. Associated research on degradation of organic compounds has primarily focused on discoloration of dyes and the decomposition of phenolic derivatives (Sugiarto and Sato, 2001; Sato, 2008; Lukes and Locke, 2005). A notable exception in scope is a pilot facility for the use of spark discharges for waste water treatment that was brought into operation by Chang and his co-workers (Yantsis et al., 2008).

A more energy efficient method is the generation of pulsed corona discharges directly in water. The energy required is generally about three orders of magnitude lower than that for spark discharges (Locke and Thagard, 2012). Sato et al. investigated a combination of streamer (i.e. corona) discharges and spark discharges in a point-to-plane geometry for the degradation of Rhodamine B (Sato, 2009). A similar setup was studied by Malik et al. for corona discharges in combination with plasma catalysts and ozone treatment for the discoloration of methylene blue (Malik et al., 2002). Lukes et al. used a hybrid gas—liquid electrical discharge reactor with corona discharges generated inside and outside the liquid for the degradation of phenol (Lukes and Locke, 2005; Lukes et al., 2004). Results of the different studies on the degradation efficacy and efficiency are again included in Table 1.

In comparison with spark discharges, corona discharges offer the advantage of generating them also in extended geometries. This has been shown for example by Malik et al. (2011, 2005). With the future implementation of the method of pulsed corona discharges generated in water in treatment facilities in mind, we have also focused on the investigation of discharges that are generated in an extended coaxial geometry directly in water. Here we are presenting results on the potential of the approach for the degradation of pharmaceuticals that have been found to have possible harmful environmental impact.

## 2. Materials and methods

### 2.1. Water treatment

Corona discharges were generated in a coaxial geometry, as shown in Fig. 1. A thin tungsten wire of 50 μm in diameter that was drawn along the center of a glass tube served as a high voltage electrode. The wire was replaced after each experiment to provide reproducible experimental conditions. The reactor had an inner diameter of 47 mm and a length between the acrylic plates of 138 mm, hence retaining a volume of 240 ml. A steel mesh was attached to the inner wall. The diameter of the openings in the mesh was 0.4 mm and the wire thickness 0.25 mm.

A mesh was chosen instead of a sheet metal electrode in order to permit optical access to the discharges. Streamers, as shown in Fig. 2, were generated along the entire length of the wire when positive high voltage pulses were applied from a 6-stage Marx-bank. The pulse generator had an erected capacitance of 12 nF

**Table 1**
Comparison of treatment efficacies and treatment parameters for the degradation of organic compounds.

| Study, reference | Substances investigated | Concentration | Treated volume | Plasma system | Degradation | Treatment time | Energy cost |
|---|---|---|---|---|---|---|---|
| Magureanu et al. (2010) | Pentoxifylline | 100 mg/l | 200 ml | coaxial DBD[a] | 92.5% | 60 min | 16 g/kWh |
| Magureanu et al. (2011) | Amoxicillin Oxacillin, Ampicillin | 100 mg/l | 200 ml | coaxial DBD[a] | >90% | 30, 10, 20 min | 27, 105, 29 g/kWh |
| Magureanu et al. (2013) | Enalapril | 50 mg/l | 300 ml | coaxial DBD[a] | >90% | 20 min | 20.66 g/kWh |
| Hijosa-Valsero et al. (2013) | Atrazine chlorfenvinfos 2,4-dipbromphenol lindane | 1–5 mg/l | 175 ml | coaxial DBD[a] | 87–89% | 5 min | 47–447 mg/kWh |
| Krause et al. (2009) | Clofibric acid Carbamazepine Iopromide | 0.1 mM (22–79 mg/l) | 200 ml | two barrier electrodes | >98% | 30 min | 500 W |
| Gerrity et al. (2010) | Meprobamate, Phenytoin, Primidone, Carbamazepine, Atenolol, Trimethoprim, (Atrazine) | 36–378 ng/l | 150 l | needle-plate | >90% | 19 min | 2.2–6.4 kWh/m$^3$ (EEO[c]) |
| Panorel et al. (2012, 2013) | Paracetamol, 17β-estradiol, Salicylic acid, Indometacin, Ibuprofen | 3–100 mg/l | 40–50 l | PCD[b] | 70–99% | 30 min | 1.5–150 g/kWh |
| Minamitani et al. (2008) | Indigo carmine | 20 mg/l | 1 l | PCD[b] | >99% | 1–60 min | 9–360 J/mg |
| Dobrin et al. (2013) | Diclofenac | 50 mg/l | 55 ml | PCD[b] | >99% | 15 min | 0.76 g/kWh (90% conversion) |
| Sugiarto and Sato (2001) | Phenol | 50 mg/l | 1 l | needle-plate | >99% | 30–60 min | 20 kV, 50 Hz |
| Sato (2009) | Rhodamine B | 10 mg/l | n.s. | needle-plate | 80% | n.s. | 70–360 J/ml |
| Malik et al. (2002) | Methylene blue | 13.25 mg/l | 20 ml | needle-plate | 95% | 90 min | 41 mg/kWh |
| Lukes and Locke (2005) | Phenol derivatives | 500 μmol/l (47–70 mg/l) | 400 ml | needle-plate | 47–80% | 60 min | 281–457 kWh/m$^3$ (EEO[c]) |

[a] Dielectric Barrier Discharge.
[b] Pulsed Corona Discharge.
[c] The EEO-value is defined as the amount of electrical energy (kWh), required to reduce the concentration of a pollutant by one order of magnitude (90%).
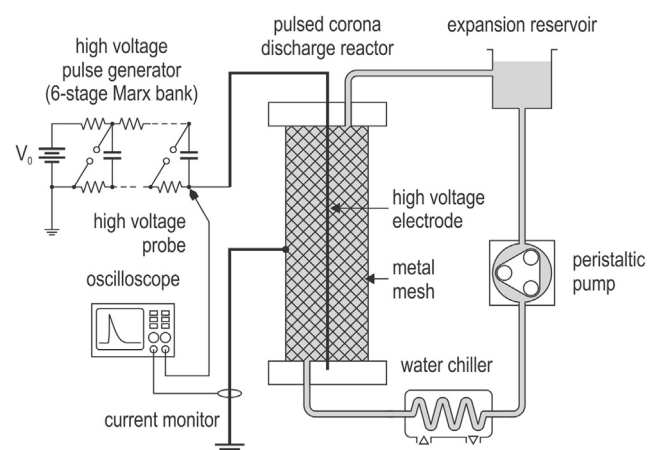


**Fig. 1.** Pulsed corona discharges were generated in a coaxial reactor with an inner diameter of 47 mm and length of 138 mm along a tungsten wire with a diameter of 50 μm. Positive high voltage pulses were applied from a 6-stage Marx bank with 20 Hz. A volume of 300 ml of water was treated in a continuous flow system with a flow rate of 120 ml/min.



**Fig. 2.** Current and voltage characteristics for a single high voltage pulse that was applied to generate corona discharges permeating the reactor volume as shown in the inset (Exposure time for the photograph was 1 s, therefore, about 20 individual discharges are superimposed in the image.) The voltage waveform is close to critically damped with peak voltage of 80 kV, pulse duration of about 270–300 ns (FWHM), and rise time of 30 ns. The current pulse shows a damped oscillation with a peak current of 200 A and a period of about 100 ns.

and an experimentally determined inductance of about 2.5 μH. The repetition rate of the pulse generator was set to 20 Hz. The charging voltage of the Marx-bank was adjusted to achieve pulse amplitudes of 80 kV when the reactor was filled with water with a conductivity of 30 μS/cm. Exponentially decaying voltage pulses with a duration of about 270–300 ns (FWHM) and rise time of 30 ns were recorded accordingly with a 120 kV/80 MHz high voltage probe (PVM-5, NorthStar Marana, AZ). Discharge parameters correspond to a resistive load with a value of 300 Ω. Lower water conductivities encourage transition of the corona discharge into a spark. The length of streamers decreases as water conductivity increases; however this is not a linear relation. For the same operating parameters, streamers of a few millimeters in length are still observed
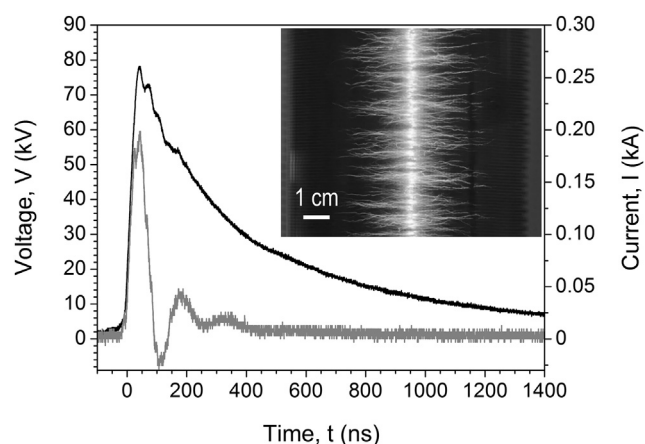
for a conductivity of 500 μS/cm. Changing conductivity has a slight effect on the pulse shape (Banaschik et al., 2014). The end point of our experiments was set to 80,000 discharges (66 min ≈ 1 h). For this duration we did not observe any significant changes in the discharge characteristics (except for a slight change in streamer length, which can be explained by a small increase of conductivity during the treatment). Pulsed currents through the reactor were measured with a Pearson current monitor (Model 5046, Pearson Electronics, Palo Alto, CA). Every voltage and current pulse was recorded on a fragmented memory storage oscilloscope for analysis (Wave Surfer 64MXs-B, LeCroy, Chestnut Ridge, NY). From recorded voltage and current waveforms we calculated the energy delivered

with each pulse by integrating the product for the duration of the signals. On average, the energy of 1.4 J was dissipated per pulse. Fig. 2 is showing typical high voltage and current pulses.

The reactor was operated in a continuous flow mode, anticipating future applications and simultaneously allowing taking water samples for analysis outside the reactor. A perceived disadvantage of the setup could be that the volume of water could not be treated entirely with every discharge. Conversely, an inherent advantage of the method is a continuous mixing. The entire system, including tubes and excess container, had a capacity of 300 ml with the reactor holding 240 ml, i.e. 80% of the total volume at all times. The liquid was driven through the system by a peristaltic pump (FH100x, Thermo Scientific, Waltham, MA) with a flow rate of 120 ml/min. This corresponds to a residence time in the reactor of 120 s or exposure to 2400 consecutive discharges. A chiller was used to prevent a temperature rise of the treated volume above 35 °C, thereby excluding possible thermal degradation of the analytes. It should be noted that in this configuration discharges are entirely generated in water, i.e. the liquid was not exposed to any plasma species that were produced by a discharge or a partial discharge in air.

## 2.2. Investigated pharmaceuticals

High pressure liquid chromatography (HPLC) grade water, acetonitrile and formic acid were purchased from Sigma–Aldrich (Taufkirchen, Germany). Due to legal constraints for diazepam, a proprietary medicinal product (Diazepam-Ratiopharm® 10 mg/ml) was purchased from a local pharmacy. All other pharmaceuticals were obtained from Sigma–Aldrich. All pharmaceuticals had purification grades of at least 98%.

The pharmaceuticals chosen for this study are known to be problematic substances for water purification technologies (Kosjek et al., 2009; Ternes et al., 2003; Zwiener and Frimmel, 2003; Larsen et al., 2004). The pharmaceuticals were selected as examples for different important substance groups and screening parameters (Schramm et al., 2006; Jekel et al., 2015) in particular including analgesics, hormones and antibiotics. Investigated pharmaceuticals, structure, respective use, and concentrations of the substances found in the environment are summarized in Table S1.

## 2.3. Procedures and degradation diagnostics

To compare different reactivity of the pharmaceuticals with respect to the plasma treatment we found it necessary to use a clean system every time. This was especially required for the phenol investigations on possible degradation mechanisms. In general, solutions of the substances in concentrations of 500 μg/l were prepared with Milli-Q purified water (Q-POD, Millipore, Billerica, MA). The conductivity of the solutions were adjusted to a value of 30 μS/cm by adding sodium chloride. Sodium chloride was chosen in part due to the fact that some of the pharmaceuticals were already obtained as sodium salt. To ensure that the concentrations of pharmaceuticals had reached an equilibrium steady-state value and were, hence, dissolved completely, solutions were prepared 24 h before treatment. A volume of 300 ml of the prepared solution was then filled into the continuous flow system. To achieve significant degradation effects, and because of the estimated recalcitrance of some pharmaceuticals, we applied 40,000 and 80,000 discharges at 20 Hz, corresponding to a total treatment time of 33 min and 66 min, respectively. For the more readily responding pharmaceuticals that were identified, e.g. ethinylestradiol and diclofenac, degradation characteristics were also studied for 6,000, 12,000 and 20,000 discharges. All experiments were repeated at least three times. The circulated volume was water-

chilled during the treatment and water temperature kept below 35 °C. Keeping temperature low and stable was motivated to exclude any thermal degradation effects on the pharmaceuticals. To further ensure that thermal decomposition was negligible we heated solutions of pharmaceuticals to 38 °C for 90 min in a water bath. Concentrations varied by less than 1% before and after the thermal treatment. Analytic separations were conducted by HPLC (Agilent 1200 Infinity Series, Agilent Technologies Santa Clara, CA) using a ZORBAX SB C18 HT rapid resolution column (2.1 × 50 mm, 1.8 μm). Isocratic or gradient elutions were used with varying eluent ratios. Eluents consisted of 0.1% formic acid in water and acetonitrile with a flow rate of 0.5 ml/min. The sample volumes that were injected varied from 5 to 30 μl and were adjusted with respect to the desired Limit of Quantification (LOQ) of at least 5 μg/l. The method was therefore able to quantify a possible degradation of at least 99%. Level of quantification was estimated as a signal-to-noise ratio (S/N) of at least ten. Concentrations before and after the treatment were quantified with a single quadrupole mass analyzer (Agilent series 6130) which was operated in Single Ion Monitoring mode (SIM), in combination with a Diode-Array Detector (DAD, Agilent, 1260 series). Peak areas of the spectra, as determined by HPLC-MS, were correlated to analyte concentrations with 6-point calibration curves ($R^2 > 0.998$).

## 2.4. Water quality parameters and reactive species

Water quality parameters, such as temperature, pH-value, conductivity and dissolved oxygen concentration were monitored with a multi parameter probe (HI 9828, Hanna Instruments, Woonsocket, RI) before and after the experiments. Samples were taken from the expansion reservoir for measurements. In addition we investigated the possible production of nitrate and nitrite as a result of the plasma treatments. First insights in the mechanisms that are responsible for the breakdown of pharmaceuticals were obtained from concentrations of hydrogen peroxide that was generated. Reaction mechanisms were then investigated in more detail using phenol as a model system.

### 2.4.1. Nitrate and nitrite concentrations

Pure Milli-Q water (300 ml) was filled into the reactor without any dissolved pharmaceuticals. After adjusting conductivity to 30 μS/cm with sodium chloride, the liquid was treated with 80,000 discharges. Samples of 80 μl were taken after the application of 10,000, 20,000, 40,000 and 80,000 discharges. The concentrations of nitrite and nitrate were then measured by a colorimetric assay kit (Cayman Chemical Company, Ann Arbor, MI) as described previously by Reuter et al. (2012). For the determination of nitrite, the treated sample was mixed with 20 μl of untreated water. After adding 50 μl Griess reagent I and 50 μl Griess reagent II, resulting in a total volume of 200 μl, nitrite reacted with the reagents forming a deep purple azo compound. The absorbance at a wavelength of 540 nm in comparison with the calibration curve yields the total concentration of nitrite. The absorbance was measured with a micro plate reader (Tecan Infinite M200 Pro, Tecan Group Ltd., Männedorf, Switzerland). The same assay was used to measure nitrate concentrations. However, nitrate first had to be reduced to nitrite with 10 μl nitrate reductase enzyme and 10 μl related cofactor which were used instead of the 20 μl untreated water (again resulting in a total volume of 200 μl). The nitrate concentration is then derived from the difference of the total concentration of nitrate plus nitrite and the total concentration of nitrite alone. Each sample was prepared and analyzed in triplicate. The detection limit of the nitrate/nitrite assay was 2.5 μM (i.e. 0.16 mg/l for nitrate and 0.12 mg/l for nitrite).

### 2.4.2. Hydrogen peroxide concentrations

Concentrations of hydrogen peroxide ($H_2O_2$) were measured by a colorimetric assay using a saturated solution of titanyl sulfate containing 15% sulfuric acid. The reaction of titanyl sulfate with hydrogen peroxide results in a yellow-colored peroxy complex. The concentration of the complex can be quantified from absorbance at 407 nm. For a calibration curve, a volume concentration of 0.0125% hydrogen peroxide dissolved in water was consecutively diluted five times; each time by a factor of two. The analysis of hydrogen peroxide concentrations of plasma-treated pure water followed procedures that were similar to the study of nitrate/nitrite concentrations. At least three individual probes of 100 μl were each mixed with 50 μl titanyl sulfate reagent and then analyzed for absorbance with a micro plate reader (Tecan Infinite M200 Pro, Tecan Group Ltd., Männedorf, Switzerland).

### 2.4.3. Investigation of radical chemistry using phenol as a chemical probe

The main purpose of using phenol was the evaluation of basic plasma chemical processes which occur during and following the treatment with discharges. Phenol is reacting readily with OH radicals (second order rate constant is of the order of $10^9 M^{-1} s^{-1}$) and many other organic compounds with aromatic structure. Moreover, phenol is reactive with other reactive species. As a rather simple molecule, phenol has specific analytic advantages with a reaction chemistry that is understood in detail and well known byproducts.

Plasmas in liquid can either interact with gas molecules dissolved in the liquid (mostly nitrogen, oxygen), or water molecules itself. Therefore plasma will form transient species ($^{\bullet}OH$, $NO_2^{\bullet}$, $^{\bullet}NO$ radicals) and long-lived chemical products ($O_3$, $H_2O_2$, $NO_3^-$ $NO_2^-$). Hydroxyl radicals and ozone are able to hydroxylate phenol (and other chemical compounds, e.g. pharmaceutical residues). Chemical reactions involving phenol and ozone can be identified from the presence of muconic acid. Conversely, radicals, such as $NO_2^{\bullet}$, $^{\bullet}NO$ (probably mediated by peroxynitrite), will form nitrated and nitrosylated products of phenol (Lukes et al., 2014). In summary, the characteristic reaction products of phenol will reveal almost all reactive species that are responsible for its degradation. Studies were conducted with aqueous solutions prepared from deionized water containing 500 μM phenol. The solution conductivity was again adjusted to at least 30 μS/cm with sodium chloride in a total treated volume of 300 ml. Altogether 80,000 discharges (treatment time 66 min) were applied. We searched mainly for hydroxylated products (hydroquinone, hydroxybenzoquinone, 1,4-benzoquinone, catechol), but also nitrated products (4-nitrosophenol, 4-nitrocatechol, 2-nitrohydroquinone, 4-nitrophenol, 2-nitrophenol) and products formed after an ozone attack (cis,trans-muconic acid, cis,cis-muconic acid). Samples of 1 ml were taken after intervals of 10,000 discharges and were analyzed with an HPLC system (Shimadzu LC-10Avp with Diode Array Detector and Fluorescence Detector). To quench hydroxyl radical post-discharge reactions, 250 μl of methanol was added to the samples.

## 3. Results

### 3.1. Degradation of dissolved pharmaceuticals

Samples of 0.5 ml were taken from the circulation system before the treatment (control), after 6,000, then 12,000, again after 20,000 and 40,000, and eventually 80,000 discharges for analysis. The flow rate of 120 ml/min corresponded to the exposure of the treated volume to 2400 discharges for a residence time of 2 min. A typical chromatogram for the degradation of diclofenac is presented with

Fig. S1a. The height of the peaks and the area under the peaks decreases with the increase of the number of discharges. The areas linearly follow the concentrations of the substances. Accordingly, peak areas of the chromatogram could be correlated with calibration curves for the quantitative analysis of degradation rates.

Initial concentrations that were in the range of micrograms per liter were chosen for the investigated pharmaceuticals. In most cases (except Gerrity et al.) this was lower than concentrations reported in previous studies (Table 1). The concentrations were still higher than those found for the contamination of potable water but already closer to concentrations found in the environment. In addition, these concentrations still allowed us to use standard analytical methods. Although we observed the decomposition of compounds, we were unable to detect any decomposition products by HPLC-MS in the total ion current (TIC) chromatogram, suggesting that the concentrations of these decomposition products are below the detection limit of our analytic method. For diclofenac and ethinylestradiol we could also conduct a spectrometric analysis, using a diode array detector (DAD) that was part of the HPLC system. With this method we were actually able to detect some decomposition products and the actual increase of their concentrations with treatment time as it is shown for example in Fig. S1b. A further advantage of the DAD was the possibility to verify retention times in the HPLC. Measurements obtained with mass spectrometer (MS) and spectrometric (DAD) agree well with each other.

The retrieval rate R was defined as the ratio of the concentration of the unchanged analyte that could be recovered after the treatment and the corresponding concentration of the untreated control. All pharmaceuticals showed a decrease with the number of applied discharges. Diclofenac and ethinylestradiol are readily decomposed. Ibuprofen, carbamazepine and trimethoprim decompose at a 3–4 times slower rate. Diazepam and diatrizoate were the most stable of the investigated substances. Diclofenac and ethinylestradiol were completely destroyed after the application of 80,000 discharges while concentrations of carbamazepine and ibuprofen were reduced by 90% and 86%, respectively. The concentration of diatrizoate was reduced by 45% and diazepam by 53%. Results are summarized in Fig. 3.

The corresponding electrical energy per order (EEO) and the energy yield, G, for a degradation of 90% is presented in Table 2. EEO is defined as electrical energy necessary to achieve the
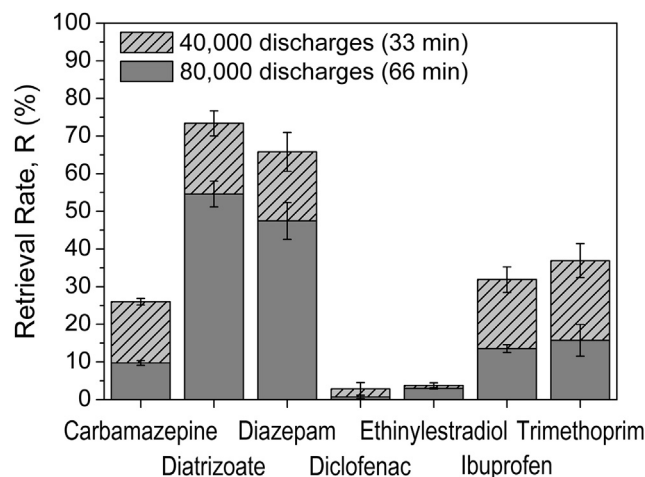


**Fig. 3.** Different pharmaceuticals have been dissolved in a concentration of 500 μg/l in water and treated with 40,000 or 80,000 discharges, corresponding to total treatment times of 33 min and 66 min, respectively. All experiments have been conducted at least in triplicates.

**Table 2**
Electrical Energy per Order (EEO) and G-value for 7 tested pharmaceuticals. Treated volume was 300 ml. EEO is defined as the amount of electrical energy (kWh), required to reduce the concentration of a pollutant by one order of magnitude (90%). G-value is calculated correspondingly for a 90% degradation.

| Pharmaceutical | EEO (kWh/m$^3$) | G-value (mg/kWh) |
| --- | --- | --- |
| Diclofenac | 27 | 45 |
| Ethinylestradiol | 32 | 38 |
| Carbamazepine | 80 | 15 |
| Ibuprofen | 97 | 13 |
| Trimethoprim | 114 | 11 |
| Diazepam | 258 | 5 |
| Diatrizoate | 430 | 3 |

decomposition of a substance by one order of magnitude or 90%. The energy yield, G, for a degradation of 90% of a substance is calculated for an assumed first order kinetic (Spinks 1976).

### 3.2. Water quality parameters

The technology of submersed corona discharges for the degradation of pharmaceuticals was investigated with the goal of improving drinking water quality. We have therefore analyzed important water quality parameters that might be affected, such as pH-value, changes in conductivity, concentrations of nitrates and nitrites and in addition concentrations of dissolved oxygen. All measurements were conducted with a multi parameter probe for samples taken from the expansion reservoir with the exception of the assessment of concentrations of nitrates and nitrites. All experiments were repeated at least three times with results and errors determined as mean values and standard deviations accordingly. Detailed results are shown in Table S2. Temperature data are not reported since the circulated volume was water-chilled during the treatment and the water temperature kept below 35 °C. We observed similar characteristics and trends for all investigated pharmaceuticals. The initial pH-values, after the pharmaceuticals had been dissolved, were in the range from 6.4 to 7.1 with standard deviations of 0.1–0.3. However, small initial differences (i.e. at the start of a treatment) are most likely due to different amounts of dissolved carbon dioxide. Notable pH-values stayed almost constant during the treatment. At most we observed a slight decrease in all experiments to values in the range from 6.2 to 6.7 and standard deviations similar to initial values. Simultaneously, conductivities were slightly increasing by 10–15 μS/cm during treatment. The most significant differences were observed for the amount of dissolved oxygen, which doubled during the application of 80,000 discharges from values of 3.6–6.3 mg/l to 6.9–13.6 mg/l.

Probably the most important water quality parameters that we monitored were the amounts of nitrate and nitrite created as a result of the plasma development as shown in Fig. S2. We observed only minor changes with results for individual measurements that were often close to the detection limit of the method of 2.5 μM. After 10,000 discharges, the concentrations of nitrate and nitrite that were found were 0.51 mg/l and 0.35 mg/l, respectively. Consecutive treatments with up to 80,000 discharges only resulted in a small further increase of these values with a final concentration of 1.29 mg/l for nitrate and 0.39 mg/l for nitrite.

### 3.3. Hydrogen peroxide production

We hypothesize that the generation of hydroxyl radicals is primarily responsible for degradation of the pharmaceuticals. Hydrogen peroxide production is often considered a useful indicator for hydroxyl radical formation in plasma systems because the recombination of OH radicals is expected to be a major pathway for

H$_2$O$_2$ generation (Eq. (1)) (Locke and Shih, 2011).

$$\cdot OH + \cdot OH \rightarrow H_2O_2 \tag{1}$$

However, yields of hydrogen peroxide can be affected by many factors and therefore the easy-to-measure H$_2$O$_2$-production should only be used for comparison and guidance of plasma mechanisms. Still analysis of hydrogen peroxide generation is an important parameter for an initial assessment of our hypothesis and for the characterization of efficacy of the interaction of a plasma with water(Lukes et al., 2014). Results for hydrogen peroxide production are shown in dependence of the number of discharges that were applied in Fig. S3. Concentrations of hydrogen peroxide seem to increase fairly linearly in the range from 0 to 30,000 discharges, reaching a value of 60 mg/l. However, for more than 30,000 discharges, the concentration appears to level off and approach saturation at a value of about 100–120 mg/l after 80,000 discharges were applied. Locke and Shih have shown, that for direct discharges in liquids, the energy required for the generation of hydrogen peroxide is generally in the range of 0.5–1 g/kWh (Locke and Shih, 2011). From the initial slope (between 0 and 30,000 discharges) we determined a value of 1.6 g/kWh for our experiments.

### 3.4. Degradation mechanism of phenol used as a chemical probe

Detection of relatively high amounts of hydrogen peroxide indicate significant production of hydroxyl radicals by plasma in water. A strong oxidation potential of 2.8 eV and almost diffusion controlled reaction rates suggest a major contribution of hydroxyl radicals to the degradation of stable pharmaceuticals. Still the question remains if and how OH radicals generated in plasma channels can be effective also in the bulk of the liquid. Using an approach adopted from the field of radiation chemistry, locally high hydroxyl radical concentrations in non-homogeneous radiation tracks in water suggest that OH radicals most likely react in the radiation track itself (i.e. recombine to H$_2$O$_2$, reform back to water, react with target compound). These radiation tracks have significant similarities to plasma channels in liquids and suggest common mechanisms for both processes (Locke and Shih, 2011). Conversely, findings in the field of sonochemistry suggest that substances with a high vapor pressure can also diffuse from the bulk into the plasma region. Furthermore non-volatile compounds could diffuse into the plasma channel although this depends on their hydrophilicity (Franclemont and Thagard, 2014).
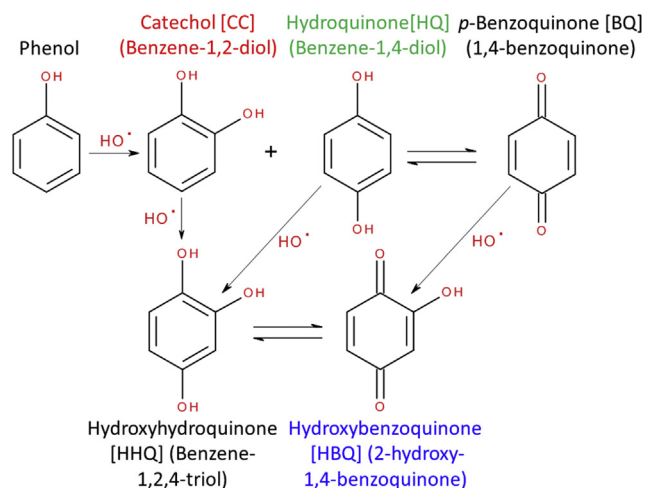


**Fig. 4.** Possible reaction pathways of phenol with hydroxyl radicals that are generated in a coaxial discharge geometry using nanosecond pulse discharges.

Decomposition mechanisms of phenol by reactions with different radicals are well understood (Lukes et al., 2014). Fig. 4 illustrates, for example, the degradation of phenol by hydroxyl radicals.

In our experiments we identified typical hydroxylated products of phenol (caused by OH radical oxidation), such as benzoquinone (BQ), hydroxybenzoquinone (HBQ), catechol (CC), and hydroquinone (HQ), as shown in Fig. 5. There was no evidence for chemical reactions involving ozone due to the absence of muconic acid, which is a typical product formed after benzene ring cleavage by ozone attack (Lukes et al., 2014). No nitrated products of phenol, as a result of reactions with reactive nitrogen species, or other peaks e.g. chlorophenols were found. Although we cannot exclude other reaction products besides hydroxylated products, their concentrations might be too low for our detection method. The amount of benzoquinone was steadily increasing during the treatment, while other by-products were decreasing or showing signs of saturation. The intermediate product hydroxyhydroquinone (HHQ) could not be identified, but its reaction product hydroxybenzoquinone (HBQ) was clearly detected.

## 4. Discussion

All investigated pharmaceuticals were effectively decomposed by 45%–99% after approximately 1 h of treatment. Notable is the degradation of the X-ray contrast agent diatrizoate which could be reduced by 45%. In comparison, Ternes et al. reported only 14% degradation for a suspension of diatrizoate in water of 5.7 μg/l and an ozone concentration of 10 mg/l (Ternes et al., 2003). In the same study, the effect of hydrogen peroxide concentrations of 10 mg/l were investigated with and without UV irradiation, but likewise, only resulted in degradation rates of 25% and 36%, respectively. Diazepam is another substance that is not very responsive to ozone treatment. Huber et al. reported that the second-order rate constant for the reaction of diazepam with ozone was very low (equivalent to a 24% degradation of a concentration of diazepam of 142 μg/l) and that direct ozone reactions were less important than oxidation by hydroxyl radicals (Huber et al., 2003). In addition, diazepam is described in literature as practically not biodegradable (Larsen et al., 2004). However, the drug was reduced by more than 50% in our experiments. Hence, in comparison with these methods, corona discharges in water seem to provide an effective method for the degradation of such stable chemical compounds.

Especially ethinylestradiol and diclofenac were almost completely destroyed. Both pharmaceuticals are on a watch list of the European Union for substances or substance groups that are monitored since March 2015 with the goal to eventually completely eliminate their release into the environment by 2020 [Water Framework Directive, Directive 2008/105/EC, Decision (EU) 2015/495 of 20 March 2015] (Commission).

So far investigations on the degradation of organic molecules by corona discharges generated in or close to water were mostly conducted in point-to-plane geometries in small volumes (Sugiarto and Sato, 2001; Sato, 2009; Malik et al., 2002). Lukes et al. have found for such a configuration EEO-values of 281–457 kWh/m$^3$ in their needle-plate experiments for the degradation of phenol derivatives for initial concentrations of 47–70 mg/l (Lukes and Locke, 2005). These values for the EEO are in the same order of magnitude as our results although the investigated substances are different. Conversely, Gerrity et al. have already determined an EEO below 2.2 kWh/m$^3$ for the destruction of carbamazepine, studied in a treatment volume of 150 l (Gerrity et al., 2010). Hereby the discharge was generated in a needle-plate geometry penetrating the water surface. Treatment conditions and water parameter are important, with larger total treatment volumes and smaller concentrations of pollutants, degradation may result in higher energy efficiencies. It should be noted that the energy efficiencies described for these systems as presented in Table 2 relate to the total electrical energy that is dissipated in discharges. Accordingly a comparison with other AOPs, e.g. UV-treatments, is likewise only possible taking into account the total costs of such treatments and total electrical energy dissipated for example by the UV-lamp (including loss mechanisms) and required for generation of chemical agents, such as $H_2O_2$.

Improvements of the energy efficiency will depend on a large extend on the use of more advanced electrode arrangements. Branched electrode designs will provide higher surfaces and reaction zones, which should increase energy efficiency. Another important parameter for the generation of radicals is the shape of the applied high voltage pulses. The generation of radicals in plasma is primarily based on the dissociation of water molecules by electron impact. Conversely, according for example to Sunka et al., electrolytic effects can be excluded and also the electrolytic decomposition associated with discharges in water is negligible (Sunka et al., 1999). Electrons need to acquire rather high energies in the plasma. Short, high voltage pulses with a fast rise time are an efficient way to impart the electrical energy primarily on electrons. For longer voltage pulses is the energy increasingly dissipated in thermal losses, which in fact is also the case for the long tail of the high voltage pulses in our experiments. Instead of using pulses with an exponential decay, future investigations focusing on efficiency should be conducted with short square pulses with fast rise times.

The main technological advantage of corona discharges generated directly in water is the effective degradation of persistent chemical compounds. In addition we observed only minor changes in water quality. Whereas plasmas that are generated in air commonly result in a drop in pH-values and significant nitrification (Oehmigen et al., 2010), we measured only small changes in pH-values. We observed concentrations for nitrate and nitrite of 1.29 mg/l and 0.39 mg/l, respectively. Drinking water standards usually mandate very strict upper limits. The drinking water ordinance in Germany for example permits no more than 50 mg/l nitrate in tap water and for nitrite a permissible maximum concentration of 0.5 mg/l. The values that we found for the application of corona discharges generated in water are comfortably below these limits. The formation of hydrogen peroxide will further
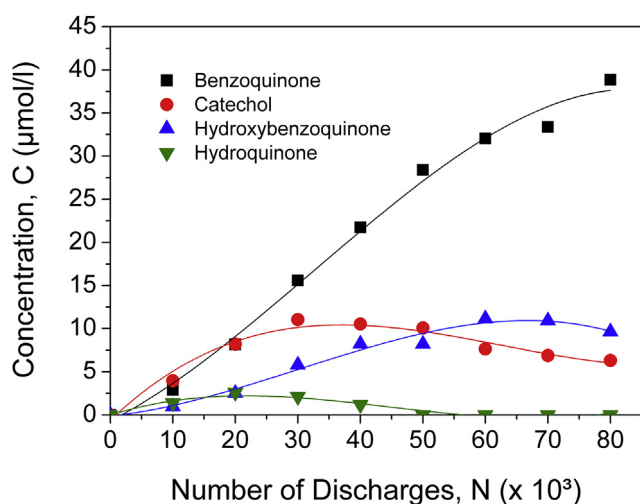


**Fig. 5.** Formation of hydroxylated products of phenol during the application of 80,000 discharges. Reaction products identified are: benzoquinone (BQ), hydroxybenzoquinone (HBQ), catechol (CC), hydroquinone (HQ).

reduce bromate, which is a regulated carcinogenic and formed after bromide oxidation for example when ozone is present (Von Gunten and Oliveras, 1998). However, cough medicine (dextromethorphan hydrobromide, ambroxol), spasmolytics (butylscopolamine-bromide) and tranquilizer (bromazepam) contain high amounts of bromide. Accordingly, bromate formation during treatment with pulsed discharges for waste water polluted with such pharmaceuticals, or in general waste water with high bromide concentrations, should be investigated in the future. The experiments presented here are a first proof-of-principle for the degradations of stable chemical compounds in a sizable volume, keeping in mind that some classes of pharmaceuticals, for example radio contrast agents, are very recalcitrant with respect to other conventional and also advanced degradation methods.

At the moment there are no mandatory legal limits for these pharmaceutical residues, but the European Commission is now demanding monitoring diclofenac and 17α-ethinylestradiol with a maximum acceptable method detection limit of 10 ng/l and 0.0035 ng/l, respectively. Therefore, upcoming legislation will eventually require the use of new abatement strategies and corona discharges generated directly in water present themselves as a feasible technology. Further developments of method and systems will most likely significantly reduce energy costs and losses.

## 5. Conclusion

Discharges in water may provide a solution for a problem that so far cannot be reasonably addressed by conventional methods. Our goal here was to study the effect of corona discharges. The experiments demonstrate the potential of the approach for the decomposition of chemical pollutants.

An inherent advantage of the method is the penetration of the treated volume with discharge filaments which is to a considerable degree independent from turbidity and does not rely on continuous supply of oxidizing agents, such as chlorine, ozone or hydrogen peroxide (Mehrjouei et al., 2015).

Water quality, especially pH-value and concentrations of nitrate and nitrite, was not changing significantly. Due to the formation of hydrogen peroxide also the formation of high borate concentrations seems to be unlikely. The absence of nitrified, chlorinated or ozonated reaction products is another advantage with respect to maintaining good water quality. Together with the observed degradation products of phenol, this allows for the conclusion that hydroxyl radicals are primarily responsible for degradation.

Energy efficiency is still a critical issue of the method and needs to be improved (Unless the conceived threat by pharmaceutical residues and other organic compounds in drinking water will render higher water treatment costs acceptable.). The efficiency is already inherently better than for a spark discharge system (500 J/pulse) as it was brought into operation by Chang and his co-workers (Yantsis et al., 2008). Further developments of the corona discharge approach will have to take pulse shaping and electrode design into account. In addition pilot installations that are operated under realistic conditions, e.g. for waste water effluents for different sites, will need to gather data on operation costs and general long term efficacy. In this respect it will also be necessary to study decomposition products for their toxicity and environmental impact and the possibility of combining corona discharges with other AOPs like photo catalysts or UV-irradiation to exploit possible synergies.

## Acknowledgment

## Appendix A. Supplementary data

Supplementary data related to this article can be found at http://dx.doi.org/10.1016/j.watres.2015.07.018.

## References

Banaschik, R., Koch, F., Kolb, J.F., Weltmann, K.D., 2014. Decomposition of pharmaceuticals by pulsed corona discharges in water depending on streamer length. Plasma Sci. IEEE Trans. 42 (10), 2736–2737.

Belfroid, A., Van der Horst, A., Vethaak, A., Schäfer, A., Rijs, G., Wegener, J., Cofino, W., 1999. Analysis and occurrence of estrogenic hormones and their glucuronides in surface water and waste water in The Netherlands. Sci. Total Environ. 225 (1), 101–108.

Brodin, T., Fick, J., Jonsson, M., Klaminder, J., 2013. Dilute concentrations of a psychiatric drug alter behavior of fish from natural populations. Science 339 (6121), 814–815.

Commission, 24 March 2015. Commission implementing decision (EU) 2015/495 of 20 March 2015 establishing a watch list of substances for Union-wide monitoring in the field of water policy pursuant to Directive 2008/105/EC of the European Parliament and of the Council. Off. J. Eur. Union L 78. ISSN: 1977-0677 58, 40–42.

Dobrin, D., Bradu, C., Magureanu, M., Mandache, N., Parvulescu, V., 2013. Degradation of diclofenac in water using a pulsed corona discharge. Chem. Eng. J. 234, 389–396.

Foster, J., Sommers, B.S., Gucker, S.N., Blankson, I.M., Adamovsky, G., 2012. Perspectives on the interaction of plasmas with liquid water for water purification. Plasma Sci. IEEE Trans. 40 (5), 1311–1323.

Foster, J.E., Adamovsky, G., Gucker, S.N., Blankson, I.M., 2013. A comparative study of the time-resolved decomposition of methylene blue dye under the action of a nanosecond repetitively pulsed DBD plasma jet using liquid chromatography and spectrophotometry. Plasma Sci. IEEE Trans. 41 (3), 503–512.

Franclemont, J., Mededovic Thagard, S., 2014. Pulsed electrical discharges in water: can non-volatile compounds diffuse into the plasma channel? Plasma Chem. Plasma Process 34 (4), 705–719.

Gerrity, D., Stanford, B.D., Trenholm, R.A., Snyder, S.A., 2010. An evaluation of a pilot-scale nonthermal plasma advanced oxidation process for trace organic compound degradation. Water Res. 44 (2), 493–504.

Giri, R., Ozaki, H., Ota, S., Takanami, R., Taniguchi, S., 2010. Degradation of common pharmaceuticals and personal care products in mixed solutions by advanced oxidation techniques. Int. J. Environ. Sci. Tech. 7 (2), 251–260.

Health, I., 2012. National Prescription Audit.

Heberer, T., 2002. Occurrence, fate, and removal of pharmaceutical residues in the aquatic environment: a review of recent research data. Toxicol. Lett. 131 (1), 5–17.

Hijosa-Valsero, M., Molina, R., Schikora, H., Müller, M., Bayona, J.M., 2013. Removal of priority pollutants from water by means of dielectric barrier discharge atmospheric plasma. J. Hazard. Mater. 262 (0), 664–673.

Hoffmann, F., Kloas, W., 2012. Estrogens can disrupt amphibian mating behavior. PLoS One 7 (2), e32097.

Huber, M.M., Canonica, S., Park, G.-Y., von Gunten, U., 2003. Oxidation of pharmaceuticals during ozonation and advanced oxidation processes. Environ. Sci. Technol. 37 (5), 1016–1024.

Jekel, M., Dott, W., Bergmann, A., Dünnbier, U., Gnirß, R., Haist-Gulde, B., Hamscher, G., Letzel, M., Licha, T., Lyko, S., Miehe, U., Sacher, F., Scheurer, M., Schmidt, C.K., Reemtsma, T., Ruhl, A.S., 2015. Selection of organic process and source indicator substances for the anthropogenically influenced water cycle. Chemosphere 125 (0), 155–167.

Jjemba, P.K., 2006. Excretion and ecotoxicity of pharmaceutical and personal care products in the environment. Ecotoxicol. Environ. Saf. 63, 113–130.

Katsoyiannis, I., Canonica, S., von Gunten, U., 2011. Efficiency and energy requirements for the transformation of organic micropollutants by ozone, O₃/H₂O₂ and UV/H₂O₂. Water Res. 45 (13), 3811–3822.

Kosjek, T., Andersen, H.R., Kompare, B., Ledin, A., Heath, E., 2009. Fate of carbamazepine during water treatment. Environ. Sci. Technol. 43 (16), 6256–6261.

Krause, H., Schweiger, B., Schuhmacher, J., Scholl, S., Steinfeld, U., 2009. Degradation of the endocrine disrupting chemicals (EDCs) carbamazepine, clofibric acid, and iopromide by corona discharge over water. Chemosphere 75 (2), 163–168.

Kümmerer, K., 2009a. Antibiotics in the aquatic environment – a review – part I. Chemosphere 75 (4), 417–434.

Kümmerer, K., 2009b. Antibiotics in the aquatic environment – a review – part II. Chemosphere 75 (4), 435–441.

Larsen, T.A., Lienert, J., Joss, A., Siegrist, H., 2004. How to avoid pharmaceuticals in the aquatic environment. J. Biotechnol. 113 (1–3), 295–304.

Locke, B.R., Shih, K.-Y., 2011. Review of the methods to form hydrogen peroxide in electrical discharge plasma with liquid water. Plasma Sour. Sci. Technol. 20 (3), 034006.

Locke, B.R., Thagard, S.M., 2012. Analysis and review of chemical reactions and transport processes in pulsed electrical discharge plasma formed directly in liquid water. Plasma Chem. Plasma Process. 32 (5), 875–917.

Lukes, P., Appleton, A.T., Locke, B.R., 2004. Hydrogen peroxide and ozone formation in hybrid gas-liquid electrical discharge reactors. Ind. Appl. IEEE Trans. 40 (1), 60–67.

Lukes, P., Dolezalova, E., Sisrova, I., Clupek, M., 2014. Aqueous-phase chemistry and bactericidal effects from an air discharge plasma in contact with water: evidence for the formation of peroxynitrite through a pseudo-second-order post-discharge reaction of $H_2O_2$ and $HNO_2$. Plasma Sour. Sci. Technol. 23 (1), 015019.

Lukes, P., Locke, B.R., 2005. Degradation of substituted phenols in a hybrid gas-liquid electrical discharge reactor. Ind. Eng. Chem. Res. 44 (9), 2921–2930.

Magureanu, M., Mandache, N.B., Parvulescu, V.I., 2015. Degradation of pharmaceutical compounds in water by non-thermal plasma treatment. Water Res. 81 (0), 124–136.

Magureanu, M., Dobrin, D., Bogdan Mandache, N., Bradu, C., Medvedovici, A., Parvulescu, V.I., 2013. The mechanism of plasma destruction of enalapril and related metabolites in water. Plasma Process. Polym. 10 (5), 459–468.

Magureanu, M., Piroi, D., Mandache, N.B., David, V., Medvedovici, A., Bradu, C., Parvulescu, V.I., 2011. Degradation of antibiotics in water by non-thermal plasma treatment. Water Res. 45 (11), 3407–3416.

Magureanu, M., Piroi, D., Mandache, N.B., David, V., Medvedovici, A., Parvulescu, V.I., 2010. Degradation of pharmaceutical compound pentoxifylline in water by non-thermal plasma treatment. Water Res. 44 (11), 3445–3453.

Malik, M.A., Kolb, J.F., Schoenbach, K.H., 2011. Streamers in water and along the insulator surface in a wire – cylinder gap. IEEE Trans. Plasma Sci. 39 (11), 2626–2627.

Malik, M.A., Minamitani, Y., Xiao, S., Kolb, J.F., Schoenbach, K.H., 2005. Streamers in water filled wire-cylinder and packed-bed reactors. IEEE Trans. Plasma Sci. 33 (2), 490–491.

Malik, M.A., Ubaid-ur-Rehman, Ghaffar, A., Ahmed, K., 2002. Synergistic effect of pulsed corona discharges and ozonation on decolourization of methylene blue in water. Plasma Sour. Sci. Technol. 11 (3), 236.

Mantzavinos, D., Psillakis, E., 2004. Enhancement of biodegradability of industrial wastewaters by chemical oxidation pre-treatment. J. Chem. Technol. Biotechnol. 79 (5), 431–454.

Mehrjouei, M., Müller, S., Möller, D., 2015. A review on photocatalytic ozonation used for the treatment of water and wastewater. Chem. Eng. J. 263 (0), 209–219.

Minamitani, Y., Shoji, S., Ohba, Y., Higashiyama, Y., 2008. Decomposition of dye in water solution by pulsed power discharge in a water droplet spray. Plasma Sci. IEEE Trans. 36 (5), 2586–2591.

Nentwig, G., 2007. Effects of pharmaceuticals on aquatic invertebrates. Part II: the antidepressant drug fluoxetine. Arch. Environ. Contam. Toxicol. 52 (2), 163–170.

Oaks, J.L., Gilbert, M., Virani, M.Z., Watson, R.T., Meteyer, C.U., Rideout, B.A., Shivaprasad, H.L., Ahmed, S., Iqbal Chaudhry, M.J., Arshad, M., Mahmood, S., Ali, A., Ahmed Khan, A., 2004. Diclofenac residues as the cause of vulture population decline in Pakistan. Nature 427 (6975), 630–633.

Oehmigen, K., Hähnel, M., Brandenburg, R., Wilke, C., Weltmann, K.D., von Woedtke, T., 2010. The role of acidification for antimicrobial activity of atmospheric pressure plasma in liquids. Plasma Process. Polym. 7 (3-4), 250–257.

Panorel, I., Preis, S., Kornev, I., Hatakka, H., Louhi-Kultanen, M., 2012. Oxidation of aqueous pharmaceuticals by pulsed corona discharge. Environ. Technol. 34 (7), 923–930.

Panorel, I., Preis, S., Kornev, I., Hatakka, H., Louhi-Kultanen, M., 2013. Oxidation of aqueous paracetamol by pulsed Corona discharge. Ozone Sci. Eng. 35 (2), 116–124.

Pintar, A., Besson, M., Gallezot, P., Gibert, J., Martin, D., 2004. Toxicity to Daphnia magna and Vibrio fischeri of Kraft bleach plant effluents treated by catalytic wet-air oxidation. Water Res. 38 (2), 289–300.

Poyatos, J., Munio, M., Almecija, M., Torres, J., Hontoria, E., Osorio, F., 2010. Advanced oxidation processes for wastewater treatment: state of the art. Water Air Soil Pollut. 205 (1–4), 187–204.

Purdom, C.E., Hardiman, P.A., Bye, V.V.J., Eno, N.C., Tyler, C.R., Sumpter, J.P., 1994. Estrogenic effects of effluents from sewage treatment works. Chem. Ecol. 8 (4), 275–285.

Reuter, S., Tresp, H., Wende, K., Hammer, M.U., Winter, J., Masur, K., Schmidt-Bleker, A., Weltmann, K.D., 2012. From RONS to ROS: tailoring plasma jet treatment of skin cells. Plasma Sci. IEEE Trans. 40 (11), 2986–2993.

Sato, M., 2008. Environmental and biotechnological applications of high-voltage pulsed discharges in water. Plasma Sour. Sci. Technol. 17 (2).

Sato, M., 2009. Degradation of organic contaminants in water by plasma. Int. J. Plasma Environ. Sci. Technol. 3 (1).

Schramm, C., Gans, O., Uhl, M., Grath, J., Scharf, S., Zieritz, I., Kralik, M., Scheidleder, A., Humer, F., 2006. Carbamazepin und Koffein–Potenzielle Screeningparameter für Verunreinigungen des Grundwassers durch Kommunales Abwasser.

Spinks, J.W.T., Woods, R.J., 1976. An Introduction to Radiation Chemistry. Wiley, New York.

Stackelberg, P.E., Furlong, E.T., Meyer, M.T., Zaugg, S.D., Henderson, A.K., Reissman, D.B., 2004. Persistence of pharmaceutical compounds and other organic wastewater contaminants in a conventional drinking-water-treatment plant. Sci. Total Environ. 329 (1), 99–113.

Stumpf, M., Ternes, T.A., Haberer, K., Baumann, W., 1996. Nachweis von natürlichen und synthetischen Östrogenen in Kläranlagen und Fließgewässern. Vom Wasser 87, 251–261.

Sugiarto, A.T., Sato, M., 2001. Pulsed plasma processing of organic compounds in aqueous solution. Thin Solid Films 386 (2), 295–299.

Sunka, P., Babický, V., Clupek, M., Lukes, P., Simek, M., Schmidt, J., Cernák, M., 1999. Generation of chemically active species by electrical discharges in water. Plasma Sour. Sci. Technol. 8 (2), 258.

Ternes, T.A., 1998. Occurrence of drugs in German sewage treatment plants and rivers1. Water Res. 32 (11), 3245–3260.

Ternes, T.A., Meisenheimer, M., McDowell, D., Sacher, F., Brauch, H.-J., Haist-Gulde, B., Preuss, G., Wilme, U., Zulei-Seibert, N., 2002. Removal of pharmaceuticals during drinking water treatment. Environ. Sci. Technol. 36 (17), 3855–3863.

Ternes, T.A., Stüber, J., Herrmann, N., McDowell, D., Ried, A., Kampmann, M., Teiser, B., 2003. Ozonation: a tool for removal of pharmaceuticals, contrast media and musk fragrances from wastewater? Water Res. 37 (8), 1976–1982.

Vogna, D., Marotta, R., Andreozzi, R., Napolitano, A., d'Ischia, M., 2004. Kinetic and chemical assessment of the $UV/H_2O_2$ treatment of antiepileptic drug carbamazepine. Chemosphere 54 (4), 497–505.

Von Gunten, U., Oliveras, Y., 1998. Advanced oxidation of bromide-containing waters: bromate formation mechanisms. Environ. Sci. Technol. 32 (1), 63–70.

Yantsis, S., Chow-Fraser, P., Li, O., Guo, Y., Chang, J., Terui, S., Watanabe, K., Itoh, M., 2008. Zooplankton mortality in Lake water treated by pulsed arc electrohydraulic discharge plasma. Int. J. Plasma Environ. Sci. Technol. 2 (2), 128–133.

Zwiener, C., Frimmel, F.H., 2003. Short-term tests with a pilot sewage plant and biofilm reactors for the biological degradation of the pharmaceutical compounds clofibric acid, ibuprofen, and diclofenac. Sci. Total Environ. 309 (1–3), 201–211.

## Publication P3

## Fenton chemistry promoted by sub-microsecond pulsed corona plasmas for organic pollutant degradation in water

R. Banaschik, P. Lukes, C. Miron, R. Banaschik, A. Pipa, K. Fricke, P.J. Bednarski and J. F. Kolb, *Electrochimica Acta*, 245 (2017) 539-548.
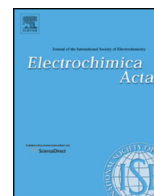
# Fenton chemistry promoted by sub-microsecond pulsed corona plasmas for organic micropollutant degradation in water

Robert Banaschik[a], Petr Lukes[b], Camelia Miron[a], Richard Banaschik[c], Andrei V. Pipa[a], Katja Fricke[a], Patrick J. Bednarski[d], Juergen F. Kolb[a,*]

[a] Leibniz Institute for Plasma Science and Technology (INP Greifswald e.V.), Felix-Hausdorff-Straße 2, 17489 Greifswald, Germany
[b] Department of Pulse Plasma Systems, Institute of Plasma Physics of the CAS, v.v.i., Za Slovankou 3, 182 00 Prague 8, Czech Republic
[c] Fraunhofer Research Institution Large Structures in Production Technology, Albert-Einstein-Straße 30, 18059 Rostock, Germany
[d] Institute of Pharmacy, University of Greifswald, Friedrich-Ludwig-Jahn-Straße 17, 17489 Greifswald, Germany

ABSTRACT

Differences in the liquid chemistry due to different ground electrode materials (titanium, stainless steel) were compared for corona discharges in water. The plasma was generated by applying positive high voltage pulses that are characterized by short rise times of about 20 ns, a peak voltage of 80 kV and pulse lengths of about 150–160 ns (FWHM). Phenol was admixed to the water for quantification of the bulk reaction chemistry, such as phenol decomposition and $H_2O_2$-formation. Optical emission spectroscopy was conducted to relate chemistry to plasma processes. Possible electrode corrosion was determined by atomic absorption spectroscopy (AAS).

The post-discharge chemistry strongly depends on ground electrode material. With stainless steel electrodes, decomposition efficiency of phenol increased by about three quarters (74.9 %) when compared with titanium electrodes. This result can be explained by dissolved metal ions corroded from the ground electrode, which catalytically decomposed the $H_2O_2$ that had been formed into hydroxyl radicals again. Ground electrodes were corroded due to electrochemical processes. Corrosion rates and overall reaction chemistries cannot readily be described similar to conventional DC electrochemical processes at low voltages. The repetitive application of sub-microsecond high voltage pulses has to be taken into account explicitly. Altogether, electrode materials, ground electrode corrosion and associated catalytic processes are more important for plasma processes in aqueous solutions than was recognized so far. Therefore, the effects need to be taken into account in the analysis of laboratory results as well as the development of respective novel water treatment technologies.

© 2017 Elsevier Ltd. All rights reserved.

## 1. Introduction

Plasmas provide different physical and chemical active processes, such as the formation of reactive species, UV-radiation, shock waves and strong electric fields. For water purification, these combined mechanisms can provide higher efficacy than traditional or more selective water treatment methods alone. Consequently, plasmas, such as pulsed corona discharges, have been successfully applied for the decomposition of organic pollutants and the killing of bacteria [1–6].

Decomposition of organic compounds is primarily mediated by the formation of transient species, e.g. hydroxyl radicals and peroxynitrites, but also due to long-lived chemical reaction products, such as ozone and hydrogen peroxide. If not consumed during oxidation processes, reactive species eventually recombine to pure water [7].

Fundamental principles of plasma generation in water include the application of nanosecond to millisecond high voltage pulses, preferably with positive polarity, in combination with high curvatures of the high voltage electrodes. For the application of short high voltage pulses is the voltage needed to instigate streamers considerably lower for positive polarity. Furthermore, streamers initiated with a positive high voltage are longer and more fractured in appearance than more bushy streamers that are obtained for negative voltages [8]. High curvatures (wire, needle tips) are hereby corresponding to higher electric fields close to the high voltage electrode, leading to plasma filaments propagating from the high voltage electrode to the ground electrode. The

propagation of the plasma channel continues as long as the electric field is high enough to sustain an electron avalanche process from the liquid interface towards the anode. For positive voltages is a positive space charge at the streamer head promoting further ionization of water molecules [9]. Radical species, hydroxyl and hydrogen radicals, are formed along the discharge channel primarily by electron-impact dissociation and subsequent reactions of the species with each other and the surrounding liquid [10]. Production rates depend on ambient parameters, such as liquid conductivity and pH-value, as well as on operating parameters, foremost duration and amplitude of the applied high voltage pulses.

It is known that the high voltage electrode material does effect streamer propagation [11]. The lifetime of a discharge system is generally determined by the resilience of the high voltage electrode, which can suffer from erosive and corrosive processes when enveloped by plasma [12].

Consequently, high voltage electrode material can influence plasma chemical processes in water due to the release of metal ions and solid particles by its erosion in the discharge. Liquid catalytic reactions during and after the plasma treatment are promoted and contributing to the reaction chemistry [13–21].

Concerning the mechanism of the discharge-induced erosion of high voltage electrodes, the electrolytic anodic oxidation and plasma sputtering of metal are expected to play the main role in the release of electrode material into the liquid [22].

There are no apparent reasons for any influence of ground electrode materials, since these electrodes are not directly subjected to the plasma in corona discharges. Accordingly, research conducted so far has focused on high voltage electrode processes, while ground electrodes and ground electrode materials received little to no attention.

However, the post-discharge chemistry that was observed for the degradation of organic pollutants by corona plasma suggests that degradation rates strongly depend on the ground electrode material (Banaschik et al., 2015). Solutions containing phenol had to be quickly mixed with methanol to stop ongoing degradation chemistry after the plasma was switched off. Responsible for the ongoing process are presumably radicals that are still forming independently from the plasma. Methanol acts as a scavenger for these radicals. These findings could not yet been explained satisfactorily by high voltage electrode corrosion alone. In coaxial discharge geometries is the high voltage electrode usually surrounded by a grounded metal electrode. Size and exposed

surface of the ground electrode are generally orders of magnitude larger than for the high voltage electrode. Therefore, processes at the ground electrode interface, corrosion and release of material into the bulk liquid might conceivable affect overall bulk reaction chemistries after all and need to be evaluated in conjunction with plasma processes accordingly.

The objective of the research presented here was to determine the influence of different ground electrode materials (titanium, stainless steel) on the liquid chemistry associated with a coaxial large volume corona discharge plasma. Plasma chemistry was investigated using phenol as a chemical probe. Byproducts of phenol decomposition and quantification of formed hydrogen peroxide allow insight in reaction chemistries and reactive species that are formed during and following the plasma treatment. Studies on chemistry were complemented by optical emission spectroscopy (OES) of the discharges in pure water. With respect to ground electrode corrosion, content of submerged and dissolved titanium or iron was measured with atomic absorption spectroscopy (AAS).

## 2. Materials and Methods

### 2.1. Experimental Setup

The discharge chamber consisted of a glass tube with an inner diameter of 47 mm and length of 138 mm, holding a volume of 240 ml. A metal mesh, made of either titanium (Ti008710/11, Goodfellow, Huntingdon, England) or stainless steel (EN 1.4571/AISI 316Ti), was attached to the inner wall of the glass tube (Fig. 1) and served as ground electrode. Surface area covered with the mesh electrode was 170 cm$^2$ with openings in the mesh of 0.19 mm (titanium) and 0.4 mm (stainless steel). Wire thickness of the titanium mesh was 0.23 mm and 0.2 mm for the stainless-steel electrode.

Due to the possible relevance of ground electrode material, metal composition and purity of the mesh electrodes were investigated with a SPECTROMAXx metal analyzer (SPECTRO Analytical Instruments GmbH, Kleve, Germany). Mesh electrodes of the same batch as used in the experiments were melted in an arc furnace applying argon (4.8) as inert gas to prevent cross contamination. The metal nugget was then polished and its composition determined at least five times.

Material of the titanium mesh electrode was proven almost pure titanium (99.7%). Only small impurities with elements such as iron, copper, and chromium were observed (Table 1).
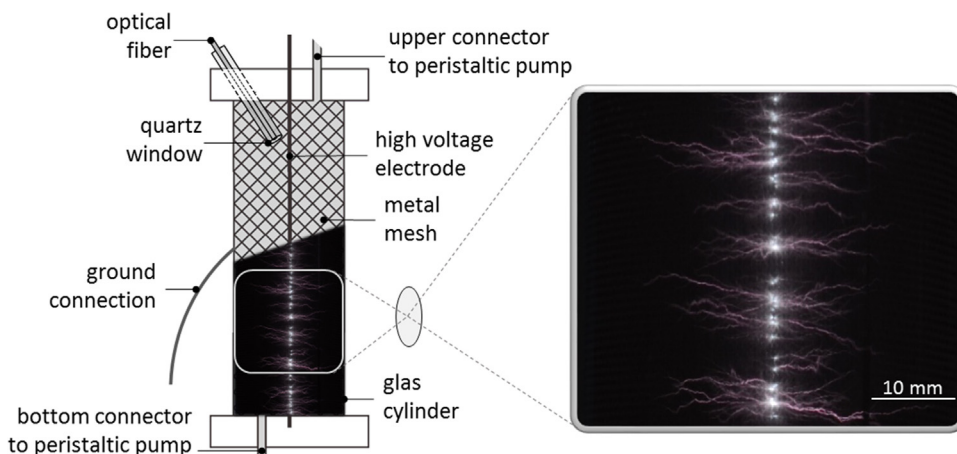


**Fig. 1.** Schematic of the experimental setup for pulsed corona discharges in liquids. A peristaltic pump with a pushing flow from the bottom to the top maintained a flow rate of 120 ml/min.

**Table 1**
Chemical composition analysis (in mass percentage) of the titanium mesh that was used as ground electrode (for n = 5 individual measurements).

|  | Ti | Fe | Mo | Cu | Mn | C |
|---|---|---|---|---|---|---|
| Component in % | 99.649 | 0.129 | 0.0454 | 0.0454 | 0.0222 | 0.0176 |
| SD in % | ±0.038 | ±0.006 | ±0.0005 | ±0.0005 | ±0.0438 | ±0.0026 |
|  | Nb | Pd | Si | Ni | Cr | Al |
| Component in % | 0.0160 | 0.0118 | 0.0108 | 0.0100 | 0.0073 | <0.002 |
| SD in % | ±0.0105 | ±0.0001 | ±0.0007 | ±0.0022 | ±0.0001 | – |

The chemical composition of the stainless-steel mesh was more complex. Main components were iron (66.7%), chromium (17.1%), nickel (11.6%) and smaller amounts of molybdenum, manganese, titanium and aluminum (Table 2). This type of high-alloy steel (EN 1.4571/AISI 316Ti) has high durability against corrosion, pitting and is applied for food preparation, chemical containers and laboratory equipment. For the major contribution, especially also with respect to chemical processes, the stainless-steel electrode is hereinafter referred to as iron electrode or iron mesh.

The high voltage electrode was made of two uncoated tungsten wires (W-005135/13, Goodfellow, Huntingdon, England) that were placed along the center of the discharge chamber and renewed between individual experiments, i.e. after the application of 80,000 discharges. Wires were manufactured by LUMA-METALL AB (Quality 821/4, LUMA-METALL AB, Kalmar, Sweden).

Positive voltage pulses were generated by a 6-stage Marx-Generator with a repetition rate of 20 Hz and applied to the high voltage electrode. Pulses are characterized by short rise times of about 20 ns, a peak voltage of 80 kV and an exponential decay resulting in pulse lengths (FWHM) of about 150–160 ns (Fig. 2).

The energy delivered with each pulse of about 1.4 J was calculated by integrating the product for the duration of the voltage and current signals. Pulsed currents through the reactor were measured with a Pearson current monitor (Model 5046, Pearson Electronics, Palo Alto, USA) connected to an oscilloscope for analysis (Wave Surfer 64MXs-B, Teledyne LeCroy, Chestnut Ridge, USA). The overall resistance, inductance and capacitance of the electrical circuit determine the pulse shape of the applied voltage, current and oscillations, respectively.

In all experiments, a volume of 300 ml of water was treated in a continuous flow system with a flow rate of 120 ml/min maintained by a peristaltic pump. A cooling system was part of the flow system and liquid temperature did not exceed 25 °C.

## 2.2. Analytic procedures and phenol degradation diagnostics

Samples for analysis were taken from an expansion reservoir (part of the water recirculation system). Studies were conducted with aqueous solutions prepared from deionized water containing 500 μM phenol. Reaction chemistry of phenol decomposition is well understood and byproducts can be used to identify several different reactive species in aqueous solutions [23,24]. Screening

**Table 2**
Chemical composition analysis (in mass percentage) of the stainless-steel mesh that was used as ground electrode (for n = 5 individual measurements).

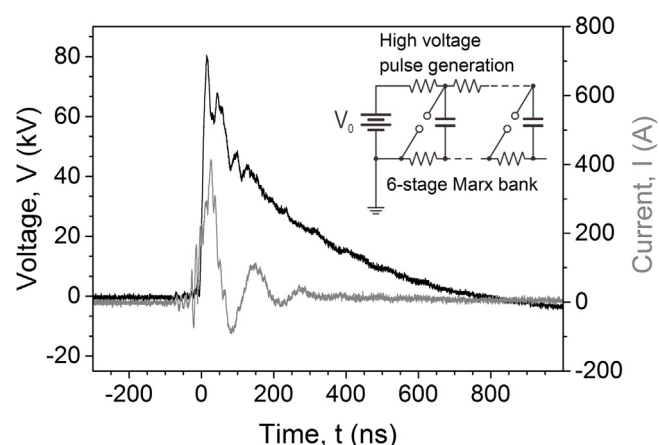|  | Fe | Cr | Ni | Mo | Mn | Si |
|---|---|---|---|---|---|---|
| Component in % | 66.74 | 17.14 | 11.63 | 1.92 | 1.10 | 0.449 |
| SD in % | ±0.11 | ±0.17 | ±0.09 | ±0.04 | ±0.01 | ±0.013 |
|  | Cu | Co | Ti | C | Nb | Al |
| Component in % |  |  |  |  |  |  |
| SD in % | 0.294 | 0.223 | 0.124 | 0.056 | 0.045 | 0.034 |



**Fig. 2.** Current and voltage characteristics for a single positive high voltage pulse that was applied to the reactor with a ground electrode made of titanium or made of iron, respectively, and water with a conductivity of 30 μS/cm.

was performed for hydroxylated products (hydroquinone, hydroxy-1,4-benzoquinone, 1,4-benzoquinone, catechol), nitrated products (4-nitrosophenol, 4-nitrocatechol, 2-nitrohydroquinone, 4-nitrophenol, 2-nitrophenol) and products formed after chemical reactions with ozone (cis,trans-muconic acid, cis,cis-muconic acid).

Because low liquid conductivities encouraged transition of the corona discharge into a spark, solution conductivity was adjusted to at least 30 μS/cm with sodium chloride. Total treatment time for each experiment was 67 min, which is equal to 80,000 discharges applied with a frequency of 20 Hz. Samples of 2 x 1 ml were taken in intervals of 10,000 applied discharges. Analysis was carried out with 250 μl methanol added immediately to the first sample of 1 ml that was taken. Methanol acted as a scavenger for radicals that could possibly be generated due to the splitting of formed hydrogen peroxide, even without plasma. The second sample of 1 ml was used for the photometric quantification of hydrogen peroxide using the titanyl sulfate method [24,25]. Procedures were the same for each ground electrode material (titanium, iron). Experiments were repeated at least three times.

Quantification of phenol and the detection of its byproducts was conducted with a Shimadzu LC-10Avp HPLC system and a Supelcosil LC-18 column (2.1 mm I.D., 25 cm, 5 μm) in combination with a Diode Array Detector (DAD) and Fluorescence Detector (Shimadzu, Kyōto, Japan). Acetonitrile (solvent A) and water (solvent B, with 1 % formic acid) were used for isocratic elution. The two-component solvent was mixed in a ratio of 10 % A and 90 % B.

## 2.3. Atomic absorption spectroscopy

Electrode corrosion, in particular corrosion of the metal mesh that served as ground electrode, was analyzed with atomic absorption spectroscopy (AAS) provided by Thermo Fischer Scientific (iCE 3500 Series, Waltham, MA). Two different operation modes were used.

Total amount of titanium dissolved in the treated solution was determined with graphite furnace atomic absorption spectroscopy (GF-AAS). Samples of 10 μl, diluted with 10 μl deionized water, were injected in pyrolytically coated electro graphite cuvettes (Thermo Fischer Scientific, Waltham, MA) and vaporized gradually up to 2500 °C. Concentration was measured using a hollow cathode lamp with a titanium cathode radiating at 365.4 nm with a bandwidth of 0.2 nm, applying Zeeman background correction.

Because of the ubiquitous occurrence of iron in environment and the fact that GF-AAS reacts quite sensitive to this metal,

concentration of iron was measured with flame atomic absorption spectroscopy (F-AAS) using an air-acetylene flame. Samples were injected directly into the air-acetylene flame (0.9 l/min) and extinction was measured at 248.3 nm with activated deuterium (D2) background correction. All experiments were repeated at least three times and concentrations were determined after correlation to the respective calibration curves.

### 2.4. Optical emission spectroscopy (OES) in water

When water is subjected to a high electric field, highly conductive channels, so called streamers, develop between the high voltage and ground electrode and plasma is spontaneously formed [8]. The light emitted by the excited species formed in the plasma in water was collected with an optical fiber immersed into the reactor. The fiber was connected to an Andor Shamrock 500 spectrograph (Andor, Belfast, UK), equipped with a Newton EMCCD camera as detector (Andor, Belfast, UK). Spectra were recorded for different wavelength regions by successively turning the grating using the Andor Solis software.

Due to the rather weak light from the streamers propagating to the ground electrode, it was necessary to point the optical fiber directly towards the tungsten high voltage electrode (Fig. 1), since density of steamers and accordingly emission intensity was higher close to the wires.

## 3. Results

### 3.1. Decomposition of phenol

Phenol decomposition can be described with a pseudo first order kinetic. The corresponding decrease in phenol concentration with the number of applied discharges (half-logarithmic plot) is shown in Fig. 3.

The figure further shows the dependences of the degradation of phenol on the electrode material. For a ground electrode made from titanium, phenol concentration decreased by 13.8 % (69 $\mu$mol/l) after the application of 80,000 discharges. An iron ground electrode resulted in a higher phenol decomposition of 24.8 %.

(124 $\mu$mol/l). The differences become distinct after the application of 20,000 discharges, indicating an increasing effect of the ground electrode material on the degradation.

### 3.2. Phenol decomposition products

The decrease in phenol concentration was accompanied by the formation of several hydroxylated products, such as 1, 4-benzoquinone, hydroxy-1,4-benzoquinone, hydroquinone and catechol. Because of their small concentrations and low stability in the solution, hydroquinone and catechol, were detected only qualitatively.

A steady increase in 1,4-benzoquinone (BQ) concentration was observed for both electrode materials (Fig. 4). Nevertheless, absolute concentrations for titanium electrodes (21.0 $\mu$M) are lower when compared to iron electrodes (35.8 $\mu$M). Notable is a slight exponential increase in 1,4-benzoquinone concentration when iron served as ground electrode material.

Compared to 1,4-benzoquinone (BQ), formation of hydroxy-1,4-benzoquinone (HBQ) possess a saturation characteristic with a maximum of 2.1 $\mu$M for titanium and 7.7 $\mu$M for the iron mesh. Concentration of hydroxy-1,4-benzoquinone is about four times lower when a titanium electrode was used.

There was no evidence for chemical reactions involving ozone (as indicated by absence of muconic acid), or reactions involving peroxynitrite (nitrated phenols). In case of ozone, muconic acid is a typical reaction product formed after a benzene ring cleavage caused by an ozone attack.

### 3.3. Hydrogen peroxide production

During plasma treatment, increasing concentrations of hydrogen peroxide were observed (Fig. 5). Different electrode materials did not affect $H_2O_2$ formation. In general, measurements indicate that hydrogen peroxide concentrations become saturated eventually. After 80,000 discharges (67 min), the maximum hydrogen peroxide concentrations were about $2.4 \pm 0.1$ mM for the titanium ground electrode and $2.45 \pm 0.1$ mM for the iron ground electrode.
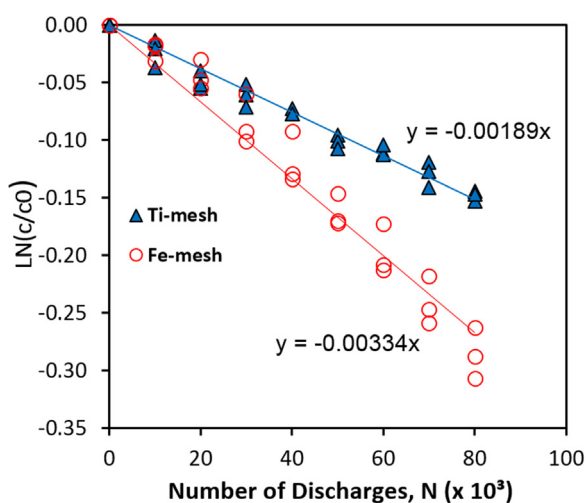


**Fig. 3.** Degradation of phenol for the continuous application of 80,000 discharges at 20 Hz. Different symbols reflect three independent experiments. Experiments were conducted with titanium (closed symbols) and stainless steel (open symbols) as ground electrode material. Linear fits of the half-logarithmic plot represent degradation rate constants of −0.00189 and −0.00334 (1/1000 pulses) for the titanium and for the iron mesh, respectively. Starting concentration of phenol was 500 $\mu$M, treated volume: 300 ml.
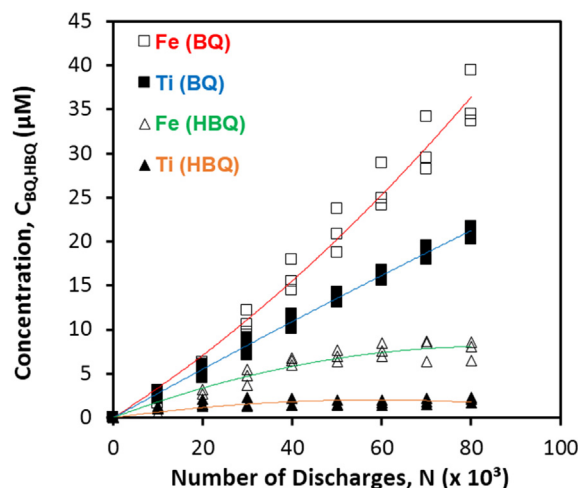


**Fig. 4.** Effect of ground electrode material (titanium, iron) on 1,4-benzoquinone (BQ) and hydroxy-1,4-benzoquinone (HBQ) formation after treatment with pulsed corona discharges. Starting concentration of phenol was 500 $\mu$M, treated volume: 300 ml. Three independent experiments were conducted with titanium (closed symbols) and iron (open symbols) as ground electrode material.
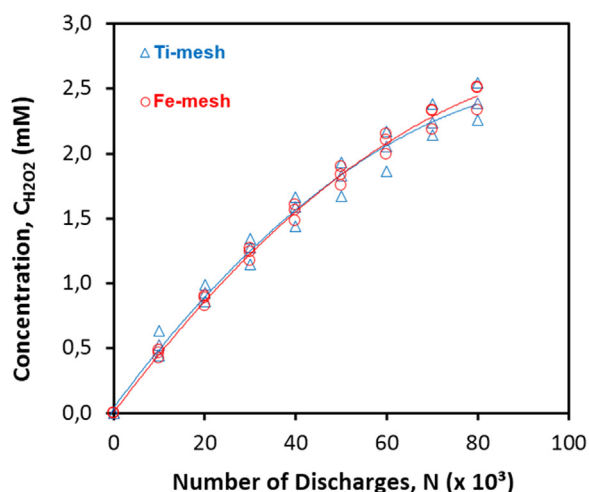
**Fig. 5.** Formation of hydrogen peroxide after application of 80,000 discharges as a function of different electrode materials (titanium, iron). Different symbols reflect three independent sets of measurements. The measurements were conducted with titanium (triangles) and iron (circles) as ground electrode materials. Concentrations reached a maximum of about $2.4 \pm 0.1$ mM (titanium) and $2.45 \pm 0.1$ mM (iron).

### 3.4. Atomic absorption spectroscopy and the determination of electrode corrosion

Electrode corrosion was assessed by quantifying the amount of titanium and iron released into the solution. For titanium ground electrodes, $0.31 \pm 0.01$ mg titanium was found in a treated volume of 300 ml, corresponding to a concentration of 1.02 mg/l. For iron ground electrodes, the amount of iron was measured to be $0.41 \pm 0.09$ mg, corresponding to a concentration of 1.35 mg/l. No titanium was detected when an iron mesh was used as ground electrode and no iron was detected when a titanium mesh was used as ground electrode.

Microscope images obtained with a Keyence digital microscope (VHX-2000, VH-Z500R – High-resolution Zoom Lens, 500-5000X, Keyence Corporation, Osaka, Japan) confirmed changes on the surface of both meshes (Fig. 6).

Furthermore, ground electrodes showed small, randomized spots of discoloration, presumably corrosion damage. Spots on the iron mesh had an orange, rust-like color, whereas spots on the titanium ground electrode were grey and hardly distinguishable.

### 3.5. Optical emission spectroscopy

Emission spectra could be collected only when the optical fiber was oriented toward the high voltage tungsten electrode (Fig. 1). If the fiber was positioned parallel to the wire electrode (at a distance >4 mm from the wire) no emission lines could be detected. Although streamers were propagating beyond this range, their density and the emission was much lower compared to closer to the wire. Near the high voltage electrode, several atomic emission lines that are associated with metals such as iron (Fe) and chromium (Cr) are observed (Fig. 7a). The metals are found in the composition of both meshes (Table 1 and Table 2). However, these metals could also have been released from the high voltage electrode, which was not investigated here, since it was kept the same in all experiments.

Nickel (Ni) lines were clearly recognized for titanium ground electrodes in the range of 338–362 nm. However, in the case of iron mesh, the strong emission of the molecular band of nitrogen ($C\ ^{3}\Pi \rightarrow B\ ^{3}\Pi$) does unfortunately not allow to conclude on the presence of nickel emission. The appearance of molecular nitrogen in the spectra was well reproducible for both electrode materials, albeit intensity was much higher when the iron mesh was used.

The spectral lines of Cu at 324.75 nm and 327.40 nm (2nd order) were also detected in the spectra for both ground electrodes (Fig. 7b). The occurrence of copper agrees with the SPECTROMAXx metal analysis (Table 1 and Table 2).
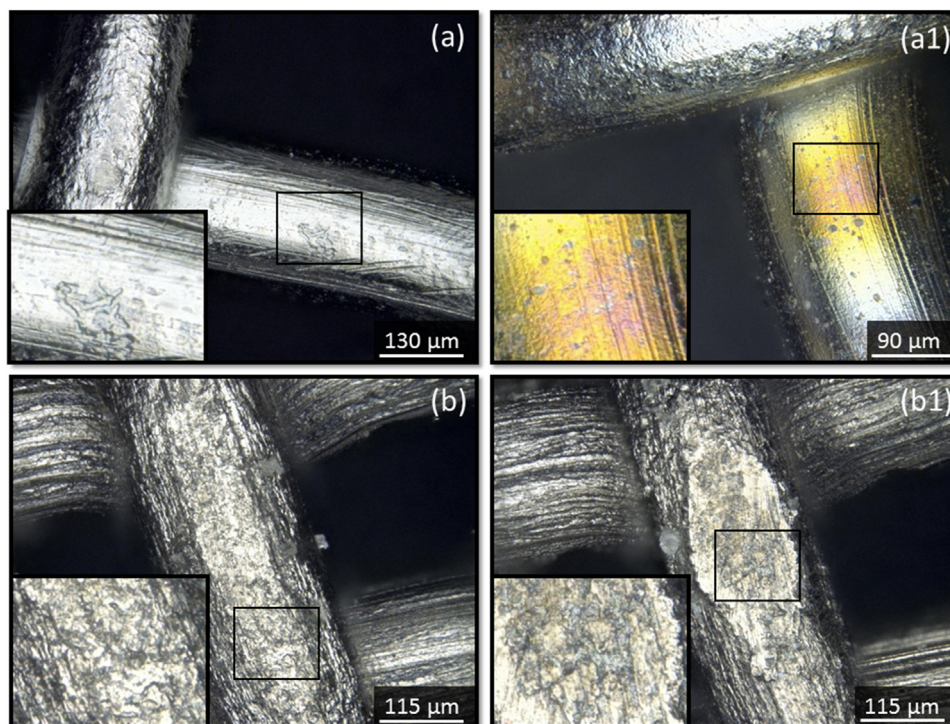


**Fig. 6.** Images of the iron (a) and titanium (b) ground electrode before the application of 80,000 discharges. After treatment, small, randomized spots of discoloration and changes in surface structure were visible for iron (a1) and titanium (b1) ground electrodes.
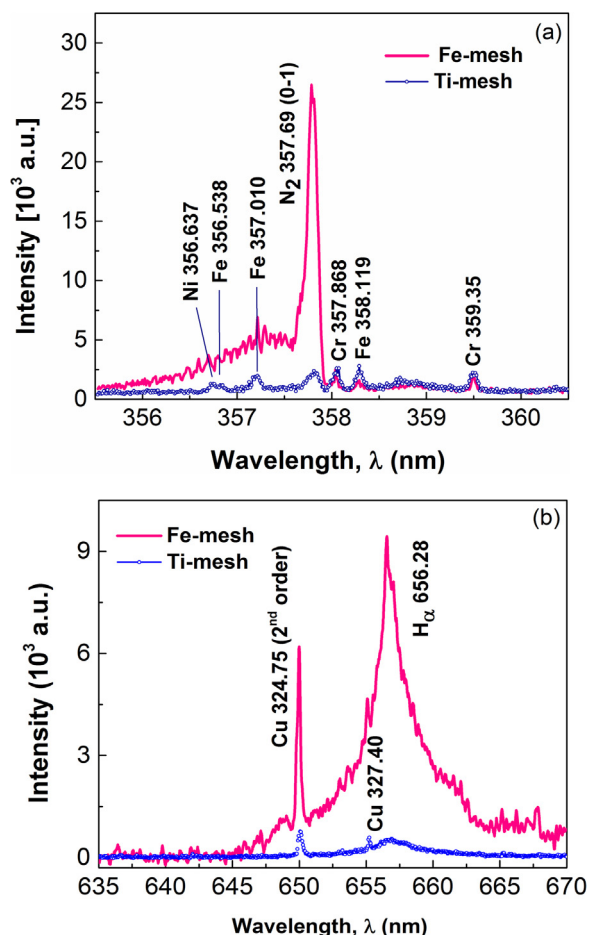
**Fig. 7.** Optical emission spectra recorded for titanium and iron mesh electrodes in the range of (a) 355–365 nm and (b) 635–670 nm.

## 4. Discussion

### 4.1. Decomposition efficiency of phenol

Ground electrode materials clearly influence degradation of phenol during plasma treatment. This is reflected by different reaction rate constants shown in Fig. 3, but also by different phenol degradation product distributions shown in Fig. 4.

Due to relative high amount of phenol used in the experiments (500 $\mu$M) a pseudo-first order kinetic for phenol decomposition was assumed. Thus, the linear slope of the degradation of phenol according to Fig. 3 was utilized to obtain the rate constant, $k$, for phenol removal. In a subsequent step, this allowed the calculation of the degradation efficiency (mg/kWh) for either titanium or iron electrodes by Eq. (1).

$$E_{Phenol} = \frac{k \times V \times C_0 \times 3600}{P} \times M_{Phenol} \qquad (1)$$

Where $k$ is the rate constant of phenol removal per one thousand pulses, $V$ the treated volume in liter (here 0.3 l) and $C_0$ the starting concentration of phenol given in mol. Applied power $P$ enters in Joule/pulse (titanium: $1.41 \pm 0.02$ J/Pulse, iron: $1.42 \pm 0.01$ J/Pulse), which in experiments was approximately the same for all experiments and for both investigated ground electrode materials. $M_{Phenol}$ describes the molar mass of phenol in g/mol. The factor 3600 results from the conversion of units into g/kWh.

A decomposition efficiency of 68.4 mg/kWh (titanium) and 119.6 mg/kWh (iron) was calculated for the different mesh electrodes. Thus, comparing values with respect to the degradation observed for titanium electrodes, phenol decomposition efficiency was higher by about three quarters (74.9 %) using the iron electrode.
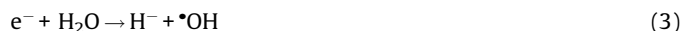
Experimental parameters and conditions, such as pulse generator and reactor geometry, were the same for all experiments and only ground electrode material was changed. Therefore, observed differences in decomposition efficiencies can directly be related to the ground electrode material itself and associated processes in the bulk liquid.

### 4.2. Reactive species responsible for phenol degradation

The generation of a plasma in water will result in the production of transient species ($^\bullet$OH, $^\bullet$NO$_2$, $^\bullet$NO radicals) and long-lived chemical products (O$_3$, H$_2$O$_2$, NO$_3^-$ NO$_2^-$) due to the plasma interacting with water and with gas molecules dissolved in the liquid. Reactive species will react with phenol forming characteristic decomposition products, such as hydroxylated and/or nitrated aromatic ring molecules [22]. Since no nitrated and ozonated products of phenol were detected, degradation chemistry seems to be dominated by hydroxyl radicals.

While direct discharges in water using high voltage pulses generally have negligible electrolysis reactions [28], plasma streamer channels share some similarities with local regions in radiation tracks when water is exposed to ionizing radiation. Values found for electron energies in pulsed corona discharges are in the range of 2 - 5 eV [27].

Electrons of lower energies up to 1 eV will predominantly only result in an excitation of water molecules. In subsequent collisions with other water molecules, OH-radicals can be formed (Eq. (2)). For electron energies between 1.5 eV and 4 eV, collisions are directly leading to dissociative attachment reactions (Eq. (3)).

$$H_2O^* + H_2O \rightarrow {}^\bullet H + {}^\bullet OH + H_2O \qquad (2)$$

$$e^- + H_2O \rightarrow H^- + {}^\bullet OH \qquad (3)$$

$${}^\bullet OH + {}^\bullet OH \rightarrow H_2O_2 \qquad (4)$$

Hydroxyl radicals that are formed either way, eventually react in a diffusion determined manner with organic pollutants in the vicinity of the streamers or recombine to more long-lived species such as hydrogen peroxide (Eq. (4)).

A direct observation of short-lived OH-radicals is difficult. A feasible method, especially in gas discharges, is optical emission spectroscopy (OES) provided the emission intensity is sufficient. Prominent lines from excited OH-molecules can be expected in the range from 306–314 nm. However, in our experiments we did not observe any OH-emissions. A possible explanation might be that OH was not generated in excited states in the discharge. In addition, it is known that for the effective quenching of $^\bullet$OH (A) by water a detection of $^\bullet$OH emissions is rather challenging [29]. The observation of OH-molecules by emission spectroscopy strongly

The emission from atomic hydrogen Balmer series (H$_\alpha$) was identified for both ground electrode materials (Fig. 7b), whereas atomic hydrogen beta and gamma of the Balmer series (H$_\beta$ and H$_\gamma$) could not be observed. Prominent emissions of the OH radical in the range of $306.4 - 314$ nm (A $^{2\Sigma^+} \rightarrow$ X $^{2\Pi}$) were previously found for pulsed electrical discharges that were generated in liquids with microsecond high voltage pulses [26,27]; these emissions could not be observed for the discharge generation with sub-microsecond pulses here.

depends on configurations and plasma generation schemes, as well as on diagnostic setups. Especially for corona discharges that were generated in water by the application of longer (microsecond) high voltage pulses, OH-lines are often found [28,30–32] Conversely, for corona plasmas, especially generated with shorter (nanosecond) high voltage pulses, they are often absent [33,34]. Altogether, more detailed studies are necessary for a better understanding of the spectroscopic data and of the underlying mechanisms.

Instead of direct observation, OH-radicals can also be confirmed from their reaction products. Since OH radical recombination is expected to be a major pathway for $H_2O_2$ generation, hydrogen peroxide is often considered a useful indicator for the generation of hydroxyl radicals in plasma systems [27,35]. Competing reactions for formation (Eq. (4)) and decomposition of hydrogen peroxide will eventually result in a steady state equilibrium, which explains the saturation characteristic that was indicated in Fig. 5.

For neutral pH-values, superoxide anion radicals are formed (Eq. (5)), whereas lower pH-values promote the formation of hydroperoxyl radicals ($HO_2^\bullet$), which can be considered the conjugated acid (p$K_a$-value of 4.8) [36].

$$^\bullet OH + H_2O_2 \rightarrow H_2O + {}^\bullet O_2^- + H^+ \qquad (5)$$

Energy efficiency for $H_2O_2$ generation and maximum hydrogen peroxide concentrations that are reached, are quite similar regardless of ground electrode material. From the initial linear increase of the hydrogen peroxide concentrations with the number of applied pulses (Fig. 5), a maximum yield of 1.08 g/kWh for titanium ground electrodes and 1.04 g/kWh for iron ground electrodes can be derived. Yields and finally achieved concentrations of $H_2O_2$ are so similar that an effect of the ground electrode material on hydrogen peroxide concentration can be excluded. Accordingly, it is unlikely that observed differences in phenol decomposition rates can be explained by either energy input or hydrogen peroxide production alone.

### 4.3. Catalytic processes induced by ground electrode corrosion

While hydroxyl radicals have a strong oxidative potential, they are rather short-lived [37] and it is unlikely that they are able to diffuse to the ground electrode from the plasma channel. However, $H_2O_2$ can be seen as an intermittent storage for OH-radicals that are not consumed in other chemical reactions. Metal ions at or from the ground electrode can then induce a catalytic decomposition of $H_2O_2$ into OH-radicals via Fenton chemistry again. Although $Ti^{3+}$ ions, as well as $Fe^{2+}$ ions, are able to provoke Fenton chemistry, the reverse reaction i.e. the reduction of the oxidized metal ion and the start of a catalytic cycle is primarily mediated by $Fe^{3+}$ ions. (Eq. (6) and (7)).

In contrast to $Fe^{3+}$ ions, are $Ti^{4+}$ ions rather small and have a high charge density, thus will easily react with water molecules to form precipitations of titanium oxo species and are only dissolvable in water for high acidic conditions [38]. It has been shown that these precipitations neither release $Ti^{3+}$ ions nor create free OH-radicals when treated with hydrogen peroxide, hence are disrupting the catalytic cycle [39].

$$Fe^{2+} + H_2O_2 \rightarrow Fe^{3+} + {}^\bullet OH + OH^- \qquad (6)$$

$$Fe^{3+} + {}^\bullet O_2^- \rightarrow Fe^{2+} + O_2 \qquad (7)$$

In case of the iron mesh, 0.41 mg of total iron (23.85 $\mu$M) was quantified with AAS. With respect to $H_2O_2$ concentration, this concentration is actually high enough to result in a $^\bullet$OH generation by Fenton chemistry in the bulk liquid, which was investigated by Grymonpré et al. In these experiments, 24 $\mu$M to 1968 $\mu$M of FeSO$_4$

Hydroquinone [HQ]
(Benzene-1,4-diol)
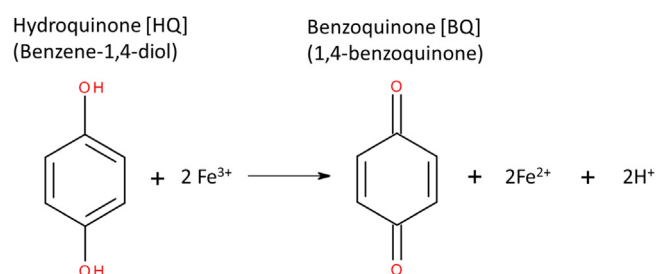
Benzoquinone [BQ]
(1,4-benzoquinone)



**Fig. 8.** The reaction of hydroquinone with iron ions released from the iron mesh is shifting the reaction equilibrium to the benzoquinone form.

were added to an aqueous phase pulsed streamer corona reactor to increase phenol decomposition [23].

Phenol byproducts may also induce additional reactions with iron ions. $Fe^{3+}$ ions can be reduced by dihydroxybenzenes, which leads, for example in the case of *para*-hydroxybenzenes, to the shift of the hydroquinone – benzoquinone equilibrium to the benzoquinone form (Fig. 8) and regeneration of $Fe^{2+}$ [40]. Thus, the catalytic cycle of iron between the (II) and (III) oxidation states can be sustained by the reaction with hydroquinone. This further facilitates the generation of hydroxyl radicals by Fenton chemistry (Eq. (6)).

This may explain why the formation of the benzoquinone (BQ) does increase exponentially for the stainless-steel ground electrode (Fig. 4), whereas titanium ground electrodes promote a linear increase.

Taking into account Fenton chemistry as source of increased phenol decomposition, leads to an interesting conclusion. About 69 $\mu$mol/l phenol was decomposed using a titanium ground electrode and 124 $\mu$mol/l using an iron electrode. Thus, with regard to iron ground electrodes, about 80 % (55 $\mu$mol/l) of phenol was not decomposed due to direct plasma – phenol interactions (streamer channels), but due to an indirect treatment, i.e. secondary reactions with OH-radicals from decomposition of $H_2O_2$, in the bulk.

Retrospective analysis of previously published data supports the conclusion on the significant contribution of ground electrode material and Fenton chemistry in plasma treatments. Lukes et al. applied a pulsed corona discharge with pulses in the $\mu$s-range for the degradation of phenol [41]. All experiments were made with a point-to-plane geometry and a tungsten needle as high voltage electrode. Pulse duration was about several microseconds with a pulse energy of 1 J/pulse and a phenol starting concentration of 500 $\mu$M to 1 mM. Decomposition efficiency was reported as 130 mg/kWh. The ground electrode was made of stainless steel and covered the entire enclosure. Later on, the same reactor was used with a titanium ground electrode of the same size and efficiency for phenol degradation decreased to 75 mg/kWh [26]. Even lower degradation efficiencies (47 mg/kWh) were reported, when a glass reactor was used with a ground electrode made from vitreous carbon [42].

### 4.4. Mechanisms of ground electrode corrosion

Whereas corrosion of the high voltage electrodes is a straightforward process, are mechanisms of ground electrode corrosion more complex. High voltage electrode corrosion in discharge setups is generally associated with the plasma generation, such as generation of reactive species, intensive heat and direct electro-physical and –chemical processes due to the high field strengths at the electrode [14,15,18]. Whereas plasma that is generated in air above a liquid surface commonly results in a drop in pH-values and significant nitrification of the liquid, this

was not observed for pulsed corona discharges generated directly in water. Thus, electrode corrosion by water acidification is negligible, especially since corrosion resistant ground electrode materials, such as stainless steel (EN 1.4571/AISI 316Ti) and pure titanium were used [5].

As a reasonable initial assumption, high concentrations of hydrogen peroxide that were formed during the treatment were suspected to be responsible for ground electrode corrosion. To test this hypothesis, an aqueous solution of 3 mM hydrogen peroxide, thus even slightly higher than concentration observed during phenol experiments, was circulated for about 67 min through the system without generating a plasma. The solution had a pH-value of about 6.4 and circulation time was equal to the entire plasma treatment time. The experiment was repeated three times, but no ground electrode material was detected in solution. Obviously, titanium and high alloy stainless steel (EN 1.4571/AISI 316Ti) are not affected by added $H_2O_2$ for the investigated concentrations and consequently ground electrode corrosion that was observed for the plasma treatment cannot be related to the presence of $H_2O_2$ alone.

Thermal damage by the plasma is also negligible, since propagating streamers are not long enough to reach the grounded electrode. Nevertheless, the effect of streamer length was evaluated. For this purpose, a four times thicker high voltage tungsten electrode (0.2 mm) was used as high voltage electrode. Thicker wire diameters result in considerable shorter streamers since the smaller electrode curvature decreases the strength of the electric field close to the high voltage electrode surface. Other parameters, i.e. treated volume, applied peak voltage (80 kV) were similar to experiments conducted for the degradation of phenol.

Although streamer did stop far from the ground electrode, comparable amounts of iron (0.37 mg) were found for otherwise the same operating parameters used during phenol degradation experiments. Furthermore, similar currents are flowing between high voltage and ground electrode, regardless of extend of the plasma that is generated.

Apparently, the current between the electrodes, or charge transferred, determines ground electrode corrosion. However, in general, corrosion is not considered in plasma chemistry when the electrode is not in contact with the plasma. Moreover, from an electrochemical point of view, the ground electrode serving as a cathode in the investigated setup should not suffer.

In classical DC electrolysis, electrodes can be distinguished as anode and cathode. In case of the experimental setup described in this work and with high voltage pulses of positive polarity applied, the high voltage electrode (wire) is the anode, while the ground electrode (mesh) serves as cathode. For the metal of the electrodes itself, a loss of electrons (at the anode) is corresponding to an oxidation of metal ions from the anode that are consequently going into solution and, hence, are associated with a corrosion of the anode (here the central wire) [43].

Consequently, it was assumed that even though the high voltage electrode may be degraded over time, integrity of the ground electrode is preserved due to an excess of electrons. However, our results show this description clearly does not seem to apply for the application of short high voltage pulses.

To verify the assumption, we suppressed plasma formation completely by using a 0.2 mm diameter wire as high voltage electrode. In addition, liquid conductivity was adjusted to 400 μS/cm by adding sodium chloride. In this case, a monopolar current pulse of about 100 ns (FWHM) with peak current of about 500 A is applied (Fig. 9). Therefore, the net charge transfer for pulsed electric field (PEF) treatment ($2.83 \times 10^{-5}$ C) is even a little higher than observed for the generation of plasma ($2.55 \times 10^{-5}$ C). The pH-value during PEF treatment stayed constant at 6.4 and since no plasma streamers were generated, also no hydrogen peroxide was formed.

In both cases, i.e. for the generation of a plasma and the application of comparable high voltage pulses only, corrosion of the ground electrode (cathode) was observed with about 0.4 mg and 0.5 mg of iron found in the liquid after application of 80,000 pulses, respectively.

Consequently, this allows the conclusion that electrode corrosion is not mediated by the plasma itself, but due to the net charge transfer that corresponds to the applied short high-pulsed electric fields.

Ghoroghchian and Bockris have early on suggested differences for electrode processes for the application of pulsed voltages [44]. Shimizu et al. have described differences in electrolytic processes for the application of short high voltage pulses in some more detail. They applied pulses in the sub-microsecond range (300 ns) to produce hydrogen by electrolysis. It was found that in such a system, electrolysis takes place with a mechanism dominated by
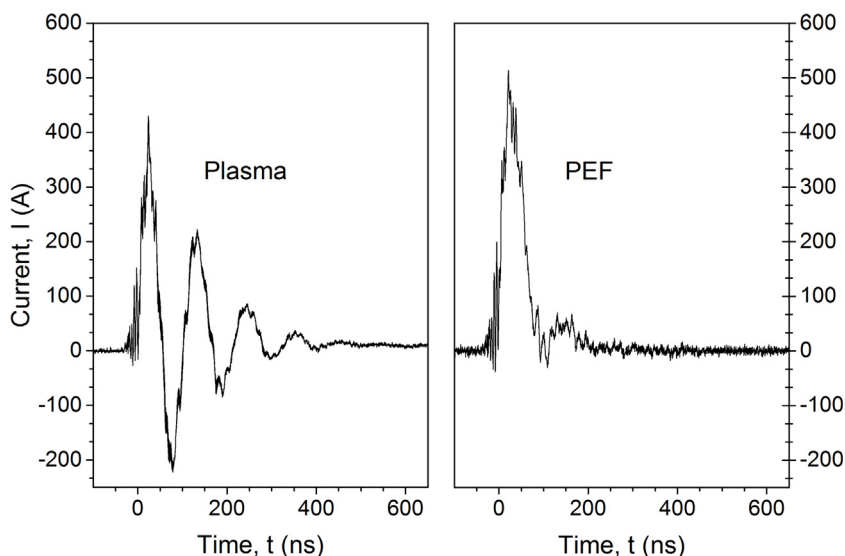


**Fig. 9.** Current pulses after plasma and pulsed electric field (PEF) treatment. Diameter of the high voltage electrode was 0.2 mm. In case of PEF-treatment, solution conductivity had to be increased to 400 μS/cm to suppress plasma generation.

electron transfer, which is distinctively different from the conventional DC electrochemical processes. The authors assumed that due to the short pulse duration, application of the electric field is too short to form a constant electric double layer close to the electrode. Instead, electrons are collected on the surface of the cathode and are quickly transferred to hydrogen ions [45].

Vanags et al., who proposed that for rapidly growing voltage differences, electrons are emitted from the cathode metal into the electrolyte, continued this work. They concluded that electrons are first solvated in the electrolyte but in a next step can dissociate water molecules to hydrogen and negatively charged hydroxyl ions ($OH^-$), which can discharge on the cathode at the moment the applied voltage decreases [46].

Neither group investigated cathode corrosion. However, the fast and substantial emission of electrons from the ground electrode might temporarily leave positively charged metal ions behind, which could go into solution. Accepting the proposed assumption of the release of metal ions from the ground electrode (cathode) with respect to charge transfer, the theoretical maximum amount of metal released can be estimated and compared with experimental results.

According to Fig. 2, the amount of charge, $Q$, transferred in a typical applied high voltage pulse can be obtained by integrating current. When multiplied with the number of applied pulses, $x_{Pulse}$ (80,000), this results in the total amount of electrical charge transferred during the treatment, which in the case of iron was about 31.1 µC.

Metal dissolved in the liquid, commonly exist in ionic form with a specific ionic charge, $z_{ion}$, depending on the oxidation state of the metal. For example, iron ions will be mostly present as ferrous ($Fe^{2+}$) or ferric ($Fe^{3+}$) ions, which would lead to the release of two or three free electrons, respectively. The other way round, how much metal (in mol) can be dissolved in water can be derived from the specific number of electrons that are withdrawn. With the Avogadro constant, $N_A$, and the molar mass of the metal, $M_{metal}$, the amount of material can be converted into mass, allowing a comparison with the data obtained from AAS measurements (Eq. (8)).

$$C_{metal} = \frac{Q \times M_{metal}}{e \times z_{ion} \times N_A} \times x_{Pulse} \qquad (8)$$

The theoretical release of material from the ground electrode according to Eq. (8) is listed for a ground electrode made of iron or titanium in Table 3.

The calculated values for metal released from the ground electrode, agrees well with the measurements.

Despite a lack of detail, such as for example considering detailed electrode composition, the analysis provides strong evidence in support of the hypothesized fast electron injection from the ground electrode, when subjected to short high voltage pulses of sub-microsecond duration.

## 5. Conclusion

Ground electrode corrosion plays an important role in pulsed corona discharges that are generated in water by the application of sub-microsecond high voltage pulses. Electrochemical processes might be the source of ground electrode corrosion when positive pulses in the sub-microsecond range are applied to the high voltage electrode. Although underlying mechanisms should be investigated further, our results support the hypothesis that ground electrode corrosion can be explained by fast electron injection from the ground electrode that is followed by a release of metal ions.

Metal ions that are released from the ground electrode can enhance decomposition rates of organic molecules, e.g. phenol. For titanium ground electrodes, the contribution of catalytic mechanisms is smaller than for ground electrodes made from stainless steel. In this case, Fenton chemistry contributes substantially to the observed phenol degradation. The use of catalytic active electrode materials may be a promising approach enhancing decomposition efficiencies of pulsed corona discharges generated in water. This way, hydroxyl radicals, which are lost due to hydrogen peroxide recombination, can be recovered. Along the same lines, also illumination with UV-light during the generation of plasmas may be beneficial.

Conversely, in fundamental studies on plasma chemical processes, electrode materials with negligible catalytic effects should be used. In addition, the possible occurrence of a variety of different metal ions, especially if alloys are used, should be considered.

## References

[1] P. Lukes, B.R. Locke, Industrial & engineering chemistry research 44 (2005) 2921–2930.
[2] A.T. Sugiarto, M. Sato, Thin Solid Films 386 (2001) 295–299.
[3] D. Gerrity, B.D. Stanford, R.A. Trenholm, S.A. Snyder, Water Research 44 (2010) 493–504.
[4] M. Hijosa-Valsero, R. Molina, H. Schikora, M. Müller, J.M. Bayona, Water Research 47 (2013) 1701–1707.
[5] R. Banaschik, P. Lukes, H. Jablonowski, M.U. Hammer, K.-D. Weltmann, J.F. Kolb, Water Research 84 (2015) 127–135.
[6] R. Banaschik, G. Burchhardt, K. Zocher, S. Hammerschmidt, J.F. Kolb, K.-D. Weltmann, Bioelectrochemistry (2016).
[7] S.B. Gupta, Investigation of a physical disinfection process based on pulsed underwater corona discharges, Forschungszentrum Karlsruhe, 2007.
[8] J. Kolb, R. Joshi, S. Xiao, K. Schoenbach, Journal of Physics D: Applied Physics 41 (2008) 234007.
[9] R.P. Joshi, S.M. Thagard, Plasma Chemistry and Plasma Processing 33 (2013) 1–15.
[10] S. Medodovic, B.R. Locke, Journal of Physics D: Applied Physics 42 (2009) 049801.
[11] M. Szklarczyk, R.C. Kainthla, J.O.M. Bockris, Journal of The Electrochemical Society 136 (1989) 2512–2521.
[12] J.F. Bonnen, S. Golovashchenko, S. Dawson, A. Mamutov, Journal of Materials Engineering and Performance 22 (2013) 3946–3958.
[13] V. Goryachev, A. Ufimtsev, A. Khodakovskii, Technical Physics Letters 23 (1997) 386–387.
[14] Š. Potocký, N. Saito, O. Takai, Thin Solid Films 518 (2009) 918–923.
[15] P. Lukeš, M. Člupek, V. Babický, P. Šunka, J.D. Skalný, M. Štefečka, J. Novák, Z. Málková, Czechoslovak Journal of Physics 56 (2006) B916–B924.
[16] P. Lukes, M. Clupek, V. Babicky, I. Sisrova, V. Janda, Plasma Sources Science and Technology 20 (2011) 034011.
[17] A. Sharma, B. Locke, P. Arce, W. Finney, Hazardous Waste and Hazardous Materials 10 (1993) 209–219.

**Table 3**
Comparison of electrode corrosion after the application of 80,000 high voltage pulses (without plasma generation). Experimental data was obtained from atomic absorption spectroscopy (AAS). According to Eq. (7), theoretical electrode corrosion (release of metal) was calculated for different ion charges ($z_{ion}$).

| Theoretical corrosion due to charge transfer | | | | | Experiment | |
|---|---|---|---|---|---|---|
| Metal | Charge transferred in µC | $M^{2+}$ ($z_{ion}$) in mg | $M^{3+}$ ($z_{ion}$) in mg | $M^{4+}$ ($z_{ion}$) in mg | AAS (mean) in mg |
| Titanium | 32.5 | 0.64 | 0.43 | 0.32 | $0.31 \pm 0.01$ |
| Iron | 31.1 | 0.72 | 0.48 | – | $0.41 \pm 0.09$ |

[18] F. Holzer, B.R. Locke, Plasma Chemistry and Plasma Processing 28 (2008) 1–13.
[19] M.J. Kirkpatrick, B.R. Locke, Industrial & Engineering Chemistry Research 45 (2006) 2138–2142.
[20] S. Međedović, B.R. Locke, Applied Catalysis B: Environmental 67 (2006) 149–159.
[21] S. Mededovic, B.R. Locke, Applied Catalysis B: Environmental 72 (2007) 342–350.
[22] P. Lukes, B.R. Locke, J.L. Brisset, Plasma Chemistry and Catalysis in Gases and Liquids (2012) 243–308.
[23] D.R. Grymonpré, A.K. Sharma, W.C. Finney, B.R. Locke, Chemical Engineering Journal 82 (2001) 189–207.
[24] P. Lukes, E. Dolezalova, I. Sisrova, M. Clupek, Plasma Sources Science and Technology 23 (2014) 015019.
[25] G. Eisenberg, Industrial & Engineering Chemistry Analytical Edition 15 (1943) 327–328.
[26] B. Sun, M. Sato, J.S. Clements, Journal of Electrostatics 39 (1997) 189–202.
[27] B.R. Locke, K.-Y. Shih, Plasma Sources Science and Technology 20 (2011) 034006.
[28] P. Sunka, V. Babický, M. Clupek, P. Lukes, M. Simek, J. Schmidt, M. Cernák, Plasma Sources Science and Technology 8 (1999) 258.
[29] P. Bruggeman, D.C. Schram, M.G. Kong, C. Leys, Plasma Processes and Polymers 6 (2009) 751–762.
[30] K.-Y. Shih, B.R. Locke, IEEE Transactions on Plasma Science 39 (2011) 883–892.
[31] B. Sun, M. Sato, A. Harano, J.S. Clements, Journal of Electrostatics 43 (1998) 115–126.
[32] M. Sato, B. Sun, T. Ohshima, Y. Sagi, Journal of Advanced Oxidation Technologies 4 (1999) 339–342.
[33] D. Dobrynin, Y. Seepersad, M. Pekker, M. Shneider, G. Friedman, A. Fridman, Journal of Physics D: Applied Physics 46 (2013) 105201.
[34] P. Lukes, M. Clupek, V. Babicky, B. Pongrac, M. Simek, J. Kolb, Proc. Plasma Science (ICOPS), 2016 IEEE International Conference on (2016).
[35] D.-X. Liu, P. Bruggeman, F. Iza, M.-Z. Rong, M.G. Kong, Plasma Sources Science and Technology 19 (2010) 025018.
[36] B.H. Bielski, D.E. Cabelli, R.L. Arudi, A.B. Ross, Journal of Physical and Chemical Reference Data 14 (1985) 1041–1100.
[37] B.R. Locke, S.M. Thagard, Plasma Chemistry and Plasma Processing 32 (2012) 875–917.
[38] S. Sakka, Handbook of sol-gel science and technology, Sol-gel processing, 1, Springer Science & Business Media, 2005.
[39] P. Tengvall, I. Lundström, L. Sjöqvist, H. Elwing, L.M. Bjursten, Biomaterials 10 (1989) 166–175.
[40] R. Chen, J.J. Pignatello, Environmental Science & Technology 31 (1997) 2399–2406.
[41] P. Lukeš, Water Treatment by Pulsed Streamer Corona Discharge: Ph.D. Thesis, Institute of Plasma Physics, AS CR, 2001.
[42] P. Lukes, B.R. Locke, Journal of Physics D: Applied Physics 38 (2005) 4074.
[43] B. Roodenburg, J. Morren, H.I. Berg, S.W. de Haan, Innovative Food Science & Emerging Technologies 6 (2005) 327–336.
[44] J. Ghoroghchian, J.M. Bockris, International Journal of Hydrogen Energy 10 (1985) 101–112.
[45] N. Shimizu, S. Hotta, T. Sekiya, O. Oda, Journal of Applied Electrochemistry 36 (2006) 419–423.
[46] M. Vanags, G. Bajars, J. Kleperis, Water electrolysis with inductive voltage pulses, INTECH Open Access Publisher, 2012.

## Publication P4

**Degradation and Metabolites of Diclofenac as Instructive Example for Decomposition of Recalcitrant Pharmaceuticals by Hydroxyl Radicals Generated with Pulsed Corona Plasma in Water**

R. Banaschik, H. Jablonowski, P.J. Bednarski and J.F. Kolb, *Journal of hazardous materials,* 342 (2018) 651-660.

# Degradation and intermediates of diclofenac as instructive example for decomposition of recalcitrant pharmaceuticals by hydroxyl radicals generated with pulsed corona plasma in water

Robert Banaschik[a], Helena Jablonowski[a,b], Patrick J. Bednarski[c], Juergen F. Kolb[a,*]

[a] *Leibniz Institute for Plasma Science and Technology e.V. (INP Greifswald), Felix-Hausdorff-Straße 2, 17489 Greifswald, Germany*
[b] *Center for Innovation Competence (ZIK) Plasmatis, Felix-Hausdorff-Strasse 2, 17489 Greifswald, Germany*
[c] *Institute of Pharmacy, University of Greifswald, Friedrich-Ludwig-Jahn-Straße 17, 17489 Greifswald, Germany*

## HIGHLIGHTS

- AOPs, including plasmas, are effective for the removal of pharmaceutical residues.
- Pulsed corona plasmas continuously provide high concentrations of hydroxyl radicals.
- Detailed degradation chemistry of diclofenac when subjected to plasma.
- Comparison and applicability of degradation mechanisms for seven pharmaceuticals.
- Assessment of risks for AOPs to form harmful degradation compounds.

## GRAPHICAL ABSTRACT
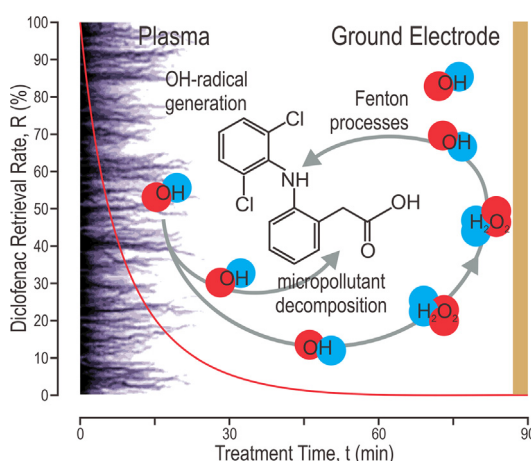


## ARTICLE INFO

## ABSTRACT

Seven recalcitrant pharmaceutical residues (diclofenac, 17α-ethinylestradiol, carbamazepine, ibuprofen, trimethoprim, diazepam, diatrizoate) were decomposed by pulsed corona plasma generated directly in water. The detailed degradation pathway was investigated for diclofenac and 21 intermediates could be identified in the degradation cascade. Hydroxyl radicals have been found primarily responsible for decomposition steps. By spin trap enhanced electron paramagnetic resonance spectroscopy (EPR), •OH-adducts and superoxide anion radical adducts were detected and could be distinguished applying BMPO as a spin trap. The increase of concentrations of adducts follows qualitatively the increase of hydrogen peroxide concentrations. Hydrogen peroxide is eventually consumed in Fenton-like processes but the concentration is continuously increasing to about 2 mM for a plasma treatment of 70 min. Degradation of diclofenac is inversely following hydrogen peroxide concentrations. No qualitative differences between byproducts formed during plasma treatment or due to degradation via Fenton-induced processes were observed. Findings on degradation kinetics of diclofenac provide an instructive understanding of decomposition rates for recalcitrant

---

* Corresponding author at: Leibniz Institute for Plasma Science and Technology e.V. (INP Greifswald), Felix-Hausdorff-Straße 2, 17489 Greifswald, Germany.
*E-mail address:* juergen.kolb@inp-greifswald.de (J.F. Kolb).

pharmaceuticals with respect to their chemical structure. Accordingly, conclusions can be drawn for further development and a first risk assessment of the method which can also be applied towards other AOPs that rely on the generation of hydroxyl radicals.

## 1. Introduction

Anthropogenic pollutants, such as pharmaceutical residues, often withstand treatment by conventional wastewater treatment processes and can accumulate in the environment [1–5]. Most pharmaceuticals have been found to have verifiable environmental adverse effects even in low concentrations [6–10]. Hence, the European Commission (EC) started monitoring pollutants including diclofenac (analgesic), 17α-ethinylestradiol and 17β-estradiol (both hormones) in 2015 [11]. The next step is the implementation of novel water purification techniques to address the problem.

Advanced oxidation processes (AOP) have been shown to effectively decompose organic compounds [12–15]. The underlying principle of AOPs is the generation of reactive species, which then degrade target pollutants. The generation of hydroxyl radicals ($^\bullet$OH) is of special interest due to their high oxidizing potential. With the goal to provide these radicals, several processes were developed that are based on the application of electric energy (electrochemical oxidation), radiation (UV, electron beams), ultrasound, admixture of chemicals ($O_3$, $H_2O_2$) or a combination of these methods ($Fe^{2+}$/UV/$H_2O_2$) [14,15].

Plasma generated directly in water or close to the water surface by an electrical discharge, is an efficient means to generate a variety of reactive species such as ozone, reactive nitrogen species and hydroxyl radicals [16–18]. Accordingly, plasmas have been demonstrated effective decomposition of organic compounds and recalcitrant pharmaceuticals [19–23] and are a promising new approach for advanced water purification techniques. Magureanu et al. investigated the degradation of pentoxifylline using a dielectric barrier discharge, which generated a plasma in the gas-liquid interface [24]. The same experimental setup was then studied for the degradation of antibiotics, such as amoxicillin, oxacillin, ampicillin [25] and enalapril [26]. Respective degradation pathways were explored and it was found that ozone and probably hydroxyl radicals are formed in significant amounts in the hybrid gas-liquid electrical discharges in the presence of oxygen. The work was expanded by Dobrin et al. by applying a pulsed corona discharge above liquid for the decomposition of diclofenac. It was assumed that ozone can act as oxidant of the organic compounds only at the gas-liquid interface or by means of radical species produced in solution. Diclofenac was effectively removed from water by ozone treatment and hydroxyl radicals were most likely involved in the further degradation of reaction products [27]. This was also suggested by Marković et al. [28].

A detailed investigation of aqueous-phase chemistry at the gas-liquid interface was performed by Lukes et al. [17]. Evidence was found for interactions of ozone, hydrogen peroxide and reactive nitrogen species that lead to the formation of hydroxyl radicals and peroxinitrite which can likewise decompose organic pollutants.

All these studies have focused on plasma generated in a gas phase in the presence of water and consequently ozone has always a significant contribution to decomposition of compounds. Conversely, corona-plasma generated directly in water does not result in the generation of ozone, nitrification or relevant changes of pH-values as it is observed for water treatment with gaseous discharges [17,29]. Accordingly, degradation pathways and mechanisms of action, as well as associated risks, have not yet been investigated.

Our previous studies have shown that reactive oxygen species, including hydroxyl radicals, play an import role in plasma mediated degradation processes when a plasma is formed directly in the liquid [19,30]. Without the need to diffuse through the gas-liquid layer first, radicals can either react directly with pollutants in the plasma channels or close to the plasma-liquid boundary [18,31], or can recombine to more long-lived species, such as hydrogen peroxide. Depending especially on electrode materials, an indirect degradation through the splitting of hydrogen peroxide (Fenton-chemistry) can then contribute to the decomposition of organic pollutants [30].

An overall understanding of processes in the bulk, especially away from the plasma, is important for any application of the method in larger volumes. However, detailed and comprehensive degradation mechanisms for pharmaceuticals are not fully understood. In particular, it is unknown why some pharmaceuticals are decomposed readily (diclofenac) whereas others seem to be more resistant (diatrizoate) when subjected to pulsed corona plasma generated in water [19]. The objective of this study was therefore to determine reaction mechanisms that are responsible for pollutant degradation during and following plasma treatment with pulsed corona plasma generated in water, choosing diclofenac as model pollutant. Since oxidation by OH-radicals is unambiguously the most interesting process, plasma degradation was compared with the generation of hydroxyl radicals and associated decomposition due to traditional Fenton-chemistry. Results of diclofenac degradation pathways were then compared to explain response of different pharmaceuticals with respect to plasma treatment and treatment with AOPs in general and to conduct an initial risk assessment.

## 2. Materials and methods

### 2.1. Generation of pulsed corona plasma

Plasma treatment was carried out in a wire to cylinder discharge geometry that has been described in detail previously [19]. Briefly, corona plasma is generated by applying positive high voltage pulses of 80 kV with a frequency of 20 Hz from a 6-stage Marx-Generator to intertwined tungsten wires with a diameter of 0.05 mm each (W-005135/13, Goodfellow, Huntingdon, England) (Fig. 1). A more detailed description is included in the supplemental material (Fig. S1).

A titanium mesh was used as ground electrode because it has been found to have less chemical interactions with plasma species in the liquid and provides a cleaner experimental system [30].

### 2.2. Decomposition of diclofenac by pulsed corona plasma

A stock solution of 0.5 mM diclofenac (159.1 mg/l of the sodium salt) was prepared with deionized Milli-Q purified water (Q-POD, Millipore, Billerica, MA). The solution conductivity was adjusted to 40 μS/cm with sodium chloride. A volume of 300 ml of the stock solution served as analytic control (no plasma treatment), whereas another volume of 300 ml was filled in the plasma discharge system including expansion reservoir and peristaltic pump (FH100x, Thermo Scientific, Waltham, MA). The solution was circulated through the chamber at a flow rate of 120 ml/min. Treated solutions
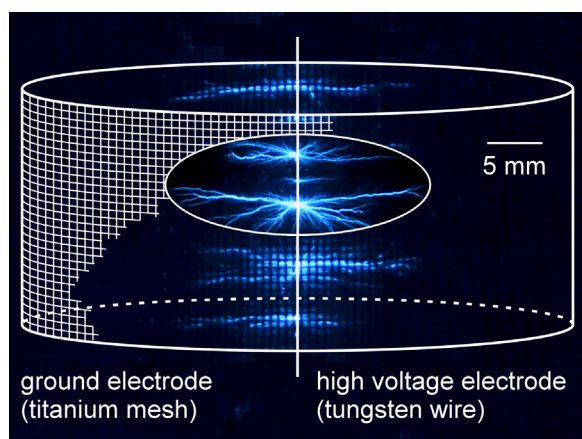
**Fig. 1.** Segment of pulsed corona plasma generated in water around two twisted 0.05 mm wires along the axis of a coaxial treatment tube of 140 mm in length in total and 47 mm in diameter. Plasma filaments are usually obscured by the mesh-electrode. An unobstructed image is shown in the oval inset.

as well as untreated controls were acidified with hydrochloric acid to a pH-value of 3 in preparation for solid phase extraction (SPE).

### 2.3. Decomposition of diclofenac due to •OH-chemistry

Fenton-chemistry was induced by introducing $Fe^{2+}$ ions from iron-salts [32]. The reagent was slightly adapted for this work as suggested by Hartman et al. [33]. In particular, iron(II) sulfate was replaced with iron(II) chloride and sulphuric acid was replaced with sodium ascorbate. With these changes, stock solutions for •OH-chemistry (as well as the plasma treated solutions) had a neutral pH-value of 6–7, increasing the stability of diclofenac.

In preliminary plasma degradation experiments, hydrogen peroxide concentrations of about 2.5 mM were observed after a treatment time of 67 min and chosen accordingly to be the starting concentration for the Fenton-chemistry experiments.

To start the catalytic hydrogen peroxide decomposition, two solutions A (diclofenac, chemicals) and B (hydrogen peroxide) were prepared. After mixing A and B, the final solution (150 ml) consisted of 0.75 mM iron(II) chloride, 2.5 mM sodium ascorbate, 0.5 mM diclofenac and 2.5 mM hydrogen peroxide.

Concentration of hydrogen peroxide during experiments was monitored with a colorimetric peroxide test (MQuant, Merck KGaA, Darmstadt, Germany). Immediately after the experiment was finished, pH-value was adjusted to 3 with hydrochloric acid and solid phase extraction was performed.

### 2.4. Solid phase extraction

Solid phase extraction (SPE) was carried out with a column made of hydrophobic polystyrene-divinylbenzene copolymer (Chromabond HR-X, Macherey-Nagel, Düren, GER).

The cartridge was first equilibrated with 5–10 ml methanol to ensure consistent interaction between the analyte and the functional groups of the sorbent. Afterwards, the cartridge was rinsed with water of the same composition as the sample. The acidified sample volume was added to the cartridge with a flow rate of about 8.5 ml/min. The cartridge was then dried with nitrogen and compounds were eluted with 3 x 3 ml acetonitrile. Eluted compounds that were dissolved in acetonitrile were used for subsequent gas chromatographic investigations.

### 2.5. Gas chromatographic identification of diclofenac byproducts

The fraction obtained after SPE was reduced to 1 ml by evaporation and 300 μl were drawn for derivatization using methoxyamine (MeOX) dissolved in pyridine and N-methyl-N-trimethylsilyl fluoroacetamide (MSTFA). Then 60 μl MeOx was added to the sample and left undisturbed at 37 °C for 90 min. Subsequently, 120 μl MSTFA was added (30 min, 37 °C).

Altogether, these steps improve separation, reduce tailing and enlarge the substrate spectrum. A pure sample without derivatization was also analyzed.

Samples of 1 μl were applied to an HP–5 ms Ultra Inert column, part of a 7890A gas chromatograph (GC–MS), including a 5975C VL mass selective detector (Agilent Technologies Santa Clara, CA). The mass detector was operated in electron impact (EI) mode and scanning was set to the range of 40–700 Da. Helium served as carrier gas and injection mode was set to splitless with an oven temperature of 100 °C. Total run time of the method was about 60 min with a temperature ramp of 5 °C/min up to 280 °C during the first 36 min.

The obtained chromatograms were processed and analyzed with AMDIS (Version 2.70), which is part of the NIST-Database 2014 (National Institute of Standards and Technology, Maryland, USA).

### 2.6. Detection of reactive oxygen species in plasma treated solution

For the detection of free radicals in plasma treated solution, spin trap enhanced electron paramagnetic resonance spectroscopy (EPR) allows a qualitative and semi-quantitative measurement [34]. An X-band (equal to a microwave frequency of 9.87 GHz) EPR (EMXmicro, Bruker BioSpin GmbH, Rheinstetten, Germany) spectroscope was used with the following instrument parameters: modulation frequency of 100 kHz, modulation amplitude of 0.1 mT, microwave power of 5.024 mW, receiver gain of 30 dB, time constant of 0.01 ms.

To distinguish between hydroxyl and superoxide anion radicals, 5-tert-butoxycarbonyl-5-methyl-1-pyrroline-N-oxide (BMPO) was added to the solution as spin trapping agent [34].

The final concentration of BMPO was 10 mM in a volume of 300 ml. During plasma treatment, 15 samples were taken at different time points (2, 8, 14, 18, 24, 29, 33, 38, 42, 47, 52, 56, 61, 65 and 70 min). The plasma treated solution was pipetted into a 50 μl borosilicate glass tube, placed in the EPR-system and analyzed immediately. As control, an untreated sample was analyzed. By the use of Xenon software with the Xenon Spin Counting module (Bruker BioSpin, Rheinstetten, Germany) the EPR spectra were evaluated.

Hydrogen peroxide formed during plasma treatment was determined by using the titanyl sulfate method. A treated sample of 0.5 ml was filled up to a total volume of 0.7 ml with titanium(IV)oxysulfate sulfuric acid and color development was determined at $\lambda = 407$ nm [35].

## 3. Results

### 3.1. Decomposition of pharmaceuticals by pulsed corona plasma

The decomposition of seven pharmaceuticals dissolved in water by pulsed corona plasma generated directly in water, has been previously reported for the treatment of 33 min and 67 min [19]. A more detailed evaluation shows that the pharmaceuticals exhibit distinctively different degradation kinetics when subjected to plasma treatment as shown in Fig. 2. Diclofenac and 17α-ethinylestradiol were readily decomposed by more than 80% within 15 min and both were almost completely removed by 1 h. Carba-
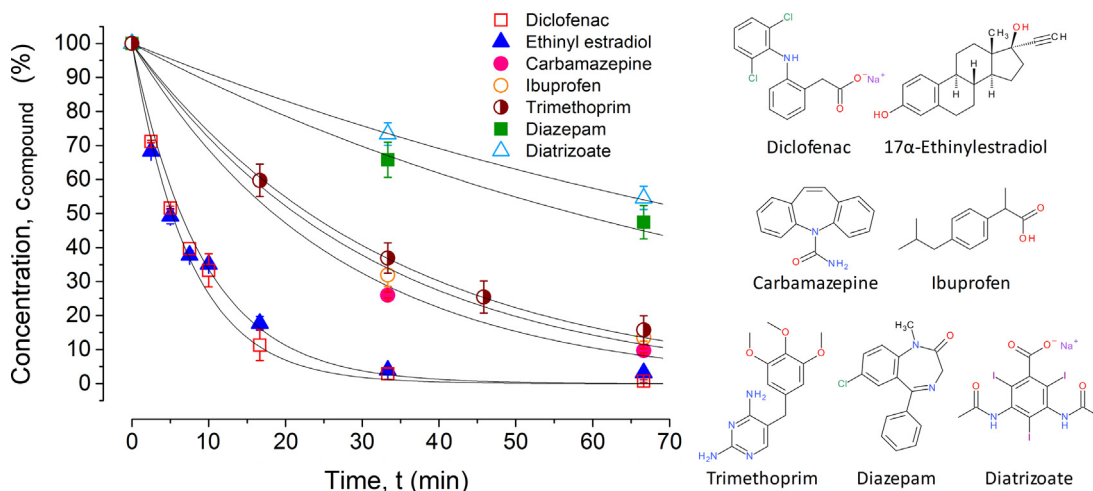
**Fig. 2.** Degradation of pharmaceuticals that were treated in individual experiments for an initial concentration in water of 0.5 mg/l with pulsed corona plasma. The plasma was instigated with a frequency of 20 Hz and a treatment with 80,000 consecutive discharges, hence, corresponding to a treatment time of 67 min.

mazepine, ibuprofen, and trimethoprim also had relatively rapid decomposition rates but after 1 h only by about 80% had been degraded. On the other hand, diazepam and diatrizoate were the most stable or slowest to be decomposed of the investigated substances, with only about 50% degraded by 1 h. Notably, the degradation of diclofenac and ethinyl estradiol follows a similar kinetic. A common characteristic is also observed for the decrease in concentrations of carbamazepine, ibuprofen and trimethoprim, although at a slower rate. Diazepam and diatrizoate are likewise degraded at comparable rates.

Since the same treatment was applied to all pharmaceuticals, different degradation rates are obviously related to individual reaction mechanisms for the same chemistry that is provided by the plasma in all cases. Reaction mechanisms have therefore been studied in detail for diclofenac and results applied to explain differences for the degradation that was observed for other compounds.

### 3.2. Decomposition of diclofenac due to plasma treatment and Fenton-chemistry

Plasma generated in water primarily provides high amounts of hydroxyl radicals. Therefore, plasma chemistry was qualitatively and quantitatively compared with an alternative production of $^{\bullet}$OH-radicals by Fenton-chemistry.

Decomposition of diclofenac by Fenton-processes followed an exponential decay (Fig. 3). The progress in the decrease is associated with the ongoing consumption of hydrogen peroxide. Most of the diclofenac was degraded during the first 60 s of the treatment with concentrations decreasing to 60%. At the same time, concentrations of hydrogen peroxide dropped by 40% below 1 mM (Fig. 4). Inherent with the decreasing concentration of hydrogen peroxide, decomposition rates of diclofenac were also decreasing. Diclofenac decomposition during plasma treatment showed a linear characteristic with a steady pollutant decay over time (Fig. 3).

Hydrogen peroxide was consumed completely after 32 min with 50% of the diclofenac being decomposed. Without hydrogen peroxide in solution, no further hydroxyl radicals could be formed. However, during plasma treatment, hydroxyl radicals were continuously generated from water with a rate that exceeds the consumption rate in various chemical reactions. Thus, hydroxyl radicals that were not consumed in reactions with pollutants could recombine to hydrogen peroxide [36].
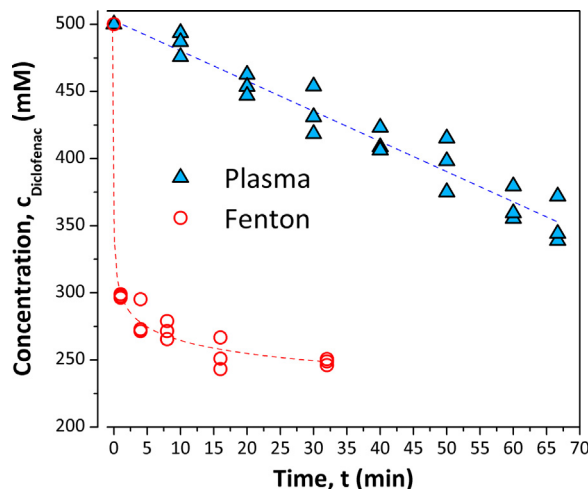


**Fig. 3.** Decomposition of diclofenac by pulsed corona plasma (solid triangles) or by the generation of OH-radicals initiated with 2.5 mM hydrogen peroxide and 0.75 mM iron(II) chloride (open circles). Initial diclofenac concentration for both experiments was 0.5 mM.
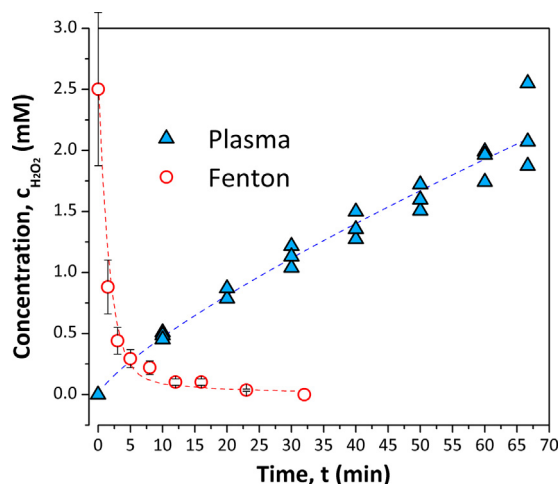


**Fig. 4.** Hydrogen peroxide concentrations for plasma treatment (solid triangles), or for $^{\bullet}$OH-chemistry with an initial admixture of 2.5 mM together with 0.75 mM iron(II) chloride (open circles).

### 3.3. Decomposition products of diclofenac

After sample preparation and analysis by GC–MS, the obtained chromatograms were analyzed with AMDIS and the NIST-Database. Typical chromatograms for the degradation of diclofenac with plasma or Fenton-chemistry are depicted in Figs. S2. and S3. It has to be noted that solid phase extraction does not only concentrate the decomposition products of diclofenac, but also concentrates traces of impurities and in general ubiquitously present compounds, e.g. sugars and fatty acids.

A summary of decomposition compounds found after the respective treatments is given in Table 1. All compounds are sorted by their retention time ($t_R$) and numbered (1–30), accordingly. In addition to the name of the compounds in column two, important diclofenac derivatives were numbered (**D1–D21**) for subsequent reference. Column three shows the NIST match value (0–999). The match value is an arbitrary unit based on the $m/z$ value and the intensities of all peaks for unknown spectra. A perfect match results in a value of 999. A match of 900 or greater is an excellent match, 800–900 a good match, 700–800 a fair match and less than 600 a very poor match. The first of the two numbers represents the direct match, i.e. comparison of an unknown compound with known compounds included in the NIST library. The second number (reverse match) is derived in the same way, but all peaks in the sample spectrum that are not found in the library spectrum are disregarded during calculation. For this work, matches had to be at least good; however, most matches were excellent. The columns named Plasma and Fenton show the occurrence ($\checkmark$) or absence (X) of a specific compound during the respective treatment that was administered in this study. The last column shows comments especially for partially identified diclofenac derivatives after •OH-attack already described in the scientific literature. Literature research hereby included •OH-chemistry of advanced oxidation processes such as sonolysis, $H_2O_2$/UV, classical Fenton and recent studies about plasmas generated in gaseous phase.

Traces of sugars, fatty acids were omitted and are not included in the table. Furthermore, not shown in the table are two compounds (**D1**, **D2**) that could not be identified in the NIST database. Both compounds had molecular masses that differed by +16 Da when compared to diclofenac, with a high probability of containing two chlorine atoms. Both compounds eluted from the GC after diclofenac. Accordingly, it is likely that these two compounds are hydroxylated diclofenac derivatives.

### 3.4. Reactive oxygen species in plasma treated solution

During plasma treatment of BMPO-containing solution, BMPO-adducts of the hydroxyl radical (•OH) and the superoxide anion radical (•$O_2^-$) were formed (Fig. 5). With increasing treatment time, the spin trap adduct concentrations for both radicals increased. Both spin trap adducts show the same trend for an increasing concentration within the same order of magnitude. The •OH-adduct was observed already after short plasma treatment time (2 min), the •$O_2^-$-adduct was detected for the first time after 38 min during plasma treatment. In the untreated controls, no spin trap adducts were determined.

Formation of hydrogen peroxide followed in general the same characteristic, i.e. increase, that was observed for the two reactive oxygen species. However, the absolute concentration of hydrogen peroxide was about three orders of magnitude higher than for the BMPO-adducts. A maximum concentration of 1.8 mM was achieved after about 70 min of plasma treatment.
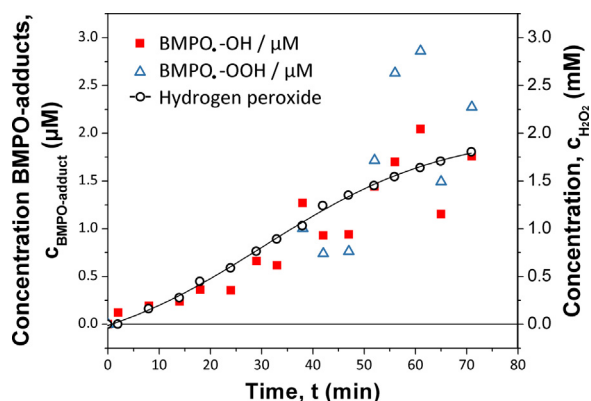


**Fig. 5.** Formation of •OH and •$O_2^-$ spin trap adducts and hydrogen peroxide (−) during plasma treatment. Initial concentration of BMPO was 10 mM.

## 4. Discussion

### 4.1. Reaction pathways and intermediates for diclofenac degradation

Whereas the possibility to continuously generate hydroxyl radicals by plasma in water is an inherent advantage of the method, the degradation by Fenton-processes depends on initial or resupplied admixtures of hydrogen peroxide and dissolved iron as described by Grymonpré et al. [42]. The high amounts of iron(II) chloride, as well as the higher initial concentrations of hydrogen peroxide, explain the increased decomposition of diclofenac during the Fenton-experiments in the first minutes of the treatment. This was achieved at the expense of sustainability, since no further diclofenac was decomposed after the hydrogen peroxide was completely consumed. However, a direct comparison of the apparently initially higher degradation rates achieved by Fenton-processes as described in Fig. 3 is not appropriate. In this study Fenton-processes were primarily investigated for comparison of degradation mechanisms.

Of 60 different identified compounds, 21 could be related directly with diclofenac degradation and are presented in Table 1. Remaining identified compounds are chemical impurities and ubiquitous present substances (e.g. sugars and fatty acids). Accordingly, some short-chain organic acids such as lactic acid (1), glycolic acid (2), benzoic acid (6), 2-hydroxybenzoic acid (14) and L-threonic acid (16) were also found for control experiments, i.e. untreated water samples. Therefore, it is unlikely that these compounds were formed during diclofenac treatment. Other compounds, such as urea (5), glycerol (8), plasticizer (23) sugars, and fatty acids are compounds ubiquitously found in water. Degradation products of chemicals that were necessary to start Fenton-chemistry, such as D-erythronolactone (12), were also disregarded, since the compound is a byproduct of sodium ascorbate decomposition. Compounds (21) and (29) represent special cases since they are also intermediates in diclofenac synthesis and can be considered both as diclofenac impurities and/or possible degradation products of diclofenac as described elsewhere [37,41].

Diclofenac is mostly stable in neutral or alkaline aqueous solutions, however, the molecule can cyclize in acidic conditions to diclofenac lactam (21), which is also known as impurity A [43,44]. All experiments were conducted under almost neutral conditions (pH 6–7) to increase the stability of diclofenac during experiments. The neutral pH-value hindered the intramolecular condensation reactions responsible for lactam formation. Short-chained organic acids were formed as diclofenac decomposition progressed, concurrently slightly decreasing pH-value. This in return promoted the formation of diclofenac lactam. Altogether, the molecule can there-

**Table 1**

Overview of chemical compounds found after diclofenac decomposition due to plasma treatment and/or •OH-chemistry induced by Fenton-processes. Compounds are sorted with respect to their retention time ($t_R$) in a GC–MS system. The table includes references to publications that describe the degradation of diclofenac by hydroxyl radicals, including identified byproducts.

| $t_R$, min # | Compound | Match | Plasma | Fenton | Comments/Occurrence in •OH-chemistry literature |
|---|---|---|---|---|---|
| **Derivatized injection, detected as silyl derivatives** | | | | | |
| 6409 (1) | Lactic acid | 956/957 | ✓ | ✓ | Probably an Impurity, also detected in control |
| 6629 (2) | Glycolic acid | 953/947 | ✓ | ✓ | Probably an Impurity, also detected in control |
| 7.474 (3) | Oxalic acid, (**D18**) | 926/929 | ✓ | ✓ | [27] [a] [37] [b] [38] [c] |
| 8.864 (4) | Malonic acid, (**D17**) | 931/943 | ✓ | ✓ | [27] [a] [37] [b] |
| 9481 (5) | Urea | 906/923 | × | ✓ | Probably an Impurity, also detected in control |
| 9927 (6) | Benzoic acid | 904/919 | ✓ | ✓ | Probably an Impurity, also detected in control |
| 9928 (7) | 2,6-Dichloroaniline, (**D6**) | 960/960 | ✓ | ✓ | [37] [b] [39] [c] [40] [d] [41] [d] |
| 10,315 (8) | Glycerol | 922/944 | ✓ | ✓ | Probably an Impurity, also detected in control (fatty acids) |
| 11,146 (9) | Succinic acid, (**D19**) | 824/913 | ✓ | × | [27] [a] |
| 11,845 (10) | Fumaric acid, (**D21**) | 903/909 | ✓ | ✓ | [27] [a] [38] [c] (*cis*-isomer maleic acid) |
| 12,226 (11) | 2,6-Dichlorophenol, (**D5**) | 928/929 | ✓ | ✓ | [37] [b] [40] [d] [41] [d] |
| 12,724 (12) | D-Erythronolactone | 905/920 | × | ✓ | Probably an Impurity, also detected in control (ascorbic acid) |
| 15,327 (13) | Malic acid, (**D20**) | 880/881 | ✓ | × | [37] [b] |
| 15,865 (14) | 2-Hydroxybenzoic acid | 905/907 | × | ✓ | Probably an Impurity, also detected in control |
| 17,159 (15) | 2-Hydroxyphenylacetic Acid (**D7**) | 935/964 | ✓ | ✓ | [37] [b] |
| 17,167 (16) | L-Threonic acid | 925/925 | × | ✓ | Probably an Impurity, also detected in control |
| 19,296 (17) | 2,6-Dichlorohydro quinone, (**D11**) | 908/908 | ✓ | ✓ | [37] [b] |
| 23,089 (18) | Homogentisic acid, (**D14**) | 944/948 | ✓ | ✓ | [39] [c] [27] [a] [37] [b] |
| 25,619 (19) | Ascorbic acid | 885/886 | × | ✓ | Chemical used in Fenton-chemistry |
| 26,572 (20) | 5-Hydroxyoxindole, (**D16**) | 894/917 | × | ✓ | Probably ring closure of: (2-Amino-5-hydroxyphenyl)acetic acid (**D15**) |
| 29,905 (21) | Diclofenac-lactam, (**D3**) | 936/939 | ✓ | ✓ | [37] [b] [40] [d] [41] [d] |
| 32,768 (22) | Diclofenac | 951/957 | ✓ | ✓ | Object of this study |
| 35,568 (23) | Dicyclohexyl phthalate | 971/973 | ✓ | ✓ | Probably an Impurity, also detected in control (plasticizer) |
| **Underivatized injection** | | | | | |
| 7543 (24) | 2-Chloroaniline, (**D13**) | 937/938 | ✓ | × | [37] [b] [40] [d] |
| 9687 (25) | Benzofuranone, (**D8**) | 851/909 | ✓ | × | Probably ring closure of: 2-Hydroxyphenyl acetic acid (**D7**) |
| 11,342* (26) | 2,6-Dichlorophenyl isocyanate, (**D4**) | 896/896 | ✓ | × | [41] [d] |
| 14,365* (27) | 3,5-Dichloro-4-amino Phenol, (**D12**) | 850/889 | ✓ | × | [27] [a] [37] [b] [38] [c] [39] [c] |
| 15,191 (28) | Oxindole, (**D10**) | 917/927 | ✓ | × | Probably ring closure of: 2-Aminophenylacetic acid (**D9**) |
| 23,337 (29) | 2,6-Dichlorodiphenyl-amine | 878/912 | ✓ | ✓ | [37] [b] [41] [d] Probably impurity due to diclofenac synthesis |
| 26,473 (30) | 2-[(2,6-Dichlorophenyl) amino]benzacetaldehyde | 887/933 | ✓ | ✓ | Probably an Impurity, also detected in control |

[a] Pulsed Corona plasma (PCD) above liquid.
[b] Hydroxyl radicals formed due to sonolysis.
[c] Hydroxyl radicals formed due to $H_2O_2$/UV.
[d] Hydroxyl radicals formed due to Fenton-chemistry.

fore be considered an indirect degradation product. Conversely, 2,6-dichlorodiphenylamine (29) was considered a diclofenac impurity since it was also detected in control samples.

Pathway and intermediates for the degradation of diclofenac by plasma treatment (P) or by Fenton-processes (F) are depicted in Fig. 6. The detailed study shows that hydroxyl radicals are responsible for the oxidation of the initial compound and almost all intermediates. No evidence was found for chemistry involving reactive chlorine, ozone or peroxynitrite. Thus, findings are in good agreement with previous studies where phenol was used as a model substance to determine different reactive species [19].

Four reaction steps (**I–IV**) predominantly characterize degradation of diclofenac. Most likely attack of the benzene rings is one of the key starting reactions [37–39]. This is illustrated by the derivatives **D1***, with a molecular mass difference of multiples of 16 Da, indicating the formation of hydroxyl/phenol groups in diclofenac. This could occur if hydroxyl radical first abstracted a hydrogen atom from carbon and then a second •OH combined with the carbon based radical. The most reactive C-atoms of the diclofenac-molecule would be expected in the 4 and 4′ position of the rings, since they are stabilized due to resonance effects. However, partially electron-withdrawing groups, such as chlorine (decrease of electron density) might also favor reactions with the C-4′. Further
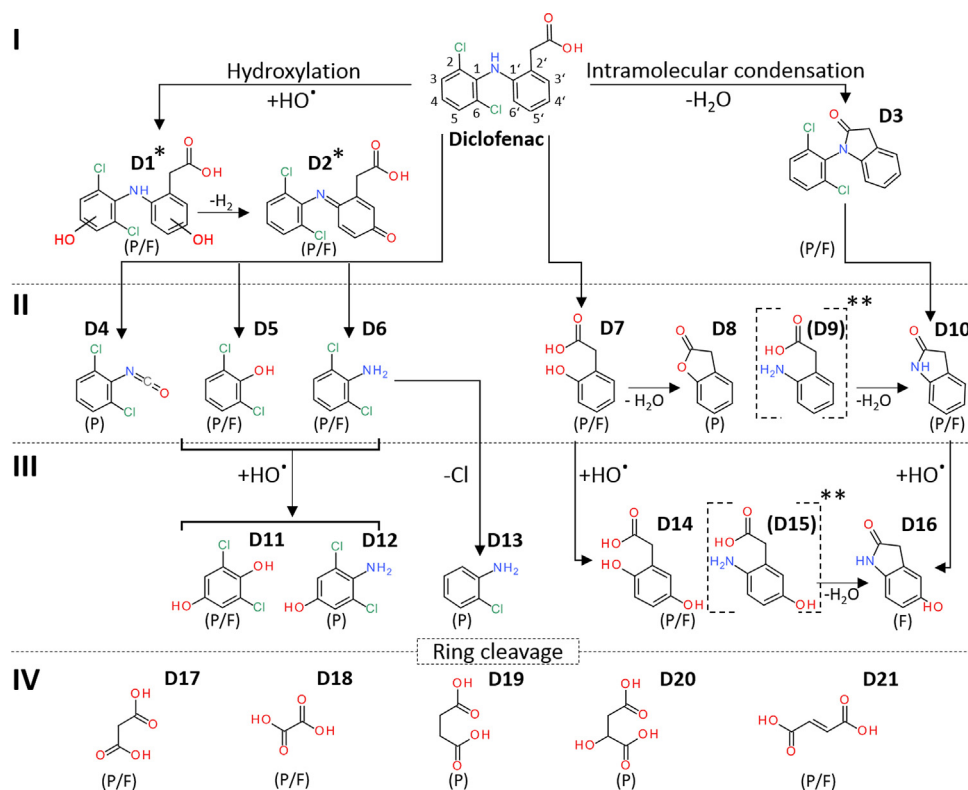
**Fig. 6.** Proposed degradation pathway and intermediates for the degradation of diclofenac by hydroxyl radicals formed during plasma treatment (P) or due to hydroxyl radicals generated by Fenton-processes (F). Apart from intermediates D9 and D15, all other byproducts were experimentally identified and verified.
*Products were identified due to their molecular mass, physicochemical properties and description in literature.
** Intermediate was not detected.

loss of $H_2$ would lead to quinone-imine intermediates, such as **D2***[38].

The cleavage of the C—N bond (**II**) results in several characteristic byproducts (**D5**-**D10**). The molecule is split into two parts; depending on the spatial orientation of the hydroxyl radical attack, the derivatives 2,6-dichlorophenol (**D5**) or 2,6-dichloroaniline (**D6**) are formed. Their respective counterparts (**D7** and **D9**) were detected as **D8** and **D10** due to acidification and ring closure during solid phase extraction.

It is worth pointing out that cleavage products for both diclofenac derivatives [(**D5**, **D10**) and (**D6, D7**)] could be detected, since previous publications only mentioned intermediates **D6** and **D7** when diclofenac was degraded with plasma generated above the liquid [27]. Derivative **D4** was only detected after plasma application, but Beldean-Galea and coworkers also reported its formation for •OH-chemistry (Fenton) [41].

Step **III** involves continuing hydroxylation and dechlorination (**D11**-**D16**), which in the end (**IV**) leads to cleavage of the benzene ring structure and formation of small organic acids (**D17**-**D21**). Accordingly, the same byproducts are observed and degradation pathways are similar for plasma treatment and Fenton-processes.

### 4.2. Reactive oxygen species responsible for pollutant degradation

Direct observation of hydroxyl radicals (e.g. by optical emission spectroscopy) is difficult due to their reactive and transient nature. For the generation of plasma with submicrosecond high voltage pulses are excited hydroxyl radicals generally not observed [30,45,46]. The generation of hydroxyl radicals was instead confirmed indirectly by spin trap enhanced EPR spectroscopy (Fig. 5).

By using BMPO as a spin trap, it was further possible to distinguish hydroxyl radicals and superoxide anion radicals [34]. The •OH-adduct was almost immediately observed, whereas the •$O_2^-$

adduct was detected after 38 min of plasma treatment. Concentrations of both BMPO-adducts increased steadily after exceeding the detection threshold.

The efficacy of the spin trap for •$O_2^-$-trapping is about 90% [47] and for •OH about 0.6% [48]. Hence, concentration of radicals that are available for pollutant degradation can be estimated to be in the range of at least 300 μM for •OH and 2.5 μM for •$O_2$ after 70 min of plasma treatment. However, many short-lived radicals immediately react already again in the vicinity of plasma filaments. Concentration measured with the spin trap can in fact be considered an estimate for OH-radicals that are available in the bulk, i.e. have not readily reacted. Conversely, hydrogen peroxide can indeed quantify overall hydroxyl radical generation as previously suggested [36]. Hereby does the comparison of mass balances imply that hydroxyl radicals were generated in a 10-fold higher concentration (1.8 mM hydrogen peroxide equals 3.6 mM •OH) than described by the spin-trap measurements. Notable the same trend and similar arguments on generation rates also apply for superoxide anions.

The time delayed formation of •$O_2^-$, as well as relative low concentration suggest the formation of •$O_2^-$ due to secondary reactions in the bulk liquid. (Fig. 7). If traces of metal ions are present in solution, they can catalytically decompose formed hydrogen peroxide providing hydroxyl radicals again. Subsequently, hydrogen peroxide acts as •OH-scavenger and forms the superoxide anion radical (•$O_2^-$), which then can reduce reactivate oxidized metal ions ($Me^{red}$/$Me^{ox}$) and can start the catalytic cycle again.

### 4.3. •OH-chemistry in micropollutant degradation

Reaction mechanisms of hydroxyl radicals with target pollutants can predominantly be described by abstraction of hydrogen atoms (Eq. (1)) and electrophilic addition to unsaturated bonds (Eq.
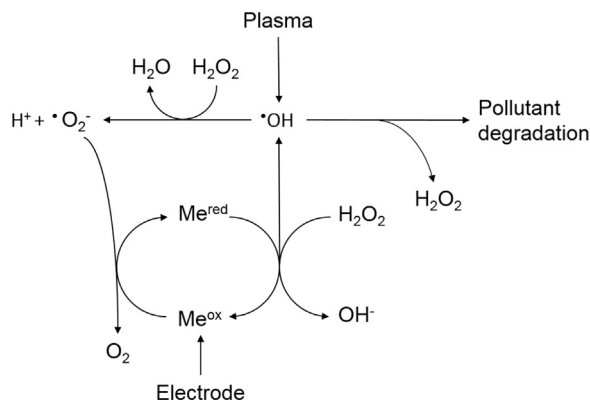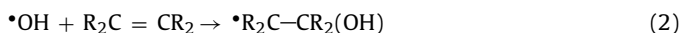
**Fig. 7.** Formation and evolution of hydroxyl radicals ($^{\bullet}$OH) during application of pulsed corona plasma. Plasma generated hydroxyl radicals can react with organic pollutants or recombine to form hydrogen peroxide. Metal ions ($Me^{red}$/$Me^{ox}$) released by electrode corrosion can catalytically decompose hydrogen peroxide providing hydroxyl radicals again. Hydrogen peroxide can further act as $^{\bullet}$OH scavenger and form the superoxide anion radical ($^{\bullet}O_2^{-}$), which then can reduce reactivate oxidized metal ions but also decompose micropollutants.

**Table 2**
Reaction rate constants of OH-radicals with investigated pharmaceutical residues. Starting with diclofenac, pharmaceuticals are sorted by their response to the plasma treatment as shown in Fig. 1.

| Pharmaceutical | Reaction rate constants ($k_{OH}$ in $10^9$ $M^{-1}$ $s^{-1}$) | Reference |
|---|---|---|
| Diclofenac | $9.29 \pm 0.11$ | [50] |
| 17α-Ethinylestradiol | $9.8 \pm 1.2$ | [13] |
| Carbamazepine | $8.8 \pm 1.2$ | [13] |
| Ibuprofen | $7.4 \pm 1.2$ | [13] |
| Trimethoprim | $8.66$ | [51] |
| Diazepam | $7.2 \pm 1$ | [13] |
| Diatrizoate | $0.96 \pm 0.02$ | [52] |

(2)). Because of steric hindrance, or if reactions described above are disfavored by multiple halogen substitutes, also electron transfers (Eq. (3)) can occur [49].

$$^{\bullet}OH + RH \rightarrow {}^{\bullet}R + H_2O \tag{1}$$

$$^{\bullet}OH + R_2C = CR_2 \rightarrow {}^{\bullet}R_2C{-}CR_2(OH) \tag{2}$$

$$^{\bullet}OH + RX \rightarrow {}^{\bullet}RX^{+} + OH^{-} \tag{3}$$

These reaction schemes can explain why some pharmaceuticals, e.g. diatrizoate, are more recalcitrant while others are decomposed readily when subjected to pulsed corona plasma generated in water (Fig. 2). Diatrizoate, a fully substituted benzene derivative, might be expected to favor reactions in which hydroxyl radicals attack the aromatic ring system. However, for diatrizoate all reactive C-atoms are blocked by functional groups. Moreover, these functional groups withdraw electrons from the aromatic ring system due to inductive effects ($-I$ effect, iodine) and resonance effects ($-M$, carbonyl group). Thus, electron density in the aromatic system is much lower when compared to diclofenac and 17α-ethinylestradiol, which are both readily decomposed because both molecules have aromatic rings that are not fully substituted. In addition, functional groups, such as the secondary amine in diclofenac or the hydroxyl group in 17α-ethinylestradiol, are both increasing the electron density ($+M$) in the aromatic ring system.

Since hydroxyl radicals are strong electrophiles, this increases the affinity of the radicals towards the target molecules. This is also reflected by the reaction rate constants of OH-radicals with the pharmaceuticals as shown in Table 2.

Carbamazepine, ibuprofen, trimethoprim and diazepam approximately have the same reaction rate constants. Their response to plasma treatment should therefore be found in

between diclofenac/17α-ethinylestradiol and diatrizoate which was indeed observed in the degradation experiments; although, it should be noted that diazepam appeared to be more recalcitrant than suggested by the reaction rate constants. Results for diazepam were well-reproducible during degradation experiments, and more research has to be conducted for a better understanding.

However, overall reaction rate constants fit well with the response observed in the degradation experiments (Fig. 2). In conclusion, aromatic ring systems, unsaturated bonds and electron donating functional groups ($+I$/$+M$) increase molecular reactivity towards plasma treatment and also towards other AOPs that are relying on the generation of hydroxyl radicals.

### 4.4. Possible hazardous byproducts formed during plasma treatment

The decomposition cascade of the initial compound by consecutive reactions with hydroxyl radicals also determines the formation of possible toxic byproducts. In case of diclofenac, aromatic ring structures with high electron densities result in several phenol derivatives and their respective counterparts such as 2,6-dichlorophenol (**D5**), 2,6-dichloroaniline (**D6**), 2-hydroxyphenylacetic acid (**D7**), 2,6-dichlorohydroquinone (**D11**), 3,5-dichloro-4-aminophenol (**D12**). Aromatic ring structures are very common in pharmaceuticals; therefore, phenol derivatives can be expected to form with many chemical compounds. Although their chemical structure is rather simple, phenols and their derivatives are well-known for their bio-recalcitrance and acute toxicity [53].

This can be further elucidated for diclofenac as an example. According to the Globally Harmonized System of Classification and Labelling of Chemicals (GHS), diclofenac is classified as harmful to aquatic life with long lasting effects (H412, category 3). 2,6-dichlorophenol (**D5**) and 2,6-dichloroaniline (**D6**) exceed this category and are classified as category 2 (H411) and category 1 (H400/H410) [54]. Substances in category 2 are considered toxic to aquatic life with long-lasting effects, whereas category 1 is considered very toxic to aquatic life with long-lasting effects.

Accordingly, the degradation of pharmaceuticals carries the risk for the generation of compounds that are even more toxic than the originally targeted substance. However, this risk is not limited to plasma but is common to all AOPs that rely on the generation of OH-radicals for oxidation processes as described above.

It is important to note that byproducts also undergo decomposition during further treatment as shown in Fig. 6. Since several intermediates are continuously formed and decomposed, the concentration of byproducts is much lower than for the original compound. Therefore, with a sufficiently long or intense treatment, the problem could be addressed.

## 5. Conclusion

Advanced oxidation processes (AOP) and plasma treatment in particular are some of the few feasible approaches to decompose recalcitrant compounds in water. Pulsed corona plasma in water can provide high concentrations of hydroxyl radicals. The fast recombination to hydrogen peroxide encourages catalytic or photolytic splitting of this intermediate storage for hydroxyl radicals to provide further water purification.

It has been found that aromatic rings, unsaturated bonds and electron donating functional groups ($+I$/$+M$) increase molecular reactivity towards plasma treatment and AOPs in general, which also explains why some pharmaceuticals are more recalcitrant than others. Nevertheless, the degradation by hydroxyl radical chemistry in principle has an associated risk for the formation

of even harmful compounds. Consequently, treatment times of AOPs should be sufficiently long to either ensure a considerable reduction of harmful byproducts, or should aim for a complete mineralization of organic pollutants. However, for practical reasons treatment times should be adjusted depending on actual pollutant concentrations and toxicity of intermediates. The comparison with Fenton-processes also offers a suggestion to improve the plasma treatment by providing means to utilize hydrogen peroxide which is generated in the plasma. This could be achieved by deliberately applying catalytic processes.

## Acknowledgments

## Appendix A.  Supplementary data

Supplementary data associated with this article can be found, in the online version, at http://dx.doi.org/10.1016/j.jhazmat.2017.08.058.

## References

[1] T.A. Ternes, M. Meisenheimer, D. McDowell, F. Sacher, H.-J. Brauch, B. Haist-Gulde, G. Preuss, U. Wilme, N. Zulei-Seibert, Removal of pharmaceuticals during drinking water treatment, Environ. Sci. Technol. 36 (2002) 3855–3863.

[2] P.E. Stackelberg, E.T. Furlong, M.T. Meyer, S.D. Zaugg, A.K. Henderson, D.B. Reissman, Persistence of pharmaceutical compounds and other organic wastewater contaminants in a conventional drinking-water-treatment plant, Sci. Total Environ. 329 (2004) 99–113.

[3] T.A. Larsen, J. Lienert, A. Joss, H. Siegrist, How to avoid pharmaceuticals in the aquatic environment, J. Biotechnol. 113 (2004) 295–304.

[4] M. Stumpf, T.A. Ternes, K. Haberer, W. Baumann, Nachweis von natürlichen und synthetischen Östrogenen in Kläranlagen und Fließgewässern, Vom Wasser 87 (1996) 251–261.

[5] R. Hirsch, T. Ternes, K. Haberer, K.-L. Kratz, Occurrence of antibiotics in the aquatic environment, Sci. Total Environ. 225 (1999) 109–118.

[6] T. Brodin, J. Fick, M. Jonsson, J. Klaminder, Dilute concentrations of a psychiatric drug alter behavior of fish from natural populations, Science 339 (2013) 814–815.

[7] G. Nentwig, Effects of pharmaceuticals on aquatic invertebrates. Part II: the antidepressant drug fluoxetine, Arch. Environ. Contam. Toxicol. 52 (2007) 163–170.

[8] F. Hoffmann, W. Kloas, Estrogens can disrupt amphibian mating behavior, PLoS One 7 (2012) e32097.

[9] C.E. Purdom, P.A. Hardiman, V.V.J. Bye, N.C. Eno, C.R. Tyler, J.P. Sumpter, Estrogenic effects of effluents from sewage treatment works, Chem. Ecol. 8 (1994) 275–285.

[10] D.J. Larsson, C. de Pedro, N. Paxeus, Effluent from drug manufactures contains extremely high levels of pharmaceuticals, J. Hazard. Mater. 148 (2007) 751–755.

[11] E. Commission, Environment and Water: proposal to reduce water pollution risks, In: European Commission, European Commission – Press release.

[12] R. Giri, H. Ozaki, S. Ota, R. Takanami, S. Taniguchi, Degradation of common pharmaceuticals and personal care products in mixed solutions by advanced oxidation techniques, Int. J. Environ. Sci. Technol 7 (2010) 251–260.

[13] M.M. Huber, S. Canonica, G.-Y. Park, U. von Gunten, Oxidation of pharmaceuticals during ozonation and advanced oxidation processes, Environ. Sci. Technol. 37 (2003) 1016–1024.

[14] J. Poyatos, M. Munio, M. Almecija, J. Torres, E. Hontoria, F. Osorio, Advanced oxidation processes for wastewater treatment: state of the art, Water Air Soil Pollut. 205 (2010) 187–204.

[15] K. Ikehata, N. Jodeiri Naghashkar, M. Gamal El-Din, Degradation of aqueous pharmaceuticals by ozonation and advanced oxidation processes: a review, Ozone: Sci. Eng. 28 (2006) 353–414.

[16] P. Lukes, B.R. Locke, Degradation of substituted phenols in a hybrid gas-liquid electrical discharge reactor, Ind. Eng. Chem. Res. 44 (2005) 2921–2930.

[17] P. Lukes, E. Dolezalova, I. Sisrova, M. Clupek, Aqueous-phase chemistry and bactericidal effects from an air discharge plasma in contact with water: evidence for the formation of peroxynitrite through a pseudo-second-order post-discharge reaction of $H_2O_2$ and $HNO_2$, Plasma Sources Sci. Technol. 23 (2014) 015019.

[18] M. Sahni, B.R. Locke, Quantification of hydroxyl radicals produced in aqueous phase pulsed electrical discharge reactors, Ind. Eng. Chem. Res. 45 (2006) 5819–5825.

[19] R. Banaschik, P. Lukes, H. Jablonowski, M.U. Hammer, K.-D. Weltmann, J.F. Kolb, Potential of pulsed corona discharges generated in water for the degradation of persistent pharmaceutical residues, Water Res. 84 (2015) 127–135.

[20] M. Magureanu, N.B. Mandache, V.I. Parvulescu, Degradation of pharmaceutical compounds in water by non-thermal plasma treatment, Water Res. 81 (2015) 124–136.

[21] I. Panorel, S. Preis, I. Kornev, H. Hatakka, M. Louhi-Kultanen, Oxidation of aqueous pharmaceuticals by pulsed corona discharge, Environ. Technol. 34 (2012) 923–930.

[22] D. Gerrity, B.D. Stanford, R.A. Trenholm, S.A. Snyder, An evaluation of a pilot-scale nonthermal plasma advanced oxidation process for trace organic compound degradation, Water Res. 44 (2010) 493–504.

[23] K.H.H. Aziz, H. Miessner, S. Mueller, D. Kalass, D. Moeller, I. Khorshid, M.A.M. Rashid, Degradation of pharmaceutical diclofenac and ibuprofen in aqueous solution, a direct comparison of ozonation, photocatalysis, and non-thermal plasma, Chem. Eng. J. 313 (2017) 1033–1041.

[24] M. Magureanu, D. Piroi, N.B. Mandache, V. David, A. Medvedovici, V.I. Parvulescu, Degradation of pharmaceutical compound pentoxifylline in water by non-thermal plasma treatment, Water Res. 44 (2010) 3445–3453.

[25] M. Magureanu, D. Piroi, N.B. Mandache, V. David, A. Medvedovici, C. Bradu, V.I. Parvulescu, Degradation of antibiotics in water by non-thermal plasma treatment, Water Res. 45 (2011) 3407–3416.

[26] M. Magureanu, D. Dobrin, N. Bogdan Mandache, C. Bradu, A. Medvedovici, V.I. Parvulescu, The mechanism of plasma destruction of enalapril and related metabolites in water, Plasma Process. Polym. 10 (2013) 459–468.

[27] D. Dobrin, C. Bradu, M. Magureanu, N. Mandache, V. Parvulescu, Degradation of diclofenac in water using a pulsed corona discharge, Chem. Eng. J. 234 (2013) 389–396.

[28] M. Marković, M. Jović, D. Stanković, V. Kovačević, G. Roglić, G. Gojgić-Cvijović, D. Manojlović, Application of non-thermal plasma reactor and Fenton reaction for degradation of ibuprofen, Sci. Total Environ. 505 (2015) 1148–1155.

[29] K. Oehmigen, M. Hähnel, R. Brandenburg, C. Wilke, K.D. Weltmann, T. von Woedtke, The role of acidification for antimicrobial activity of atmospheric pressure plasma in liquids, Plasma Process. Polym. 7 (2010) 250–257.

[30] R. Banaschik, P. Lukes, C. Miron, R. Banaschik, A.V. Pipa, K. Fricke, P.J. Bednarski, J.F. Kolb, Fenton chemistry promoted by sub-microsecond pulsed corona plasmas for organic micropollutant degradation in water, Electrochim. Acta 245 (2017) 539–548.

[31] R.P. Joshi, S.M. Thagard, Streamer-like electrical discharges in water: part II. Environmental applications, Plasma Chem. Plasma Process. 33 (2013) 17–49.

[32] F. Haber, J. Weiss, Über die katalyse des hydroperoxydes, Naturwissenschaften 20 (1932) 948–950.

[33] R.K. Hartmann, Handbook of RNA biochemistry, Wiley-VCH, 2005.

[34] H. Tresp, M.U. Hammer, J. Winter, K. Weltmann, S. Reuter, Quantitative detection of plasma-generated radicals in liquids by electron paramagnetic resonance spectroscopy, J. Phys. D: Appl. Phys. 46 (2013) 435401.

[35] G. Eisenberg, Colorimetric determination of hydrogen peroxide, Ind. Eng. Chem. Analyt. Ed. 15 (1943) 327–328.

[36] B.R. Locke, K.-Y. Shih, Review of the methods to form hydrogen peroxide in electrical discharge plasma with liquid water, Plasma Sources Sci. Technol. 20 (2011) 034006.

[37] J. Hartmann, P. Bartels, U. Mau, M. Witter, W. Tümpling, J. Hofmann, E. Nietzschmann, Degradation of the drug diclofenac in water by sonolysis in presence of catalysts, Chemosphere 70 (2008) 453–461.

[38] L.A. Pérez-Estrada, S. Malato, W. Gernjak, A. Agüera, E.M. Thurman, I. Ferrer, A.R. Fernández-Alba, Photo-Fenton degradation of diclofenac: identification of main intermediates and degradation pathway, Environ. Sci. Technol. 39 (2005) 8300–8306.

[39] D. Vogna, R. Marotta, A. Napolitano, R. Andreozzi, M. d'Ischia, Advanced oxidation of the pharmaceutical drug diclofenac with $UV/H_2O_2$ and ozone, Water Res. 38 (2004) 414–422.

[40] S. Bae, D. Kim, W. Lee, Degradation of diclofenac by pyrite catalyzed Fenton oxidation, Appl. Catal. B: Environ. 134 (2013) 93–102.

[41] M.S. Beldean-Galea, V. Coman, F. Copaciu, D. Thiebaut, J. Vial, Simultaneous identification of Fenton degradation by-products of diclofenac, ibuprofen and ketoprofen in aquatic media by comprehensive two-dimensional gas chromatography coupled with mass spectrometry, Rev. Roum. Chim. 59 (2014) 1021–1027.

[42] D.R. Grymonpré, A.K. Sharma, W.C. Finney, B.R. Locke, The role of Fenton's reaction in aqueous phase pulsed streamer corona reactors, Chem. Eng. J. 82 (2001) 189–207.

[43] F. Wang, J. Finnin, C. Tait, S. Quirk, I. Chekhtman, A.C. Donohue, S. Ng, A. D'souza, R. Tait, R. Prankerd, The hydrolysis of diclofenac esters: synthetic prodrug building blocks for biodegradable drug–polymer conjugates, J. Pharm. Sci. 105 (2015) 773–785.

[44] Ph.Eur., European pharmacopoeia, Council Of Europe: European Directorate for the Quality of Medicines and Healthcare, Strasbourg, 2016.

[45] D. Dobrynin, Y. Seepersad, M. Pekker, M. Shneider, G. Friedman, A. Fridman, Non-equilibrium nanosecond-pulsed plasma generation in the liquid phase (water PDMS) without bubbles: fast imaging, spectroscopy and leader-type model, J. Phys. D: Appl. Phys. 46 (2013) 105201.

[46] P. Lukes, M. Clupek, V. Babicky, B. Pongrac, M. Simek, J. Kolb, On the mechanism of OH radical formation by nanosecond pulsed corona discharge in water, Plasma Science (ICOPS), 2016 IEEE International Conference on, IEEE (2016) (1-1).

[47] N. Bézière, M. Hardy, F. Poulhès, H. Karoui, P. Tordo, O. Ouari, Y.-M. Frapart, A. Rockenbauer, J.-L. Boucher, D. Mansuy, Metabolic stability of superoxide adducts derived from newly developed cyclic nitrone spin traps, Free Radic. Biol. Med. 67 (2014) 150–158.

[48] H. Tong, A.M. Arangio, P.S. Lakey, T. Berkemeier, F. Liu, C.J. Kampf, W.H. Brune, U. Pöschl, M. Shiraiwa, Hydroxyl radicals from secondary organic aerosol decomposition in water, Atmos. Chem. Phys. 16 (2016) 1761–1771.

[49] V.I. Parvulescu, M. Magureanu, P. Lukes, Plasma Chemistry and Catalysis in Gases and Liquids, John Wiley & Sons, 2012.

[50] W.J. Cooper, W. Song, Advanced oxidation degradation of diclofenac, in: Radiation Treatment of Wastewater for Reuse with Particular Focus on Wastewaters Containing Organic Pollutants, 2012 (168).

[51] X. Luo, Z. Zheng, J. Greaves, W.J. Cooper, W. Song, Trimethoprim Kinetic and mechanistic considerations in photochemical environmental fate and AOP treatment, Water Res. 46 (2012) 1327–1336.

[52] F.J. Real, F.J. Benitez, J.L. Acero, J.J. Sagasti, F. Casas, Kinetics of the chemical oxidation of the pharmaceuticals primidone, ketoprofen, and diatrizoate in ultrapure and natural waters, Ind. Eng. Chem. Res. 48 (2009) 3380–3388.

[53] S. Ahmed, M. Rasul, W.N. Martens, R. Brown, M. Hashib, Heterogeneous photocatalytic degradation of phenols in wastewater: a review on current status and developments, Desalination 261 (2010) 3–18.

[54] PubChem, 2,6-DICHLOROANILINE, In: National Center for Biotechnology Information, 2017.

# Publication P5

## Comparison of Pulsed Corona Plasma and Pulsed Electric Fields for the Decontamination of Water Containing Legionella Pneumophila as Model Organism

R. Banaschik, G. Burchhardt, K. Zocher, S. Hammerschmidt, J.F. Kolb, K.-D. Weltmann, *Bioelectrochemistry*, 112 (2016) 83-90.

# Comparison of pulsed corona plasma and pulsed electric fields for the decontamination of water containing *Legionella pneumophila* as model organism

Robert Banaschik [a], Gerhard Burchhardt [b], Katja Zocher [a], Sven Hammerschmidt [b,*], Juergen F. Kolb [a,*], Klaus-Dieter Weltmann [a]

[a] Leibniz Institute for Plasma Science and Technology e.V. (INP Greifswald), Felix-Hausdorff-Straße 2, 17489 Greifswald, Germany
[b] Department Genetics of Microorganisms, Interfaculty Institute for Genetics and Functional Genomics, Ernst Moritz Arndt University of Greifswald, Friedrich-Ludwig-Jahn-Straße 15a, 17489 Greifswald, Germany

## ARTICLE INFO

## ABSTRACT

Pulsed corona plasma and pulsed electric fields were assessed for their capacity to kill *Legionella pneumophila* in water. Electrical parameters such as in particular dissipated energy were equal for both treatments. This was accomplished by changing the polarity of the applied high voltage pulses in a coaxial electrode geometry resulting in the generation of corona plasma or an electric field. For corona plasma, generated by high voltage pulses with peak voltages of $+80$ kV, *Legionella* were completely killed, corresponding to a log-reduction of 5.4 (CFU/ml) after a treatment time of 12.5 min. For the application of pulsed electric fields from peak voltages of $-80$ kV a survival of log 2.54 (CFU/ml) was still detectable after this treatment time. Scanning electron microscopy images of *L. pneumophila* showed rupture of cells after plasma treatment. In contrast, the morphology of bacteria seems to be intact after application of pulsed electric fields. The more efficient killing for the same energy input observed for pulsed corona plasma is likely due to induced chemical processes and the generation of reactive species as indicated by the evolution of hydrogen peroxide. This suggests that the higher efficacy and efficiency of pulsed corona plasma is primarily associated with the combined effect of the applied electric fields and the promoted reaction chemistry.

© 2016 Elsevier B.V. All rights reserved.

## 1. Introduction

*Legionella pneumophila* are Gram-negative bacteria that were first described in 1979 after an outbreak of pneumonia among members of the American Legion. The elongated non-spore forming aerobic microorganisms with a length of 2–5 μm proliferate in amoeba but can also replicate within alveolar macrophages. Although 15 serogroups of *Legionella pneumophila* are confirmed, serogroup 1 (sg1) is most frequently associated with severe infections [1]. Legionellosis can traditionally be distinguished in two clinical pictures. One is described as Legionnaires' disease (named after the first observed outbreak) causing severe pneumonia. The other is the so called Pontiac fever whose etiopathology is rather moderate, flue-like and most of all self-limiting. The difference to Legionnaires' disease is the lack of pneumonic symptoms [2,3].

In modern societies *Legionella* often persist in water tanks, cooling systems or air conditioning systems causing a severe respiratory disease when contaminated water or aerosol is inhaled by human beings. Several countries reported an increase in cases of legionellosis [4,5]. The Department of Epidemiology (Atlanta, USA) investigated data provided by the Center of Disease Control (CDC) for the years 1990 to 2005. They recognized an increase of 70% from 1310 cases in 2002 to 2223 cases in 2003. Two years later the rate of new infections increased to 12,000 in 2005.

Additional efforts are needed to develop highly efficient disinfection systems to reduce Legionella species in water containing environments [6].

To eradicate *Legionella* several physical and chemical disinfection methods have been described including thermal treatment (superheat-and-flush or instantaneous heating-system), copper/silver ionization, UV-light or hyperchlorination. However, these disinfection methods have limitations [7]. Thermal treatment has disadvantages such as high costs and duration because only temperatures above 60 °C for extended times lead to an almost complete killing of *L. pneumophila*. UV-light is only recommended in combination with superheat-and-flush to provide comprehensive protection. Additionally, prefiltration is necessary to prevent accumulation of chalk residues on the quartz sleeves housing the UV source, which otherwise would

\* Corresponding authors.
 *E-mail addresses:* sven.hammerschmidt@uni-greifswald.de (S. Hammerschmidt),
juergen.kolb@inp-greifswald.de (J.F. Kolb).

decrease UV light emission. Chlorine is highly corrosive and can cause severe plumbing damage. A coating of the pipe system is necessary. This, however, cannot eliminate leakage completely. Furthermore, it was demonstrated that *Legionella* is rarely sensitive to chlorine [7,8]. Thus, more advanced disinfection methods are necessary and motivate the development of new treatment techniques such as pulsed electric fields (PEF) and pulsed corona plasma, respectively. Both of them have already proved to be effective, bio-compatible and environmental friendly [9].

Potential applications of PEF treatment are food processing, medical treatment or water treatment [10–14]. If parameters like pulse polarity, conductivity and electrode shape are adjusted correctly, alternatively non-thermal, i.e. corona plasma, can be formed. It has been demonstrated that non-thermal plasma generated directly in water does have a variety of physical and chemical effects known to be effective for pollutant degradation, bacterial killing, including the killing of spores [9,15–20]. Beside the occurrence of strong electric fields, ultraviolet radiations, shockwaves and probably most importantly chemical reactive species such as hydroxyl radicals and hydrogen peroxide ($H_2O_2$) are generated by the plasma [21]. Nevertheless, processes responsible for bacterial killing with pulsed corona plasma are not fully understood. Especially the role of the electric field in comparison to effects mediated by the plasma itself is unclear. Therefore it is still ambiguous which of the methods is more efficient and causes a higher log-reduction of colony forming units (CFU), requires less time and/or less energy.

Differences between pulsed corona plasma and PEF were already compared previously although in different experimental setups. Slightly higher decontamination efficiency was found for plasma when *Escherichia coli* was used as model organism. Corona plasma was generated in a wire to plate geometry, applying pulses of 600 ns at a repetition rate of 0.1 Hz and with peak voltages of 120 kV. The results were correlated to PEF-treatments conducted in a plate-to-plate setup for an applied homogenous pulsed electric field of 80 kV/cm with pulse durations of 60 ns, 300 ns and 2 μs. In this setting shorter pulses in sub-microsecond range appeared to be more effective than longer pulses [22,23].

Comparative studies were also performed using *Pseudomonas fluorescens* as a model microorganism. Plasma was formed in a needle to plate system when applying pulses of 20 kV with a duration of 6 μs. Air or nitrogen could be bubbled through the needle to enhance energy efficiency. When plasma was applied directly to water, it was found to be more energy efficient than PEF-treatment, which was conducted in plate-to-plate geometry for a homogeneous field of 66 kV/cm and a pulse length of 150 μs [24].

Although the plasma was not generated directly in water a further study showed that the combination of plasma and PEF treatment had synergistic killing effects dependent in which order the methods were applied. Using a plasma jet close to the liquid surface first and afterwards PEF treatment led to an almost complete killing of *Staphylococcus aureus*. Pulsed electric fields were applied with a plate to plate configuration using peak voltage of 3 kV, pulse duration of 100 μs and a repetition rate of 1 Hz [9].

However, all these studies were facing the problem that plasma source and PEF source were not directly comparable due to two different experimental setups for either the application of plasma or the electric field.

In this study two different methods were compared for their effect on the viability of pathogenic *Legionella* in water. An experimental setup was established, which allowed the generation of plasma and pulsed electric fields, respectively.

All experiments were performed with the same experimental setup and an equal peak voltage of about 80 kV. Almost the same amount of energy in either the plasma or PEF treatment was delivered per discharge or pulsed field. This was accomplished by changing the polarity of the applied short high voltage pulses, which resulted either in the generation of corona plasma or an electric field only. This allowed a direct comparison on the effectiveness and differences in killing mechanisms for both methods.

## 2. Materials and methods

### 2.1. Electrical setup

A coaxial electrode geometry was used for plasma and PEF treatment, respectively. For a more robust electrode design two twisted tungsten wires (W-005135/13, Goodfellow, Huntingdon, England) with a diameter of 0.05 mm each (pure, uncoated) were aligned in the middle of a glass tube and served as high voltage electrode. The glass tube had a length of 67 mm and a diameter of 34.5 mm. Ground electrode was a metal mesh of stainless steel that was fixed on the inner wall of the class tube. High voltage electrode was replaced after each experiment to establish the most comparable conditions for all experiments. The assembled reactor was holding a volume of 68 ml. Positive or negative high voltage pulses could be applied to the center electrode by a 6-stage Marx-bank with a repetition rate of 20 Hz. The setup was described previously in more detail [19,25]. An inherent advantage of this setup is the possibility to create either a pulsed corona plasma using positive polarity high voltage pulses (Fig. 1) or just a pulsed electrical field using negative polarity high voltage pulses.

During application of positive high voltage pulses in a wire to cylinder or needle to plate system, a strong electric field is located close to the surface of the high voltage electrode (wire). Although the field weakens over distance, electron avalanches result in streamer propagating to the outer electrode (metal mesh) forming a plasma. Negative polarity uses to be less attractive for electron avalanches. If streamers formed at all, they are significantly shorter than with a positive polarity [26,27]. The described mechanism can be employed to develop an experimental setup (pulse width, reactor chamber, conductivity) in which only a positive discharge is formed, even when negative pulses with the same peak voltage were used.

Pulses applied by the Marx-bank are characterized by short rise times of about 20 ns, a peak voltage of 80 kV and an exponential decay resulting in pulse lengths (FWHM) of about 140 ns for positive (plasma) and approximately 240 ns for negative (PEF) polarity (Fig. 2).

Although pulse length for PEF treatment is increasing, the calculated pulse energy is almost similar for both polarities. This can be explained by current flows that compensate for differences in applied voltages. Beyond 400 ns energy dissipated in pulses applied for plasma and PEF
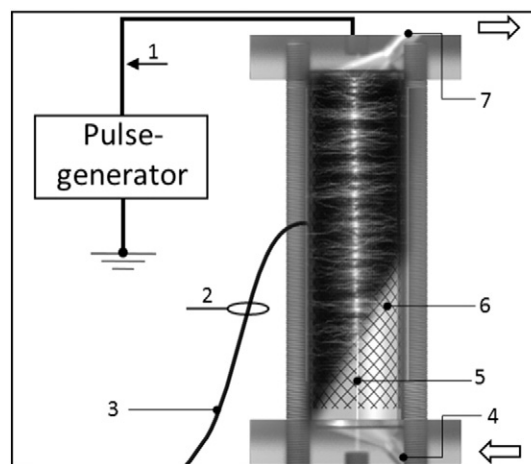


**Fig. 1.** Pulsed corona plasma in coaxial geometry with increased exposure time. (1) voltage measurement, (2) current measurement, (3) ground connection, (4) bottom connector to peristaltic pump, (5) tungsten high voltage electrode, (6) ground electrode (stainless steel mesh), (7) upper connector to peristaltic pump. Arrows indicate the flow direction of *Legionella* suspension. Positive or negative high voltage pulses were applied to the center electrode from a 6-stage Marx-bank with a repetition rate of 20 Hz. Conductivity of treated suspension was adjusted to 60 μS/cm. A flow rate of 140 ml/min was maintained by a peristaltic pump, which was placed before the setup with a pushing flow from the bottom to the top as indicated by arrows.
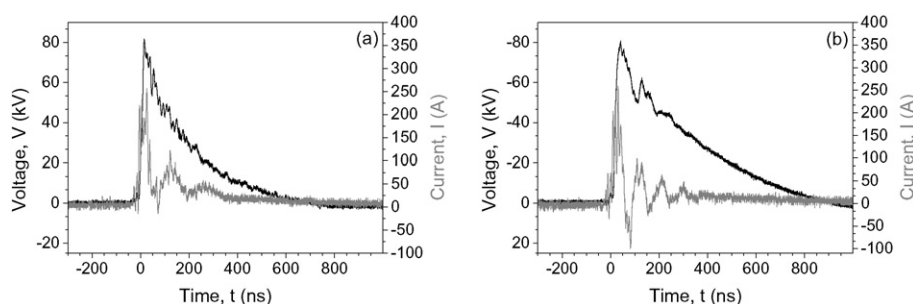
**Fig. 2.** Current and voltage characteristics for a single positive (a) and negative (b) high voltage pulse that was applied to generate a corona plasma or an electric field. Voltage waveform is close to critically damped with peak voltage of 80 kV, pulse duration of about 140 and 240 ns (FWHM). The current pulses show a damped oscillation with peak currents of 130 A for positive and 120 A for negative polarity. Calculated energy of both pulses was 1.1 J.

treatment is rather low. Therefore a slightly longer exponential decay observed for PEF treatment led only to a small increase of energy consumption. Energy delivered with each pulse (1.1 J) was calculated by integrating the product for the duration of the voltage and current signals. Voltage was measured with a 120-kV/80-MHz high voltage probe (PVM-5, NorthStar Marana, AZ). Current was measured with a Pearson current monitor (Model 5046, Pearson Electronics, Palo Alto, CA). Current monitor was terminated with 50 Ω at the oscilloscope to monitor fast rise times of the current pulses. Voltage and current were recorded for analysis (Wave Surfer 64MXs-B, LeCroy, Chestnut Ridge, NY).

A peristaltic pump (FH100x, Thermo Scientific, Waltham, MA) was used to move the bacterial suspension with a flow rate of 140 ml/min through the setup. Total treated volume including tubes and expansion tank was 140 ml. Samples for each experiment were taken after 7500, 15,000 and 30,000 consecutive discharges. This corresponded to a treatment time of 6.25 min, 12.5 min and 25 min. Taking the volume of the discharge chamber, total volume and flow rate into account, theoretical exposure time to plasma or PEF for a single cell during 1 min of treatment/pumping was 600 discharges or high voltage pulses. To exclude thermal effects due to heating, suspension was cooled with ice cold water to keep the temperature below 28 °C.

### 2.2. Cultivation of Legionella pneumophila

Cultivation of *L. pneumophila* Philadelphia 1 JR32 [28] was performed in BCYE medium supplemented with 0.04% L-cysteine and 0.025% Fe-III(NO₃). In general *L. pneumophila* was inoculated on BCYE agar medium and grown at 34 °C for 2 days. Grown bacteria were transferred to 30 ml BYE medium starting with an $OD_{600\ nm}$ of 0.1 and incubated in a shaking water bath at 34 °C until they reach an $OD_{600\ nm}$ of 0.35. Bacteria were harvested at room temperature at 3270 g for 10 min. Bacterial sediment was resuspended in sterile 20 ml distilled water and centrifuged again to remove residual culture fluid. Approximately 10 ml of grown *Legionella* were transferred to 130 ml sterile distilled water. Conductivity of suspension was adjusted to 60 μS/cm by adding 0.1 M NaCl and pH-value was determined. The reaction chamber was completely filled up with this bacterial suspension and connected to a reservoir by pipes, which were connected to the peristaltic pump (Fig. 1). At specific time intervals 4–6 ml samples were taken to determine $OD_{600\ nm}$, pH-value, conductivity, $H_2O_2$ concentration. After each time point serial dilutions of treated bacterial suspensions were prepared and 0.1 ml of each sample was plated on BCYE agar plates followed by an incubation step at 34 °C. After three days *Legionella* colonies appeared and were counted after 5 days of incubation.

#### 2.2.1. Determination of hydrogen peroxide concentration

Plasma effects often correlate with the formation of highly reactive species. Of particular interest is the hydroxyl radical with a strong oxidation potential of 2.8 eV. Although hydroxyl radicals cannot be measured easily, detection of relatively high amounts of hydrogen peroxide can prove production by plasma in water, because a major

pathway for hydrogen peroxide is the hydroxyl radical recombination in the plasma channels (Eq. (1)) [19,29].

$$\centerdot OH + \centerdot OH \rightarrow H_2O_2 \tag{1}$$

Furthermore, $H_2O_2$ is known for the mediation of cytotoxic effects and can be used as disinfectant itself. Hence, additive effects of hydrogen peroxide to bacterial killing should be taken into account and the $H_2O_2$ concentration has to be quantified.

For determination of $H_2O_2$ a 1 ml sample was centrifuged at 3500g for 6 min, the supernatant was transferred into a new tube and 0.5 ml Titanium(IV)oxysulfate sulfuric acid was added [30]. Color development was determined at $OD_{407\ nm}$. The concentration of $H_2O_2$ was estimated with a calibration curve and a range between 0 and 6 mM $H_2O_2$.

#### 2.2.2. Sample preparation for scanning electron microscopy

Applying strong electric fields to cell membranes often induces the formation of pores, thereby causing leakage and possibly cell death [22]. Furthermore, in streamer breakdown processes the formation of shockwaves can be expected as an integral part [31]. Thus, effects on bacterial morphology seem to be conceivable.

To visualize possible effects treated and untreated bacterial suspensions were investigated by scanning electron microscopy. Microscopic images were generated from samples after plasma and PEF treatment, respectively. A sample of 4 ml was centrifuged at 3500g for 6 min and resuspended in 1 ml distilled water supplemented with 1% para-formaldehyde. Bacteria were loaded on a 0.2 μm pore size polycarbonate filter and stored in fixation solution (5 mM Hepes, 50 mM NaN₃, 1% glutaraldehyde, 4% para-formaldehyde, pH 7.4) until use for the scanning electron microscopy. Further preparation of samples was as described previously [32]. Finally, *Legionella* loaded filters were examined in a scanning electron microscope EVO LS10 (Carl Zeiss Microscopy GmbH, Oberkochen, Germany).

### 2.3. Statistical analysis

Bacteria for control and bacteria exposed to plasma and/or PEF were derived from the same culture and all experiments were conducted at least in triplicate. In graphs, each bar represents the mean of three independent experiments with standard deviation. Student's *t*-test was chosen for statistical analysis with significance for a p-value $<0.05$. Tests were carried out in Microsoft Excel 2013 and Prism 6.01.

## 3. Results

### 3.1. Plasma and PEF treatment

The experimental setup enabled to study the impact of pulsed corona plasma or pulsed electric fields on bacterial suspensions of *L. pneumophila* in water. Bacterial suspension was always adjusted to a

conductivity between 60 and 62 μS, pH-value of 6.0 and a temperature range between 25 and 27 °C. A flow rate of 140 ml/min was maintained using a peristaltic pump. For the same treatment, i.e. without the application of either plasma or PEF, the suspension was circulated 25 min through the discharge chamber.

Bacterial concentration after 25 min decreased by <10% (p = 0.03) when compared to control. Thus, mechanical stress caused by the continuous flow had only a minor effect on the survival of *Legionella* (Fig. S1).

The *Legionella* suspension was exposed to pulsed corona plasma (Fig. 3). Treatment of *Legionella* suspensions with pulsed corona plasma (a) or PEF (b). 7500, 15,000 and 30,000 consecutive discharges or pulsed electric fields for a peak voltage of 80 kV and repetition rate of 20 Hz were applied. This is equal to a treatment time of 6.25 min, 12.5 min and 25 min (Fig. 3a). Plasma treatment for 6.25 min corresponding to 7500 consecutive discharges resulted in a loss of viable *Legionella* by 33% (log 1.79). Longer treatment with plasma for 12.5 min resulted in a complete bacterial killing and no *Legionella* colonies were monitored on agar plates. Consequently also no viable bacteria were detected after 25 min.

By using the same experimental setup for PEF treatment it was possible to determine survival of *Legionella* without plasma generation (Fig. 3b). Experimental parameters for the application of high voltage pulses, such as peak voltage and conductivity were kept constant but polarity of the power source was changed. Negative applied voltage pulses therefore only generated an electrical field along the wire without igniting a corona plasma. Similar to plasma treatment a CFU log reduction of approximately 32% (log 1.9) was achieved after 6.25 min of treatment. However, compared to plasma treatment, doubling the treatment time did not completely kill *Legionella* and CFU/ml decreased only for approximately log 2 for each sampling point. Thus, compared to plasma treatment almost log 1 of *Legionella* survived this experiment after 25 min treatment.

Antimicrobial effects of plasma treatment were accompanied by an increased formation of hydrogen peroxide reaching a maximum of about 2 mM $H_2O_2$ after 25 min. In comparison, PEF treatment resulted in $H_2O_2$ concentrations in the range of 0.13 mM after 25 min (Fig. 4). Formation of hydrogen peroxide for plasma and PEF treatment after 7500, 15,000 and 30,000 consecutive discharges with a repetition rate of 20 Hz. This equals a treatment time of 6.25 min, 12.5 min and 25 min. High voltage pulses of 80 kV were applied (Fig. 4).

In most organisms hydrogen peroxide is produced during cell-metabolism, however, due to its oxidative potential it is regarded as cytotoxic. To assess the effect of $H_2O_2$ *L. pneumophila* was incubated with 1 mM $H_2O_2$. This concentration was chosen because it appears after 12.5 min of plasma treatment, where no viable bacteria were observed anymore. Samples were taken at 4 different time points, similar to
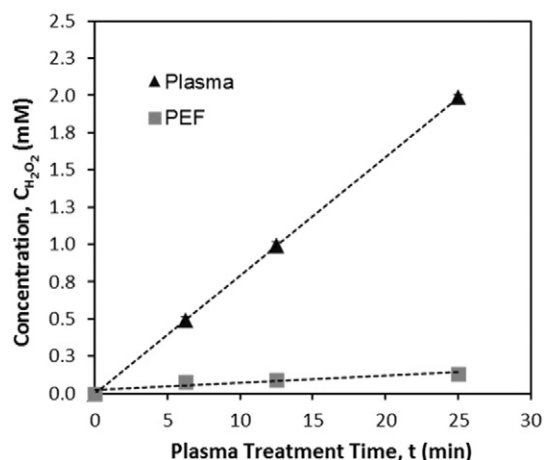


Fig. 4. Formation of hydrogen peroxide for plasma and PEF treatment after 7500, 15,000 and 30,000 consecutive discharges with a repetition rate of 20 Hz. This equals a treatment time of 6.25 min, 12.5 min and 25 min. High voltage pulses of 80 kV were applied. Each data point represents the mean of 3 independent experiments with standard deviation of 0.02 mM $H_2O_2$ for plasma and 0.04 mM $H_2O_2$ for PEF treatment. (Hence, error bars are actually smaller than the symbols in the graph.)

experiments conducted with plasma or PEF. After 12.5 min the CFU/ml decreased by about 23% (log 1.47). After 25 min incubation with 1 mM hydrogen peroxide less than log 1.9 CFU/ml of *Legionella* were killed (Fig. 5).

### 3.2. Scanning electron microscopy

The bacterial morphology after plasma and PEF treatment was illustrated by scanning electron microscopy (Fig. 6). During both treatments a bacterial damage and an alteration of *Legionella* appearance was observed when compared to untreated bacteria. After *L. pneumophila* was exposed to PEF no obvious difference in cell shape was observed. For increasing treatment times, i.e. increasing number of pulses applied, the number of ruptured cells observed post-exposure to PEF was substantially lower when compared to treatments with plasma generating pulses. Occasionally bacteria appeared deflated and surrounded by small vesicles. Obvious damage of the unit membrane led to lysis and release of the cytoplasmic content. Findings for PEF treatment can also be applied to plasma treatment, however, cell damage was generally more severe. In addition it seemed that more bacteria were completely disrupted after plasma treatment and an increase of cell debris was visible. Longer treatment of 25 min encouraged the formation of plaque-like structures. No cell damage was observed when *L. pneumophila* was exposed to 1 mM hydrogen peroxide (Fig. S2).
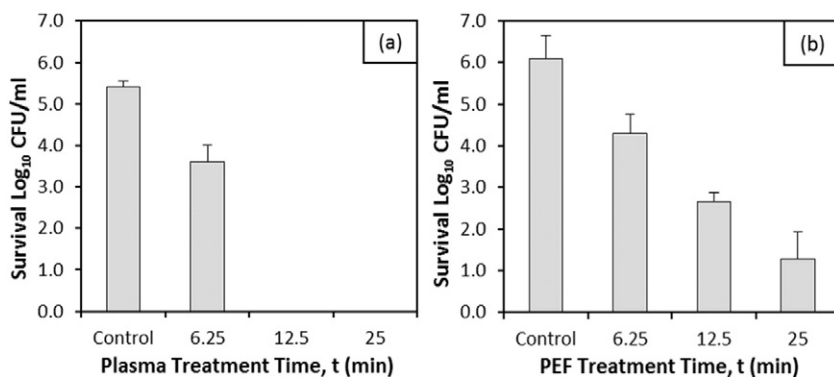


Fig. 3. Treatment of *Legionella* suspensions with pulsed corona plasma (a) or PEF (b). 7500, 15,000 and 30,000 consecutive discharges or pulsed electric fields for a peak voltage of 80 kV and repetition rate of 20 Hz were applied. This is equal to a treatment time of 6.25 min, 12.5 min and 25 min. Each bar represents the mean of three independent experiments with standard deviation (n = 3). For plasma treatment no viable *Legionella* were counted after 12.5 min and 25 min, respectively. Comparing plasma and PEF treatment, statistical significance was observed for t = 12.5 min (p = 0.0003). The CFU was determined after 5 days of incubation at 34 °C. Detection limit: 10 CFU/ml.
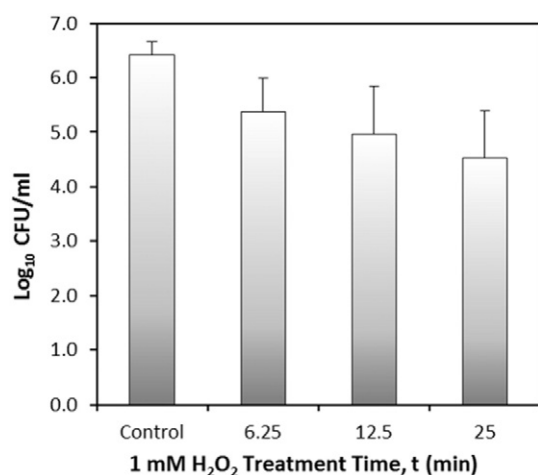
**Fig. 5.** Incubation of *Legionella* suspension with 1 mM $H_2O_2$. Samples were taken for time points that were similar to plasma treatment and PEF treatment, respectively. In general, a small but statistical significant decrease in bacteria concentration was observed in comparison to controls after 6.25 min (p = 0.02), 12.5 min (p = 0.01) and 25 min (p = 0.01). Each bar represents the mean of 5 independent experiments with standard deviation.

## 4. Discussion

Antibacterial effects of pulsed corona plasma and pulsed electric fields for decontamination of water containing *Legionella pneumophila* Philadelphia 1 JR32 as model microorganism were investigated. Increasing incidences of legionellosis motivate the development of alternative methods for water disinfection such as application of plasma or pulsed electric fields. Understanding the processes responsible for bacterial killing may help to increase efficiency of these methods. In this study both methods have been directly compared with the same experimental setup when the same energy was dissipated.

Both methods in common is the application of short high voltage pulses, which have been shown to be potentially more efficient in comparison to longer pulses for PEF treatment [22]. Supplied energy for PEF and plasma treatment can be dissipated in different ways. For PEF treatment energy will be consumed mainly for building up the electric field and the associated current flowing through the medium which increases water temperature due to Joule heating. These effects also occur during plasma treatment but in addition shockwaves, UV-radiation and reactive species are formed.

Energy per pulse by plasma or PEF treatment was calculated from current voltage measurements (Table 1). In both cases fast rising high voltage pulses with almost similar peak voltages of 80 kV were applied. Voltage pulses had an exponentially decay and pulse length was measured as full width at half maximum (FWHM). When plasma filaments are forming in the discharge volume the overall resistance of the reactor is slightly decreasing, resulting in a shorter duration of the voltage pulse that is observed (Fig. 2). Simultaneously overall current is increasing and therefore the pulse energy dissipated into plasma and/or electric field, was in the order of 1.03–1.16 J per pulse. Conductivity of *Legionella* suspension stayed almost constant during plasma and PEF application. The initial pH-value of 6 slightly decreased to a value of 5.5 during plasma treatment. Conversely, no change of pH-value was detected and the conductivity did not change during PEF treatment.

A complete killing of *L. pneumophila* was achieved after 12.5 min with plasma treatment, whereas log 2.54 CFU/ml were still alive after 12.5 min for only PEF exposure. In this case viable *Legionella* were still determined on agar plates even after 25 min of PEF treatment. Taking into account eradicated number of bacteria (CFU/ml), treated volume, energy per pulse, efficiencies can be calculated for both methods (Table 2).

For the investigated experimental setup, 124 kJ are necessary to kill *Legionella* in one liter of water (log 5.4 CFU/ml) using pulsed corona plasma. Conversely, for pulsed electric fields only, >221 kJ per liter are required for a complete killing of *Legionella*. In case of plasma, less energy is required than for thermal treatment. For thermal treatment, the temperature of water with a heat capacity of $c_W = 4.2$ kJ $kg^{-1}$ $K^{-1}$ has to be increased to 70 °C [33]. If starting temperature is around 25 ° C this change in temperature ($\Delta T = 45$ K) requires approximately 188 kJ/l.

Peak voltage (80 kV) and pulse shape were almost the same for both treatments and all experiments. For the given electrode geometry the electric field was the same for both methods and only polarities of the applied high voltage pulses were different. Accordingly, application of pulsed corona plasma using a coaxial electrode geometry seems to be superior to a PEF treatment of equal energy input. Apparently, plasma mediated effects enhance bacterial killing using the applied energy more effectively.
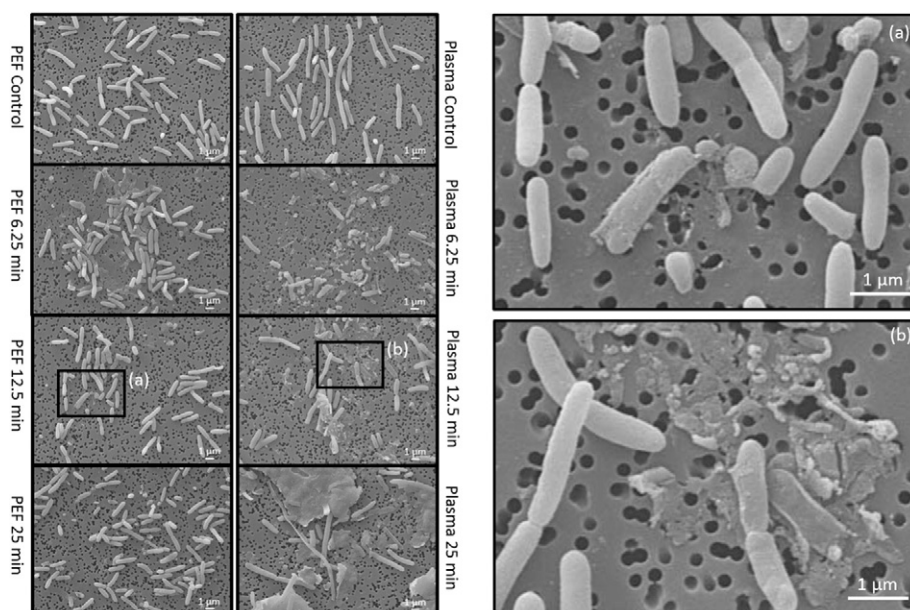


**Fig. 6.** Scanning electron microscopy pictures of *L. pneumophila* after plasma and PEF treatment, respectively.

**Table 1**
Pulse and energy parameters (MEAN) with standard deviation (SD) after application of 30,000 consecutively applied high voltage pulses, which is equal to a treatment time of 25 min. High voltage pulses were applied with a repetition rate of 20 Hz.

|  | Rise time in ns | Pulse-width in ns | Peak-voltage in kV | Peak-current in A | Pulse-energy in J |
|---|---|---|---|---|---|
| Plasma (mean) | 16 | 145 | 80.86 | 128.10 | 1.16 |
| SD | ±0.05 | ±3.97 | ±0.61 | ±5.05 | ±0.05 |
| PEF (mean) | 19 | 228 | −80.65 | −143.45 | 1.03 |
| SD | ±2.08 | ±27.90 | ±0.22 | ±5.74 | ±0.17 |

Nevertheless, killing effects mediated by the electric field itself (log 3.4 CFU/ml) have to be considered as an integral part of plasma treatment contributing to overall killing of log 5.4 CFU/ml. Formally this circumstance can be expressed as a ratio of 63% PEF and 37% plasma based on observed log reduction. However, it has to be kept in mind that nature is most likely more complicated and it can be assumed that killing of log 3.4 is much easier than killing of log 5.4. Also findings should not be generalized for other microorganisms and are dependent on the experimental setup, pulse shape and the applied electric field.

For pulsed electric field exposures, the killing of bacteria can be explained by the irreversible poration of cell membranes. The at least required electric field for membrane poration can be estimated from Schwan's equation [34]. Hereby the assumption of a spherical shape is in fact a poor approximation for the shape of *Legionella pneumophila*. For elongated (prolate) cell shapes have Gimsa and independently Kotnik shown, that the induced (peak) transmembrane potential for an orientation of the major axis of the cell in parallel to the applied electric field will be more than twice as high at the poles for prolate cells in comparison to spherical cells of the same volume [35,36]. Further away from the poles is the membrane potential higher (by at most a factor of 2) for spherical cells. Altogether the cumulative effect on the cell membrane as estimated for prolate cells in comparison to spherical cells is therefore probably very similar, especially when taking into account that the poration at the poles together with the continuously changing orientation of the cells is probably sufficient for the killing of bacteria. Accordingly Schwan's equation is providing a reasonable approximation determining the effective volume around the high voltage electrode where an adverse effect on the cells can be expected. The estimate of an effective volume is arguably more strongly affected by the decay of the electric field with distance from the high voltage electrode than by the more gradual differences arising from the cell shape.

The minimal field strength $E_{min}$ necessary for electroporation can be described by the general first order formulation of Schwan's equation (Eq. (2)) for the induced transmembrane potential, $\Delta\Psi$ [35]:

$$\Delta\Psi = 1.5 * E * r * \cos\theta * \left(1 - e^{\frac{-t}{\tau_m}}\right) \qquad (2)$$

where $t$ is the time of the pulse and $\tau_m = (0.5 * (\rho_a + \rho_b)) * C * r$ the characteristic charging time and with $\rho_a$ and $\rho_b$ are conductivities of the solvent and the cytoplasm, $C$ the capacity of the cell membrane and $r$ the radius of the cell.

At a sufficiently high voltage across the cell membrane which is generally assumed to be on the order = 1 V [37], pores are formed and the cell membrane becomes permeable. Dependent on field strength, pulse duration and number of pulses applied, a pore can be formed permanently or only temporarily. As a consequence, pores can induce leakage and possibly cell death [12,22,38,39].

However, in the chosen geometry the electric field is not homogeneous and only a fraction of cells in the vicinity of the high voltage electrode will be exposed to the required field. To estimate field strength alongside the high voltage electrode with respect to reactor dimensions the following equation was employed (Eq. (3)):

$$E = \frac{V_0}{\ln \frac{b}{a}} * \frac{1}{R} \qquad (3)$$

where $V_0$ is the applied voltage, $a$ and $b$ the radii of the wire and reactor. $R$ is the chosen distance between the wire and the reactor wall. For an applied voltage of 80 kV the electrical field strength $E$ close to the high voltage tungsten wire is 2745 kV/cm and decreases exponentially to 8.1 kV/cm close to the outer electrode (Fig. 7).

According to the exponential decrease of the electrical field strength, induced membrane potential is decreasing with increasing distance from the high voltage electrode. The necessary electric field, $E_{min}$, for inducing a transmembrane potential difference of $\Delta\Psi = 1$ V, was calculated with 30.4–31.2 kV/cm for a solvent conductivity of 60–62 μS/cm. With these assumptions and the applied peak voltage of 80 kV the necessary field strength is achieved up to a distance of about 0.45 cm from the wire surface. Thus, effects of PEF were mediated in a cylindrical zone around the high voltage electrode with a volume of 4.1 to 4.3 cm³.

It has to be noted that the analysis is not taking into account the decreasing value of the applied voltage with time as shown in Fig. 2. Therefore, the interaction volume might actually be much smaller for the threshold voltage that is equivalent to the minimum required electric field. The problem is alleviated by the flow system together with the high number of applied high voltage pulses. As consequence a large fraction of bacteria will eventually pass through the interaction zone, most likely repeatedly, and be prone to poration accordingly. Conversely, the killing rates that are achieved in the coaxial geometry for the dissipated energy are certainly still much lower than could be expected for the exposure to a homogeneous electric field and the efficiencies reported in Table 2 could be further increased. However, the objective of the study was not optimizing the PEF exposure but instead to compare them with the competing approach exploiting the generation of plasma filaments, for the same energy input per applied high voltage pulse. In addition, to the electric field around the wire, high electric fields are also formed around the plasma filaments.

**Table 2**
Energy efficiency for plasma treatment and PEF treatment for killing of *Legionella pneumophila* Philadelphia 1 JR32. Each column represents the mean of three independent experiments (n = 3). Comparing plasma and PEF treatment killing effects statistical significance was observed for 12.5 min (p = 0.004).

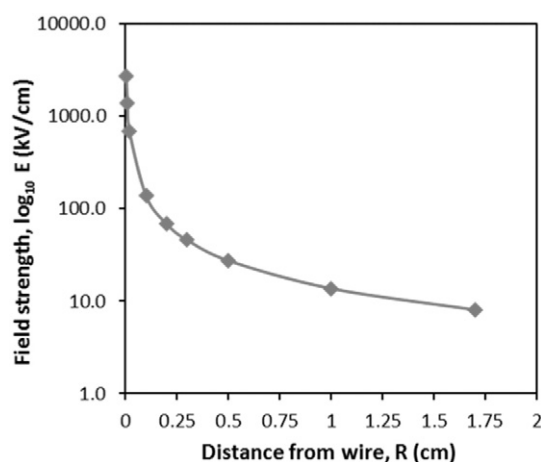|  | Killing after 12.5 min in CFU/ml | Killing after 25 min in CFU/ml | Energy per pulse applied in J | Efficiency per log reduction in kJ/l | Efficiency for eradication in kJ/l |
|---|---|---|---|---|---|
| Plasma (mean) | log 5.4 | log 5.4 | 1.16 | 23.03 | 124.44 |
| SD | ±0.15 | ±0.15 | ±0.02 | ±0.85 | ±5.15 |
| PEF (mean) | log 3.42 | log 4.82 | 1.03 | 46.97 | >221.15 |
| SD | ±0.46 | ±0.57 | ±0.08 | ±5.90 | ±35.60 |

**Fig. 7.** Estimated electric field strength *E* as a function of distance from the wire at the center for an application of a high voltage of 80 kV. Field strength was calculated with respect to reactor dimensions, electrode curvature and applied voltage.

More importantly the mechanisms that are provided by the plasma can further be directed towards the killing of bacteria in addition to the electric field. Several studies proposed that in particular the generation of reactive species by the interaction of a plasma with water provides a most effective means for the killing of bacteria [40–43]. Chemical reactions responsible for the formation of reactive species in a plasma are often quite complex. They are dependent on many parameters like plasma source, gas mixture and/or immersion in a liquid. As a result of this reactive species for a variety of plasma sources may differ.

In pulsed corona plasma generated directly in water, hydroxyl radicals seem to be the dominant transient species [19]. Although hydroxyl radicals have only a lifetime of a few nanoseconds in aqueous solution they can form long-lived chemical products such as $H_2O_2$ [29]. Increased concentration of hydrogen peroxide was observed for plasma experiments conducted in this work. As an uncharged species $H_2O_2$, with its ability to penetrate membranes, is causing oxidative stress to compounds also inside the cell. Together with the applied electric field and the associated membrane poration, reactive species could enter cells more easily.

After 12.5 min, i.e. the time point where no viable colonies could be found, a concentration of 1 mM $H_2O_2$ was determined. Presumably this concentration can lead to severe damage due to oxidation of the DNA of the bacteria by generation of 8-oxo-guanidine or at proteins by generation of disulfide bridges [44,45]. However, when *Legionella* was exposed to 1 mM $H_2O_2$ only (i.e. without the associated generation of corona plasma or pulsed electric fields), a log reduction of only log 1.47 (CFU/ml) after 12.5 min was observed. Due to its own catalase and alkyl hydroxide reductase *L. pneumophila* is able to convert $H_2O_2$ into nontoxic compounds when applied in low concentration [46]. It should be mentioned that catalase activity is different in several Legionella strains [47].

However, we cannot exclude that other bacteria react less sensitive to $H_2O_2$ exposure than *Legionella*. A striking example is the opportunistic pathogen *Streptococcus pneumoniae*, which does not produce a catalase but is highly resistant against reactive oxygen species including $H_2O_2$ [48]. Meanwhile, hydrogen peroxide alone cannot explain increased cell disruption during plasma treatment when compared to PEF. No cell damage of *L. pneumophila* was detected by scanning electron microscopy when *Legionella* was exposed to 1 mM hydrogen peroxide (Fig. S2).

Although, the generation of reactive species, including hydrogen peroxide seems to be primarily responsible for the killing of *Legionella*, some other corona plasma characteristics could also contribute. These are in particular UV emissions, shockwaves and local heating generated directly within the plasma filaments. For example shear forces induced by shockwaves or water vapor expansion due to local heating during streamer propagation may be an explanation for increased cell damage observed during plasma treatment [31]. However, these effects are most likely only effective in close vicinity of the filaments while long-lived chemical species could be found throughout the liquid.

Altogether the combination of plasma induced mechanism, such as the generation of reactive species, with pulsed electric fields that are provided in the investigated configuration result in a much more efficient killing of *Legionella* than the exposure to pulsed electric fields alone.

## 5. Conclusion

The aim of this study was an unambiguous comparison of two promising emerging methods for the elimination of *Legionella pneumophila* from water. The experimental setup was designed to generate pulsed electric fields or pulsed corona plasma by changing the polarity of the applied high voltage pulses. It could be shown that killing of *L. pneumophila* was possible with both methods. However, pulsed corona plasma seems to be more efficient. Herby the effects of pulsed electric fields and the generation of reactive species are combined. Electroporation of the cell membrane due to the established electric field might favor the uptake of reactive species such as $H_2O_2$ into the *Legionella*. Once inside the cell radicals can develop their cytotoxic effects resulting in an enhanced bacterial killing. Based on these findings the application of pulsed corona plasma can be further optimized. Conversely, water treatments that are currently conducted by pulsed electric fields could be improved by a combination with plasma induced chemistry. This way, it might be possible to reduce the duration of applied electric fields and increase the energy efficiency of the treatment.

## Appendix A. Supplementary material

Supplementary data to this article can be found online at http://dx.doi.org/10.1016/j.bioelechem.2016.05.006.

## References

[1] D. García, N. Gómez, P. Mañas, S. Condón, J. Raso, R. Pagán, Occurrence of sublethal injury after pulsed electric fields depending on the micro-organism, the treatment medium ph and the intensity of the treatment investigated, J. Appl. Microbiol. 99 (2005) 94–104.

[2] M. Swanson, B. Hammer, Legionella pneumophila pathogenesis: a fateful journey from amoebae to macrophages, Annu. Rev. Microbiol. 54 (2000) 567–613.

[3] B.S. Fields, R.F. Benson, R.E. Besser, Legionella and Legionnaires' disease: 25 years of investigation, Clin. Microbiol. Rev. 15 (2002) 506–526.

[4] C. Joseph, Legionnaires' disease in Europe 2000–2002, Epidemiol. Infect. 132 (2004) 417–424.

[5] P. Stöcker, B. Brodhun, U. Buchholz, Legionärskrankheit in Deutschland unter besonderer Berücksichtigung der im Krankenhaus oder in einer Pflegeeinrichtung erworbenen Erkrankungen, 2004–2006, Bundesgesundheitsbl. Gesundheitsforsch. Gesundheitsschutz 52 (2009) 219–227.

[6] K. Neil, R. Berkelman, Increasing incidence of legionellosis in the United States, 1990–2005: changing epidemiologic trends, Clin. Infect. Dis. 47 (2008) 591–599.

[7] Y.S. Lin, J.E. Stout, V.L. Yu, R.D. Vidic, Disinfection of water distribution systems for Legionella, Semin. Respir. Infect. 13 (1998) 147–159.

[8] J.M. Kuchta, A.M. McNamara, R.M. Wadowsky, R.B. Yee, Susceptibility of Legionella pneumophila to chlorine in tap water, Appl. Environ. Microbiol. 46 (1983) 1134–1139.

[9] Q. Zhang, J. Zhuang, T. von Woedtke, J.F. Kolb, J. Zhang, J. Fang, K.-D. Weltmann, Synergistic antibacterial effects of treatments with low temperature plasma jet and pulsed electric fields, Appl. Phys. Lett. 105 (2014) 104103.

[10] S.J. Beebe, P.M. Fox, L.J. Rec, K. Somers, R.H. Stark, K.H. Schoenbach, Nanosecond pulsed electric field (nsPEF) effects on cells and tissues: apoptosis induction and tumor growth inhibition, Plasma Sci. IEEE Trans. 30 (2002) 286–292.

[11] R. Nuccitelli, U. Pliquett, X. Chen, W. Ford, R. James Swanson, S.J. Beebe, J.F. Kolb, K.H. Schoenbach, Nanosecond pulsed electric fields cause melanomas to self-destruct, Biochem. Biophys. Res. Commun. 343 (2006) 351–360.

[12] S. Toepfl, V. Heinz, D. Knorr, High intensity pulsed electric fields applied for food preservation, Chem. Eng. Process. Process Intensif. 46 (2007) 537–546.

[13] H. Akiyama, T. Sakugawa, T. Namihira, K. Takaki, Y. Minamitani, N. Shimomura, Industrial applications of pulsed power technology, Dielectr. Electr. Insul. IEEE Trans. 14 (2007) 1051–1064.

[14] X. Chen, J.F. Kolb, R.J. Swanson, K.H. Schoenbach, S.J. Beebe, Apoptosis initiation and angiogenesis inhibition: melanoma targets for nanosecond pulsed electric fields, Pigment Cell Melanoma Res. 23 (2010) 554–563.

[15] P. Lukes, M. Clupek, V. Babicky, P. Sunka, Ultraviolet radiation from the pulsed corona discharge in water, Plasma Sources Sci. Technol. 17 (2008) 024012.

[16] M. Dors, E. Metel, J. Mizeraczyk, E. Marotta, Coli bacteria inactivation by pulsed corona discharge in water, Int. J. Plasma Environ. Sci. Technol. 2 (2008) 34–37.

[17] A.T. Sugiarto, M. Sato, Pulsed plasma processing of organic compounds in aqueous solution, Thin Solid Films 386 (2001) 295–299.

[18] B. Jiang, J. Zheng, S. Qiu, M. Wu, Q. Zhang, Z. Yan, Q. Xue, Review on electrical discharge plasma technology for wastewater remediation, Chem. Eng. J. 236 (2014) 348–368.

[19] R. Banaschik, P. Lukes, H. Jablonowski, M.U. Hammer, K.-D. Weltmann, J.F. Kolb, Potential of pulsed corona discharges generated in water for the degradation of persistent pharmaceutical residues, Water Res. 84 (2015) 127–135.

[20] V. Joubert, C. Cheype, J. Bonnet, D. Packan, J.-P. Garnier, J. Teissié, V. Blanckaert, Inactivation of Bacillus subtilis var. niger of both spore and vegetative forms by means of corona discharges applied in water, Water Res. 47 (2013) 1381–1389.

[21] P. Sunka, V. Babický, M. Clupek, P. Lukes, M. Simek, J. Schmidt, M. Cernák, Generation of chemically active species by electrical discharges in water, Plasma Sources Sci. Technol. 8 (1999) 258.

[22] K.H. Schoenbach, F.E. Peterkin, R.W. Alden III, S.J. Beebe, The effect of pulsed electric fields on biological cells: experiments and applications, Plasma Sci. IEEE Trans. 25 (1997) 284–292.

[23] A. Abou-Ghazala, S. Katsuki, K. Schoenbach, F. Dobbs, K. Moreira, Bacterial decontamination of water by means of pulsed corona discharges, pulsed power plasma science, PPPS-2001. Dig. Tech. Pap. IEEE 2001 (2001) 612–615.

[24] E. Van Heesch, A. Pemen, P.A. Huijbrechts, P.C. van der Laan, K. Prasinski, G.J. Zanstra, P. De Jong, A fast pulsed power source applied to treatment of conducting liquids and air, Plasma Sci. IEEE Trans. 28 (2000) 137–143.

[25] R. Banaschik, F. Koch, J.F. Kolb, K.D. Weltmann, Decomposition of pharmaceuticals by pulsed corona discharges in water depending on streamer length, Plasma Sci. IEEE Trans. 42 (2014) 2736–2737.

[26] B. Sun, M. Sato, J.S. Clements, Optical study of active species produced by a pulsed streamer corona discharge in water, J. Electrost. 39 (1997) 189–202.

[27] M.A. Malik, A. Ghaffar, S.A. Malik, Water purification by electrical discharges, Plasma Sources Sci. Technol. 10 (2001) 82.

[28] E. Wintermeyer, B. Ludwig, M. Steinert, B. Schmidt, G. Fischer, J. Hacker, Influence of site specifically altered Mip proteins on intracellular survival of Legionella pneumophila in eukaryotic cells, Infect. Immun. 63 (1995) 4576–4583.

[29] B.R. Locke, K.-Y. Shih, Review of the methods to form hydrogen peroxide in electrical discharge plasma with liquid water, Plasma Sources Sci. Technol. 20 (2011) 034006.

[30] G. Eisenberg, Colorimetric determination of hydrogen peroxide, Ind. Eng. Chem. Anal. Ed. 15 (1943) 327–328.

[31] J. Kolb, R. Joshi, S. Xiao, K. Schoenbach, Streamers in water and other dielectric liquids, J. Phys. D. Appl. Phys. 41 (2008) 234007.

[32] S. Handtke, R. Schroeter, B. Jürgen, K. Methling, R. Schlüter, D. Albrecht, S.A. van Hijum, J. Bongaerts, K.-H. Maurer, M. Lalk, Bacillus pumilus reveals a remarkably high resistance to hydrogen peroxide provoked oxidative stress, PLoS One 9 (2014).

[33] B. Kim, J. Anderson, S. Mueller, W. Gaines, A. Kendall, Literature review—efficacy of various disinfectants against legionella in water systems, Water Res. 36 (2002) 4433–4444.

[34] V.H. Pauly, H. Schwan, Über die Impedanz einer Suspension von kugelförmigen Teilchen mit einer Schale, Z. Naturforsch. B 14 (1959) 125–131.

[35] T. Kotnik, D. Miklavčič, Analytical description of transmembrane voltage induced by electric fields on spheroidal cells, Biophys. J. 79 (2000) 670–679.

[36] J. Gimsa, D. Wachner, Analytical description of the transmembrane voltage induced on arbitrarily oriented ellipsoidal and cylindrical cells, Biophys. J. 81 (2001) 1888–1896.

[37] T. Kotnik, W. Frey, M. Sack, S.H. Meglič, M. Peterka, D. Miklavčič, Electroporation-based applications in biotechnology, Trends Biotechnol. (2015).

[38] N. Rowan, S.J. Macgregor, J. Anderson, R. Fouracre, O. Farish, Pulsed electric field inactivation of diarrhoeagenic Bacillus cereus through irreversible electroporation, Lett. Appl. Microbiol. 31 (2000) 110–114.

[39] S. Spilimbergo, F. Dehghani, A. Bertucco, N.R. Foster, Inactivation of bacteria and spores by pulse electric field and high pressure $CO_2$ at low temperature, Biotechnol. Bioeng. 82 (2003) 118–125.

[40] F. Liu, P. Sun, N. Bai, Y. Tian, H. Zhou, S. Wei, Y. Zhou, J. Zhang, W. Zhu, K. Becker, Inactivation of bacteria in an aqueous environment by a direct-current, cold-atmospheric-pressure air plasma microjet, Plasma Process. Polym. 7 (2010) 231–236.

[41] K. Oehmigen, M. Hähnel, R. Brandenburg, C. Wilke, K.D. Weltmann, T. von Woedtke, The role of acidification for antimicrobial activity of atmospheric pressure plasma in liquids, Plasma Process. Polym. 7 (2010) 250–257.

[42] Z. Machala, L. Chládeková, M. Pelach, Plasma agents in bio-decontamination by dc discharges in atmospheric air, J. Phys. D. Appl. Phys. 43 (2010) 222001.

[43] N. Bai, P. Sun, H. Zhou, H. Wu, R. Wang, F. Liu, W. Zhu, J.L. Lopez, J. Zhang, J. Fang, Inactivation of Staphylococcus aureus in water by a cold, $He/O_2$ atmospheric pressure plasma microjet, Plasma Process. Polym. 8 (2011) 424–431.

[44] E.L. Domingue, R. Tyndall, W. Mayberry, O. Pancorbo, Effects of three oxidizing biocides on Legionella pneumophila serogroup 1, Appl. Environ. Microbiol. 54 (1988) 741–747.

[45] J.J. Foti, B. Devadoss, J.A. Winkler, J.J. Collins, G.C. Walker, Oxidation of the guanine nucleotide pool underlies cell death by bactericidal antibiotics, Science 336 (2012) 315–319.

[46] J.J. LeBlanc, R.J. Davidson, P.S. Hoffman, Compensatory functions of two alkyl hydroperoxide reductases in the oxidative defense system of Legionella pneumophila, J. Bacteriol. 188 (2006) 6235–6244.

[47] L. Pine, P. Hoffman, G. Malcolm, R. Benson, M. Keen, Determination of catalase, peroxidase, and superoxide dismutase within the genus legionella, J. Clin. Microbiol. 20 (1984) 421–429.

[48] M. Saleh, S.G. Bartual, M.R. Abdullah, I. Jensch, T.M. Asmat, L. Petruschka, T. Pribyl, M. Gellert, C.H. Lillig, H. Antelmann, Molecular architecture of Streptococcus pneumoniae surface thioredoxin-fold lipoproteins crucial for extracellular oxidative stress resistance and maintenance of virulence, EMBO Mol. Med. 5 (2013) 1852–1870.

# Publications and Conference Contributions

## Publications in Peer Reviewed Journals

### 2017

„Degradation and Metabolites of Diclofenac as Instructive Example for Decomposition of Recalcitrant Pharmaceuticals by Hydroxyl Radicals Generated with Pulsed Corona Plasma in Water"
R. Banaschik, H. Jablonowski, P.J. Bednarski, J.F. Kolb, Journal of hazardous materials 342 (2018) 651-660.

"Fenton chemistry promoted by sub-microsecond pulsed corona plasmas for organic pollutant degradation in water"
R. Banaschik, P. Lukes, C. Miron, R. Banaschik, A. Pipa, K. Fricke, P.J. Bednarski, J.F. Kolb, Electrochimica Acta, 245 (2017) 539-548.

„Comparison of extraction of valuable compounds from microalgae by atmospheric pressure plasmas and pulsed electric fields"
K. Zocher, R. Banaschik, C. Schulze, T. Schulz, J. Kredl, C. Miron, M. Schmidt, S. Mundt, W. Frey, J.F. Kolb, Plasma Medicine, (2017)

### 2016

"Comparison of pulsed corona plasma and pulsed electric fields for the decontamination of water containing *Legionella pneumophila* as model organism"
R. Banaschik, G. Burchhardt, K. Zocher, S. Hammerschmidt, J.F. Kolb, K.-D. Weltmann, Bioelectrochemistry, 112 (2016) 83-90.

### 2015

"Potential of pulsed corona discharges generated in water for the degradation of persistent pharmaceutical residues"
R. Banaschik, P. Lukes, H. Jablonowski, M.U. Hammer, K.-D. Weltmann, J.F. Kolb, Water research, 84 (2015) 127-135.

## 2014

"Decomposition of Pharmaceuticals by Pulsed Corona Discharges in Water Depending on Streamer Length"
R. Banaschik, F. Koch, J.F. Kolb, K.D. Weltmann, Plasma Science, IEEE Transactions on, 42 (2014) 2736-2737.

# Conference Proceedings

"Degradation of Pharmaceutical Residues in Water with Pulsed Corona Discharges Generated Directly in Water by Sub-Microsecond High Voltage Pulses"
J.F. Kolb, R. Banaschik, C. Miron, F. Koch, P. Lukes, K.-D. Weltmann, Symposium on High Pressure Low Temperature Plasma Chemistry-Book of contributions: HAKONE XIV. Greifswald: INP Greifswald and IfP Greifswald, 2014 - (Brandenburg, R.; Stollenwerk, L.), O-06-31-O-06-31 ISBN N

# Oral Presentations

## Invited talks

## 2014

"Degradation of Selected Pharmaceuticals with Pulsed Corona Discharges Generated in Water"
R. Banaschik, P. Lukes, J.F. Kolb, K.-D. Weltmann, 41st IEEE International Conference on Plasma Science (ICOPS), May 25-29, 2014, Washington, DC, USA.

"Degradation of Stable Pharmaceutical Residues in Water by Nanosecond Pulsed Corona Discharges in Water"
J.F. Kolb, R. Banaschik, C. Miron, K.-D. Weltmann, 9th International Symposium on Non-Thermal/Thermal Plasma Pollution Control Technology and Sustainable Energy (ISNTP-9), June 16-20, 2014, Dalian, China.

## Talks

## 2017

"Plasma liquid chemistry of pulse discharges generated in water depending on pulse duration and ground electrode materials"
R. Banaschik, P. Lukes, C. Miron, H. Jablonowski, A. Pipa, K. Fricke, J. Kredl, T. Schulz, K.-D. Weltmann, P. Bednarski, J. F. Kolb, 44th IEEE International Conference on Plasma Science (ICOPS), May 21-25, 2017 Atlantic City, USA

## 2015

"Investigation of Reaction Mechanism for the Degradation of Pharmaceutical Residues by Pulsed Corona Discharges Generated in Water"
R. Banaschik, P. Lukes, J.F. Kolb, P. Bednarski, K.-D. Weltmann, COST TD1208 2nd Annual Meeting, "Electrical discharges with liquids for future applications", Barcelona, 23-26 March 2015.

"Degradation of Pharmaceutical Residues in Water by Pulsed Corona Discharges – Investigation of Reaction Mechanism"
R. Banaschik, P. Lukes, Camelia Miron, J.F. Kolb, P. Bednarski, K.-D. Weltmann, 42st IEEE International Conference on Plasma Science (ICOPS), May 24-28, 2015, Antalya, Turkey.

## 2014

"Pulsed Corona Discharges Generated in Water with Sub-Microsecond High Voltage Pulses for the Degradation of Pharmaceuticals"
R. Banaschik, F. Koch, C. Miron, J. Zhuang, P. Lukes, J.F. Kolb, K.-D. Weltmann, COST TD1208 Annual Meeting, "Electrical discharges with liquids for future applications," Lisbon, 10-13 March 2014.

# Poster Presentations

## 2016

"Pulsed Corona Plasma and Pulsed Electric Fields for the decontamination of water containing Legionella pneumophila"
R. Banaschik, G Burchhardt, K. Zocher, S. Hammerschmidt, J. F. Kolb, K.-D. Weltmann, 13th International Bioelectrics Symposium (BIOELECTRICS 2016), September 12-15, 2016, Rostock, Germany.

## 2015

"Pulsed Corona Discharges Generated in Water with Sub- Microsecond High Voltage Pulses for the Degradation of Pharmaceutical Residues"
R. Banaschik, P. Lukes, P. Bednarski, J. F. Kolb, DPG-Frühjahrstagung, März 2-5, 2015, Bochum, Germany

"Disinfection by Pulsed Discharges in Water: When Pulsed Electric Fields are not enough"
J. F. Kolb, R. Banaschik, P. Lukes, P. Bednarski, K.-D. Weltmann, 1st World Congress on Electroporation, Pulsed Electric Fields in Biology, Medicine, Food and Environmental Technologies, September 6-10, 2015, Portorož, Slovenia

## 2013

"Degradation of Pharmaceutical Residues with Pulsed Corona Discharges Generated in Water"
R. Banaschik, F. Koch, J. Zhuang, C. Miron, J.F. Kolb, K.-D. Weltmann, 10th International Bioelectrics Symposium (BIOELECTRICS 2013), September 16-19, 2013, Karlsruhe, Germany.

# Acknowledgment